University of Alberta

Characterization and Identification of Low Affinity Dihydropyridine Binding Sites on Skeletal Muscle Ca^{2+} Channels

by

Dingjiu Bao ©

A thesis submitted to the Faculty of Graduate Studies and Research in partial fulfillment of the requirements for the degree of Master of Science

Division of Neuroscience

Edmonton, Alberta

Spring, 1997

ABSTRACT

L-type calcium channels are enriched in the transverse tubule membrane system of skeletal muscle. A novel technique, using velocity sedimentation, has been developed to isolate transverse tubule membranes rapidly (30 min) and efficiently from skeletal muscle microsomal membranes.

Fluorescence techniques have been used to investigate low affinity dihydropyridine binding sites in skeletal muscle calcium channels. Amlodipine, a dihydropyridine derivative, is fluorescent in aqueous solution. Transverse tubule membranes are themselves highly fluorescent, as is the purified calcium channel protein. The binding of amlodipine to transverse tubule membranes is accompanied by an enhancement of amlodipine fluorescence, when excited either directly or via energy transfer from membrane proteins, and a quench in intrinsic protein fluorescence. Binding is to a specific and saturable population of low affinity sites with a K_d around 4 μM. Other non-fluorescent dihydropyridines competitively inhibit amlodipine binding with micromolar affinities and the binding of these drugs can be determined directly by their ability to quench the protein fluorescence. By monitoring the quench in protein fluorescence these sites have been shown to be present in the purified L-type calcium channel. In addition, studies of the kinetics of ligand dissociation have indicated that the low affinity sites are allosterically coupled to well studied high affinity sites.

It has also been demonstrated that slow voltage-dependent calcium channels are present in isolated transverse tubule membranes. Functional responses of these calcium channels can be studied by using rapid filtration techniques to measure voltage-dependent [$^{45}Ca^{2+}$] fluxes on physiologically relevant time scales.

Studies of the pH-dependence of amlodipine binding to its high affinity sites suggest that this derivative (pKa = 8.7) binds more tightly in its unprotonated (neutral) form. Based on these and previous results, it is suggested that the ionized molecule may have restricted accessibility to its intramembrane binding domain.

ACKNOWLEDGMENTS

First of all, I would like to thank my supervisor, Dr. Susan Dunn, for the opportunity to study and take part in the research in her laboratory. Thanks, Susan, for your excellent supervision, encouragement, support, and patience over the last three years.

I wish to express my gratitude for the encouragement, help, and understanding of my supervisory committee, Dr. Bill Dryden and Dr. Ian Martin.

I would like to thank Dr. Teresa Krukoff, Dr. Amy Tse, Dr. Fred Tse and Dr. Bill Colmers for their efficient guidance, encouragement and help during my program.

Special thanks to my colleagues and friends, Rick, Glen, Margaret, Lori, Liren, and Martin for their kindness, support, technical assistance and the help in improving my English.

Finally, the financial support of the Alberta Heritage Foundation for Medical Research, Medical Research Council of Canada, Faculty of Medicine, Division of Neuroscience and Faculty of Graduate Studies and Research is gratefully acknowledged.

TABLE OF CONTENTS

LIST OF TABLES

LIST OF FIGURES

LIST ABBREVIATIONS

A_{595}	protein absorbance reading at wavelength 595 nm
ACS	aqueous counting scintillant
Ala	alanine
ATP	adenosine triphosphate
B_{max}	maximal binding density
Ba^{2+}	barium ion
BSA	bovine serum albumin
BTZ	benzothiazepine
Ca^{2+}	calcium ion
$CaCl_2$	calcium chloride
cAMP	cyclic adenosine monophosphate
cA-PK	cAMP-dependent protein kinase
cGMP	cyclic guanosine monophosphate
Cd^{2+}	cadmium ion
cDNA	complementary DNA
CHAPS	3-[(3-cholamidopropyl)-dimethylammonio]-1-propanesulfonate
Ci	curie
cpm	counts per minute
C-terminal	carboxyl terminal
DEAE	diethylaminoethyl
DHP	1,4-dihydropyridine
DNA	deoxyribonucleic acid
DOCC	depletion-operated calcium channel
E-C	excitation-contraction
EDTA	ethylenedinitrilo tetraacetic acid
EGTA	ethylene glycol-bis (β-aminoethyl ether) N,N,N',N'- tetraacetic acid
Em	equilibrium membrane potential
em	emission wavelength
ex	excitation wavelength
EX	extracellular location
FTX	funnel-web spider toxin

G-protein	guanine nucleotide binding protein
Gs	stimulatory GTP binding protein
GTP	guanosine triphosphate
HCl	hydrochloric acid
HEPES	4-(2-hydroxyethyl)-1-piperazineethanesulfonic acid
HVA	high voltage activated
Ile	isoleucine
IN	intracellular location
IP_3	inositol triphosphate
K^+	potassium ion
K_d	dissociation constant
KCl	potassium chloride
kD	kilo dalton
LVA	low voltage activated
mA	milliampere
MES	2-N-morpholino ethanesulfonic acid
Me_2SO	dimethylsulfoxide
$MgCl_2$	magnesium chloride
MW	molecular weight
Ni^{2+}	nickel ion
NaCl	sodium chloride
NaN_3	sodium azide
ND	not determined
PAA	phenylalkylamine
PC	phosphatidycholine
PEG	polyethelene glycol
PKA	protein kinase A
PKC	protein kinase C
PMSF	phenylmethylsulfonyl fluoride
pS	pico Siemens
PVDF	polyvinylidene difluoride
rpm	rotations per minute
SDS-PAGE	sodium dodecylsulfate polyacrylamide gel electrophoresis
S4	the fourth transmembrane segment
S5	the fifth transmembrane segment
S6	the sixth transmembrane segment

sFTX	synthetic funnel-web spider toxin
SMOCC	second messenger-operated calcium channel
SR	sarcoplasmic reticulum
TBS	Tris buffered saline
TBST	Tris buffered saline containing 0.1% Tween 20
TM	transmembrane location
T-tubule	transverse tubule
Tris	Tris (hydroxymethyl) aminomethane
Tyr	tyrosine
U	unit
V	volt
VDCC	voltage-dependent calcium channel
VICC	voltage-independent calcium channel
v/v	volume per volume
w/v	weight per volume
WGA	wheat germ agglutinin
°C	degrees Celsius
ω-CgTx	ω-conotoxin

1. INTRODUCTION

1.1. Calcium and Calcium Channels

1.1.1. Introduction

Calcium ions (Ca^{2+}) play a key role in controlling many physiological processes. A steep concentration gradient between extracellular and intracellular Ca^{2+} is maintained such that the concentration of extracellular Ca^{2+} is 1-10 mM whereas the intracellular free Ca^{2+} concentration ranges from 0.1 to 10 μM, depending on the state of the cell (Hosey and Lazdunski, 1988). Because of the low background levels of Ca^{2+}, elevation of intracellular Ca^{2+} concentrations can lead to activation of a number of diverse physiological processes as well as cellular toxicity and death. Regulation of cellular Ca^{2+} levels is thus crucial for the proper functioning of an individual cell. Several different types of Ca^{2+} transport systems, present both on the cellular plasma membrane and on the membranes of intracellular organelles, serve to maintain the low concentration of intracellular free Ca^{2+} (Carafoli, 1987). Defects in the regulation of Ca^{2+} movements and storage are believed to be associated with a variety of acute and chronic losses of cellular function, resulting in a number of experimental and clinical disease states (Hosey and Lazdunski; 1988; Hoffman, 1995).

1.1.2. Plasmalemmal Ca^{2+} Channels

Ca^{2+} entry through plasma membrane Ca^{2+} channels represents a major pathway for the cellular control of calcium in many cell types including both excitable and non-excitable cells (Hosey and Lazdunski, 1988; Felder *et al.*, 1994). Although the plasma membrane is normally impermeable to Ca^{2+}, opening of these Ca^{2+} channels allows Ca^{2+} to diffuse passively across the plasma membrane down its electrochemical gradient into the cell. According to fundamental differences in gating mechanisms, plasma Ca^{2+} channels are usually categorized as voltage-dependent Ca^{2+} channels (VDCCs) and voltage-independent Ca^{2+} channels (VICCs) (Hosey and Lazdunski, 1988; Felder *et al.*, 1994).

VDCCs are gated pores that open in response to depolarization of the plasma membrane and highly selectively allow the entry of Ca^{2+} into the cell. By sensing depolarization and facilitating the flow of Ca^{2+}, VDCCs translate electrical signals on the membrane surface into intracellular chemical signals. Ca^{2+} entry into a cell triggers a variety of intracellular processes, including membrane excitability, muscle contraction, and secretion of neurotransmitters (Snutch and Reiner, 1992; Catterall, 1994). The existence of distinct types of VDCCs was first demonstrated by differences in electrophysiological properties, then by pharmacological distinctions (Miller, 1992; McCleskey, 1994). More recently, molecular biological approaches have revealed even greater diversity among VDCCs, with diversity arising from the existence of multiple genes, as well as from alternative splicing mechanisms (Tsien *et al.*, 1991; Hofmann *et al.*, 1994). These VDCCs are discussed in detail in the following section.

Ca^{2+} influx also occurs through VICCs, which have been identified by electrophysiological and biochemical techniques. These channels are activated by many ligands including neurotransmitters, hormones, cytokines, and antigens (Felder *et al.*, 1994). VICCs constitute a large family of proteins with their own regulatory mechanisms. Three main mechanisms have been proposed (Felder *et al.*, 1994). In receptor-operated Ca^{2+} channels (ROCCs), the channels are closely coupled to membrane receptors and are independent of regulation by diffusible second messengers, including Ca^{2+}. Depletion-operated Ca^{2+} channels (DOCCs) are regulated by the concentration of Ca^{2+} in the intracellular Ca^{2+} stores and provide a source for refilling of these stores. Second messenger-operated Ca^{2+} channels (SMOCCs) are regulated by IP_3, IP_4 and intracellular Ca^{2+} that are generated following receptor activation. However, these channels are independent of the filling state of intracellular Ca^{2+} stores. It has been shown that Ca^{2+} flux through these three types of VICCs can be modulated by guanyl nucleotide binding protein (G protein) coupled receptors. Examples of VICCs include an ROCC in smooth muscle

that is activated by ATP (Benham and Tsien, 1987), muscarinic receptor-stimulated DOCC in N1E-115 neuroblastoma cells (Mathes and Thompson, 1994), and IP_3-stimulated SMOCC in lacrimal acinar cells (Bird *et al.*, 1991). Although VICCs have been implicated in the regulation of cell growth and differentiation, their physiological roles are still somewhat speculative. Ongoing studies include isolation of VICC channels, cloning and mapping of their distribution, and characterizing the diversity and physiological function of the various family membranes (Felder *et al.*, 1994)

1.1.3. Voltage-Dependent Ca^{2+} Channels (VDCCs)

VDCCs represent the best characterized plasmalemmal Ca^{2+} entry pathway, primarily because powerful and specific channel blocking agents are available (Triggle and Janis 1987; Campbell *et al.*, 1988). At least four major classes of VDCCs (L, T, N, and P) exist based on electrophysiological and pharmacological criteria as well as on their distribution and postulated cellular functions (Tsien *et al.*, 1991; Miller, 1992; Triggle, 1994).

L-type calcium channels, the best characterized class, are high-voltage-activated (HVA; positive to -10 mV) and mediate long-lasting Ca^{2+} currents with large unitary conductance (25-30 pS) (Fox *et al.*, 1987a, b). Inactivation of L-type channels is relatively slow and displays both Ca^{2+}-dependence and voltage-dependence (Chad, 1989; Pelzer *et al.*, 1990). These channels are more permeable to Ba^{2+} than to Ca^{2+}, and are more potently blocked by Cd^{2+} than by Ni^{2+} (Triggle *et al.*, 1989). L-type channels are inhibited by three distinct class of organic compounds: dihydropyridines (DHPs), phenylalkylamines (PAAs), and benzothiazepines (BTZs) (Triggle and Janis, 1987). L-type channels are found in virtually all excitable tissues and in many non-excitable cells. They are the major pathway for voltage-gated Ca^{2+} entry in heart and smooth muscle, and they are related to the generation of action potentials and to signal transduction events at the cell membrane (Kostyuk, 1989; Bertolino and Llinas, 1992).

Their voltage-dependence of activation and their rates of inactivation distinguish T-type Ca^{2+} channels from high-voltage-activated Ca^{2+} channels. T-type channels are low-voltage-activated (LVA), carry a small (8 pS) transient current, and exhibit rapid and purely voltage-dependent inactivation (Bean, 1989). In contrast to L-type channels, T-type channels are resistant to dihydropyridine compounds, less sensitive to Cd^{2+} and more sensitive to Ni^{2+}, amiloride and octanol (Tang *et al.*, 1988; Bertolino and Llinas, 1992). T-type channels are also found in a wide variety of excitable and non-excitable cells although they are virtually absent in some cells such as adrenal chromaffin cells or sympathetic neurons (Bean, 1989; Carbone and Swandulla, 1989; Hess, 1990). Because Ca^{2+} enters through T-type channels at negative membrane potentials, these channels are likely to be responsible for pacemaker activity and neuronal oscillatory activity (Llinas, 1988; Tsien *et al.*, 1991). Due to the lack of selective ligands, T-type channels have not been isolated and their structure has not yet been determined.

N-type Ca^{2+} channels are also high-voltage-activated (-40 to -30 mV) but they differ pharmacologically from L-type channels in being resistant to DHPs and blocked by ω-conotoxin (ω-CgTx) GVIA, a toxic peptide isolated from a fish-hunting marine snail (Olivera *et al.*, 1985; Stanley and Atrakchi, 1990). N-type channels often exhibit a smaller single channel conductance (13-20 pS) and a greater tendency to inactivate with depolarized holding potentials than L-type channels (Plummer *et al.*, 1989). They are restricted largely to neurons although there is great variability from one neuron to another, e.g. they are largely absent from cerebellar Purkinje cells and possibly also from cerebellar granule cells (Tsien *et al.*, 1991). The N-type channels play a role in some forms of neurotransmitter release from mammalian cells (Bertolino and Llinas, 1992; Gonzalez Burgos *et al.*, 1995).

A fourth distinct type of VDCCs is the P-type which was initially identified in cerebellar Purkinje cells (Llinas *et al.*, 1989). They activate over a range of potentials less negative than -50 mV and show very slow inactivation. P-type channels are insensitive to

both dihydropyridine derivatives and ω-conotoxin GVIA, but are blocked by native funnel-web spider venom and by a polyamine (FTX) extracted from such venom, as well as by a synthetic polyamine (sFTX) (Llinas *et al.*, 1989). More recently, ω-Aga-IVA, a peptide isolated from the venom of the funnel-web spider, *Agelenopsis aperta*, has been reported to selectively block P-type channels (Mintz *et al.*, 1992). Using sFTX affinity chromatography, proteins were isolated from guinea pig cerebellum and squid optic lobe that manifested single-channel properties similar to those of native P-type channels when reconstituted into lipid bilayers (Llinas *et al.*, 1989). P-type channels have now been cloned, and their primary structure has been determined (Mori *et al.*, 1991; Starr *et al.*, 1991). P-type channels appear to be the most widely distributed Ca^{2+} channels in the mammalian central nervous system as detected by immunohistochemical studies (Hillman *et al.*, 1991; Bertolino and Llinas, 1992; Westenbroek *et al.*, 1995). Their postulated functions include serving both as a generator of intrinsic activity and as a modulator of neuronal integration and transmitter release (Bertolino and Llinas, 1992; Gonzalez Burgos *et al.*, 1995).

A neuron can have all four types of channels, whereas muscle cells have only L and sometimes T channels (Benham *et al.*, 1987; Dirken and Beam, 1995; Gonzalez Burgos *et al.*, 1995). In many neurons, a combination of known channel-selective blockers fails to block all Ca^{2+} current, suggesting the presence of additional types of Ca^{2+} channels (McCleskey, 1994). Recently, other types of VDCCs have been reported i.e. Q-type channels, which are blocked by ω-conotoxin-MVIIC from the marine snail *Conus magus*; and R-type channels, which are resistant to most toxins (Wheeler *et al.*, 1994; Perez-Reyes and Schneider, 1995).

1.2. L-type Ca^{2+} Channels in Skeletal Muscle

Two types of Ca^{2+} channels, L- and T-type, have been identified in skeletal muscle (Bean, 1989). The best studied are L-type channels which are DHP-sensitive. Although

DHP-sensitive Ca^{2+} channels are present in essentially all excitable cells, by far the most abundant source is rabbit skeletal muscle, where they are localized to the transverse tubule (T-tubule) membranes (Fosset *et al.*, 1983). Thus, L-type Ca^{2+} channels in the T-tubule membranes of skeletal muscle have served as the major biochemical and molecular model for studies of Ca^{2+} channels (Catterall, 1995; Perez-Reyes and Schneider, 1995).

1.2.1. Biochemical and Molecular Properties of the Subunits of Skeletal Muscle L-Type Ca^{2+} Channels

The high density of L-type Ca^{2+} channels in skeletal muscle T-tubule membranes and the specific high-affinity binding of dihydropyridine Ca^{2+} channel antagonists to L-type Ca^{2+} channels have facilitated their purification and structural analysis (Catterall, 1995). The L-type Ca^{2+} channel protein has been purified using traditional purification procedures involving detergent (digitonin or CHAPS) solubilization, lectin-Sepharose affinity chromatography, DEAE ion exchange chromatography and sucrose-density gradient sedimentation (Curtis and Catterall, 1984; Borsotto *et al.*, 1985). The purified channel is an oligomeric protein in which the principle α_1 subunit is associated in a complex with β, γ and disulfide linked α_2/δ subunits in a stoichiometry of 1:1:1:1:1 (Catterall, 1988). The primary structures of all of these subunits have been defined by cloning their corresponding cDNAs (Tanabe *et al.*, 1987; Ellis *et al.*, 1988; Ruth *et al.*, 1989; DeJongh *et al.*, 1990; Jay *et al.*, 1990). The predicted topology and biochemical characteristics of DHP receptor subunits in skeletal muscle are shown in Figure 1 and Table 1, respectively.

The α_1 subunit is the central functional subunit of the channel protein, leaving the other subunits as likely determinants of more subtle channel properties (Miller, 1992). Photoaffinity labelling studies have demonstrated that the α_1 subunit carries binding sites for DHPs and for other organic Ca^{2+}-channel blockers (Striessnig *et al.*, 1986 and 1987; Naito *et al.*, 1989) and, in expression studies, this subunit has been shown to form a

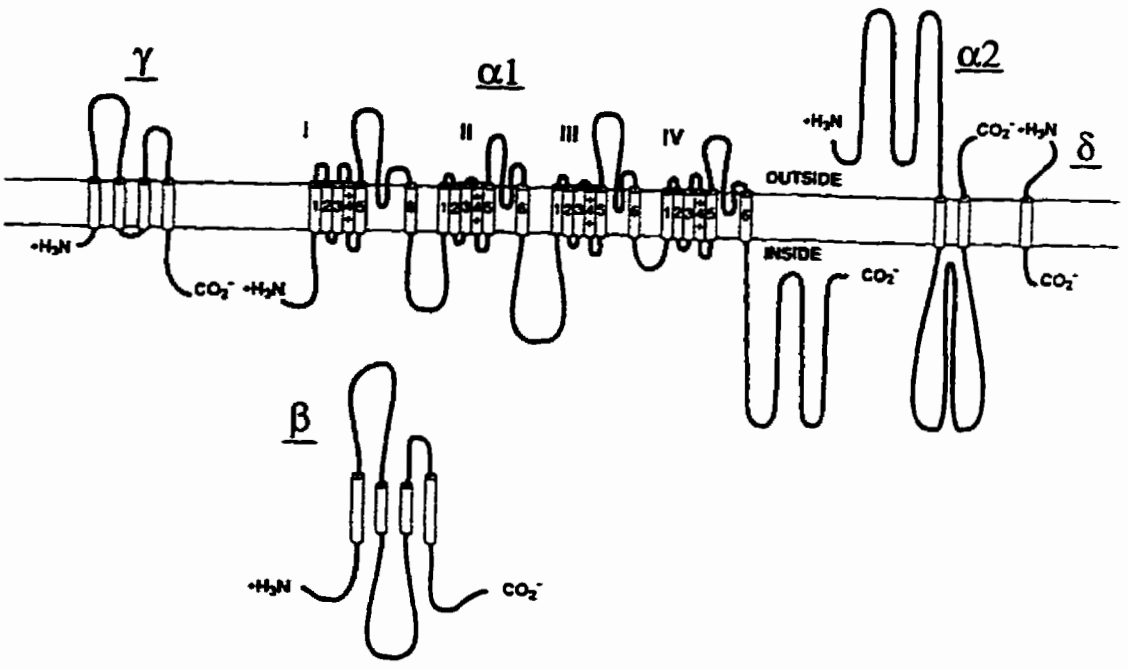

Figure 1. Proposed topology of skeletal muscle Ca^{2+} channel subunits. Transmembrane folding models of the subunits derived from primary structure determination and analysis. Cylinders represent predicted α-helical segments in the transmembrane regions of the α_1, $\alpha_2\delta$, and γ subunits and in the peripherally associated β subunit. The transmembrane folding patterns are derived only from hydropathy analysis for $\alpha_2\delta$ and γ and from a combination of hydropathy analysis and analogy with the current models for the structures of sodium and potassium channels for α_1. The transmembrane arrangement of $\alpha_2\delta$ is not well-defined by hydropathy analysis and the indicated structure should be taken as tentative (Catterall, 1992).

Table 1.

Biochemical Properties of the Subunits of L-type Ca^{2+} Channels in Skeletal Muscle

	α_1		β	γ	α_2	δ
	Full size (<5%)	**Truncated** (>95%)				
Molecular Weight (kDa)	212	175	57	30	140	30
Location	TM	TM	IN	TM	TM/EX	TM/EX
Glycosylation	-	-	-	++	+++	+
Phosphorylation	+	+	+	-	-	-

TM: transmembrane location
IN: intracellular location
EX: extracellular location

functional voltage-dependent Ca^{2+} channel (Tanabe *et al.*, 1988; Perez-Reyes *et al.*, 1989). The α_1 subunit of skeletal muscle L-channels displays 30-40% homology to the α_1 subunit of voltage-dependent sodium channels (Tanabe *et al.*, 1987). This subunit has four internal homologous domains (I-IV), each containing six putative transmembrane segments (S1-S6) (Tanabe *et al.*, 1987). The fourth transmembrane segment (S4) of each of these domains contains positively charged amino acids (arginine or lysine) every third or fourth residue and this region has been proposed to constitute the voltage-sensing region of the channel protein (Catterall, 1988). The loops that connect transmembrane segments S5 and S6 in each domain contain short membrane-associated segments, designated SS1/SS2, that are thought to form the ion selectivity filter (Heinemann *et al.*, 1994; Catterall, 1995). Two forms of α_1 subunit, $\alpha_{1(175)}$ and $\alpha_{1(212)}$, have been detected in rabbit skeletal muscle (De Jongh *et al.*, 1989 and 1991; Lai *et al.*, 1990). The minor $\alpha_{1(212)}$ (less than 5%) is full-length whereas the major $\alpha_{1(175)}$ (more than 95%) is truncated during posttranslational proteolytic cleavage of its carboxyl terminal domain between residues 1685 and 1699 (De Jongh *et al.*, 1991).

The β subunit (57 kDa) is a hydrophilic protein that is not glycosylated and, therefore, is likely to be located on the intracellular side of the membrane (Takahashi *et al.*, 1987; Ruth *et al.*, 1989). The β subunit is phosphorylated by multiple protein kinases, including protein kinase C and cAMP-dependent protein kinase (Curtis and Catterall, 1985; Jahn *et al.*, 1988; O'Callahan *et al.*, 1988). Substantial evidence indicates that there is a strong association between the α_1 and β subunits (Curtis and Catterall, 1984; Takahashi *et al.*, 1987; Leung *et al.*, 1988). Furthermore, a conserved motif in the loop between domain I and domain II of the α_1 subunit has been identified to be a binding site for the β subunit (Pragnell *et al.*, 1994). Co-expression of the β subunit with the α_1 subunit alters both functional and the pharmacological properties of Ca^{2+} channel (see below).

The α_2/δ subunits (140/30 kDa), encoded by the same gene, are linked to each other by disulfide bonds and are apparently highly conserved in most tissues including neurons, cardiac and smooth muscle (DeJongh *et al.*, 1990; Jay *et al.*, 1991; Miller, 1992; Hofmann and Flockerzi, 1994). Both subunits are highly glycosylated and this underlies the usefulness of lectin affinity chromatography in the purification of the channel complex (Striessnig *et al.*, 1987; Curtis and Catterall, 1986). Opinions differ as to the physical arrangement of the α_2/δ subunits in relation to the other subunits and to the membrane (Catterall *et al.*, 1988; Campbell *et al.*, 1988; Jay *et al.*, 1991; Catterall, 1995). However, both subunits do contain hydrophobic sequences which suggests that each subunit may have transmembrane segments (Takahashi *et al.*, 1987; Isom *et al.*, 1994).

The γ subunit is unique to skeletal muscle (Jay *et al.*, 1990; Bosse *et al.*, 1990; Catterall, 1995). It is a hydrophobic glycoprotein with an apparent molecular mass of 30 kDa (Takahashi *et al.*, 1987). The deduced primary structure contains four predicted hydrophobic transmembrane segments and multiple sites for N-linked glycosylation (Jay *et al.*, 1990; Bosse *et al.*, 1990; Catterall, 1995).

1.2.2. The Roles of DHP Receptors in Skeletal Muscle

Although L-type Ca^{2+} channels or DHP receptors are abundant in skeletal muscle T-tubule membranes, their functional significance remains to be established. Skeletal muscle DHP receptors play distinct roles as compared to those in either cardiac or smooth muscle. In skeletal muscle, electrically stimulated contraction has been observed in Ca^{2+}-free medium (Armstrong *et al.*, 1972; Frank, 1982), suggesting that the influx of extracellular Ca^{2+} is not an obligatory step in muscle contraction. Furthermore, skeletal muscle L-channels activate very slowly, reaching peak current amplitude only after 100-200 ms (Beaty *et al.*, 1987), whereas Ca^{2+} release from sarcoplasmic reticulum (SR) begins and terminates within a few milliseconds after depolarization (Melzer *et al.*, 1986). Thus, this

Ca^{2+} current is too slow to account for the rapidity of Ca^{2+} release from SR. Therefore, unlike in cardiac or smooth muscle, the function of DHP receptors as Ca^{2+} channels in skeletal muscle is not directly responsible for muscle contraction. Furthermore, it is unlikely that the influx of Ca^{2+} through these channels is the trigger for Ca^{2+}-induced Ca^{2+} release from the SR.

1.2.2.1. Function as Voltage Sensors for Excitation-Contraction (E-C) Coupling

DHP receptors in skeletal muscle do, however, play a unique role in mediating skeletal muscle excitation-contraction (E-C) coupling, a process which links changes in membrane potential to muscle contraction (Rios and Pizarro, 1991). It has been suggested that during E-C coupling, DHP receptors may function as voltage sensors (Rios and Pizarro; Lamb, 1992). A small electrical signal, known as asymmetric charge movement, is thought to reflect the activation of these voltage-sensors (Schneider and Chandler, 1973) and this, by some unknown mechnism, triggers the release of Ca^{2+} from the SR which initiates the events that lead to muscle contraction (Rios and Pizarro, 1991). DHP antagonists suppress the activity of the voltage sensors in the T-tubule membranes (Rios and Brum, 1987). In addition, the release of Ca^{2+} from the SR in skeletal muscle has been shown to be T-tubule depolarization-induced and DHP receptor-dependent (Anderson and Meissner, 1995). Solid evidence for the crucial role of DHP receptors in E-C coupling has also come from studies of cultured muscle cells from mice with a muscular dysgenesis mutation in which native Ca^{2+} channels are absent (Beam *et al.*, 1986). Transfection of deficient myocytes with cDNA encoding the α_1 subunit of L-channels restored charge movement, E-C coupling, and the ability to contract (Tanabe *et al.*, 1988; Adams *et al.*, 1990). Whether contraction is skeletal-like (i.e. independent of extracellular Ca^{2+}) or cardiac-like (i.e. dependent on the extracellular Ca^{2+}) was dependent on which kind of α_1 subunit cDNA had been injected (Tanabe *et al.*, 1990a). Furthermore, the structural

element for the unique skeletal muscle E-C coupling has been identified by constructing chimerae of skeletal and cardiac clones and shown to be the loop between domains II and III (Tanabe *et al.*, 1990b). Recently, a subdomain in the II-III loop, Thr^{671}-Leu^{690}, has been identified to be responsible for triggering SR Ca^{2+} release in skeletal muscle (El-Hayek *et al.*, 1995).

1.2.2.2. Function as VDCCs

Although the initiation of contraction in skeletal muscle is independent of extracellular Ca^{2+}, the DHP receptors can mediate Ca^{2+} entry in response to membrane depolarization, as can the receptors in cardiac and smooth muscle. Studies of [$^{45}Ca^{2+}$]flux in isolated T-tubule membrane vesicles has demonstrated the presence of both DHP-sensitive and voltage-dependent Ca^{2+} channels in this preparation (Dunn, 1989). Purified DHP receptors or isolated α_1 subunits from skeletal muscle T-tubule membranes have been successfully reconstituted into phospholipid vesicles or planar lipid bilayers and shown to form functional Ca^{2+} channels (Affolter and Coronado, 1985; Curtis and Catterall, 1986; Flockerzi *et al.*, 1986; Pelzer *et al.*, 1989; Ma *et al.*, 1991). The expression of the α_1 subunit in L-cells, a murine fibroblast-derived cell line, led to the formation of DHP-sensitive Ca^{2+} channels, although with different electrophysiological characteristics from those of native skeletal muscle Ca^{2+} channels (Perez-Rayes *et al.*, 1989). Furthermore, expression of the α_1 subunit in cultured muscle cells from dysgenic mice restored Ca^{2+} current, in addition to charge movement and E-C coupling (Tanabe *et al.*, 1988; Adams *et al.*, 1990; Beam *et al.*, 1992).

In several studies it has been shown that the Ca^{2+} currents in skeletal muscle or in reconstituted preparations are smaller than expected if all DHP receptors are functional Ca^{2+} channels (Schwartz *et al.*, 1985; Curtis and Catterall, 1986; Pelzer *et al.*, 1989). The small Ca^{2+} current may be the consequence of the low channel open probability (Lamb, 1992; Ma

et al., 1991). Furthermore, purification and reconstitution procedures can cause protein denaturation or subunit losses (Nunoki *et al.*, 1989; Mundina-Weilenmam *et al.*, 1991). In a recent study, a retrograde signal from the ryanodine receptor was shown to enhance the ability of skeletal muscle DHP receptors to function as Ca^{2+} channels (Nakai *et al.*, 1996). This may explain the difficulty of expression of skeletal muscle L-channels in a non-muscle system, in which the interaction between DHP receptors and ryanodine receptors does not occur (Perez-Rayes *et al.*, 1989).

1.2.2.3. Dual Roles of DHP Receptors in Skeletal Muscle

The current view is that DHP receptors in skeletal muscle are likely to play dual roles (Lamb, 1991; Dunn *et al.*, 1993; Catterall, 1995). Their primary physiological role is to serve as voltage sensors in E-C coupling. By unknown mechnisms, voltage-driven conformational changes of the L-channels activate Ca^{2+} release from SR (Rios and Brum, 1987; Adams and Beam, 1990; Catterall, 1991; Rios and Pizarro, 1991). As voltage-gated Ca^{2+} channels, DHP receptors mediate slow Ca^{2+} currents. Potentiation of L currents may serve to replenish cellular Ca^{2+} during periods of sustained muscle activity and to increase intracellular Ca^{2+} in response to tetanic stimulation, leading to increased contractile force (Dulhunty and Gage, 1988; Frank and Oz, 1992; Lamb 1992; Scuptoreanu *et al.*, 1993).

1.2.3. Modulation of Skeletal Muscle L-Type Ca^{2+} Channels

As described above, DHP receptors in T-tubule membranes of skeletal muscle perform dual functions as voltage sensors and as functional VDCCs. However, it has been estimated that only about 5% of the total number of DHP receptors function as Ca^{2+} channels (Schwartz *et al.*, 1985). Several mechanisms may contribute to regulation of the ion conductance activity of these channels.

1.2.3.1. Two Forms of the α_1 Subunit

As mentioned above, two size forms of the skeletal muscle α_1 subunit have been demonstrated to exist and both have been shown to form functional VDCCs. There are six conserved consensus sites for cAMP-dependent protein phosphorylation on the full length α_1 subunit, but three of these potential phosphorylation sites, which are located in the carboxy-terminal tail, are absent in $\alpha_{1(175)}$ (DeJong *et al.*, 1989; Rotman *et al.*, 1995). Since it is well established that Ca^{2+} flux through L-type channels is regulated by cAMP-dependent protein kinase (see below), a change in the relative proportion of $\alpha_{1(212)}$ and $\alpha_{1(175)}$ may have the potential to modify the observed channel characteristics profoundly (Catterall, 1991; DeJong *et al.*, 1994). A recent study by Catterall's group shows that $\alpha_{1(212)}$ is subjected to calpain proteolysis to remove the major sites of cAMP-dependent phosphorylation (DeJong *et al.*, 1994). Calpain is a Ca^{2+}-activated neutral protease which is physiologically important for the regulation of Ca^{2+} currents (Belles *et al.*, 1988; Romanin *et al.*, 1991).

1.2.3.2. Regulation by Protein Phosphorylation and G-Protein Interactions

As in many other cells, the Ca^{2+} channels in skeletal muscle are regulated by neurotransmitters and hormones via receptor mediated events that involve second-messenger-mediated protein phosphorylation systems and direct interaction with G proteins (Dunn *et al.*, 1993). α_1 and β subunits of skeletal muscle L-type channel are substrates *in vitro* for many protein kinases including cAMP-dependent protein kinase (cA-PK), protein kinase C (PKC) , casein kinase II, and a multifunctional Ca^{2+}/calmodulin-dependent protein kinase (Takahashi *et al.*, 1987; O'Callahan and Hosey, 1988; Jahn *et al.*, 1988; Ruth *et al.*, 1989). Purified and reconstituted Ca^{2+} channels are activated by phosphorylation of their α_1 and β subunits by cA-PK (Hymel *et al.*, 1988 ; Nunoki *et al.*, 1989; Mundina-Weilenmann *et al.*, 1991). Addition of cA-PK increased open probability of purified,

reconstituted channels and also native channels from T-tubule vesicles (Flockerzi *et al.*, 1986). It is likely that this phosphorylation represents the mechanism by which L-type Ca^{2+} channels are activated by β-adrenergic stimulation in skeletal muscle (Arreola *et al.*, 1987). Further studies in cultured skeletal muscle cells indicated that α_1 subunit may be phosphorylated by cA-PK in intact cells (Lai *et al.*, 1990) and voltage-dependent phosphorylation of the α_1 subunit by cA-PK can modulate channel activity in response to repetitive depolarizing stimuli (Sculptoreanu *et al.*, 1993).

The Ca^{2+} channel function of DHP receptors in skeletal muscle has also been shown to be modulated directly by G-proteins (Yatani *et al.*, 1988; Brown *et al.*, 1989; Hamilton *et al.*, 1991). The α subunit of G_s has been shown to be closely associated with Ca^{2+} channels in skeletal T-tubule membranes (Hamilton *et al.*, 1991). In the absence of cAMP, cGMP, Ca^{2+}, inositol triphosphate and /or protein kinase C, both an activated G-protein and purified $G_s\alpha$ have been shown to increase the open channel probability by about 13-25 fold (Yatani *et al.*, 1988).

1.2.3.3. Regulation by Auxiliary Subunits

Like other voltage-gated cation channels, the principal subunit of VDCCs (α_1) is expressed in cells as a specific protein complex with several auxiliary subunits. L-type channels in skeletal muscle are a complex of five subunits. Although the α_1 subunit alone can form a functional L-channel in both expression and purification and reconstitution studies, it is subject to modulation by the auxiliary subunits. Of the four auxiliary subunits, the β subunit has been the most extensively studied. Coexpression of the skeletal muscle α_1 and β subunit accelerated the activation and inactivation kinetics by more than 10-fold (Lacerda *et al.*, 1991; Varadi *et al.*, 1991). In addition, coexpression of the cardiac α_1 subunit with the skeletal muscle β subunit led to increased α_1-mediated inward currents due to a facilitation of channel opening upon membrane depolarization (Nishimura *et al.*, 1993).

As noted above, the skeletal muscle β subunit is a substrate for phosphorylation by a number of protein kinases. Moreover, the β subunit is selectively dephosphorylated by phosphoprotein phosphatases (Lai *et al.*, 1993). Since protein phosphorylation/ dephosphorylation can influence the activity of Ca^{2+} channels, the effects of the β subunit may be due, in part, to phosphorylation/dephosphorylation mechanisms (Catterall, 1995).

In contrast to the substantial functional effects of the β subunit on Ca^{2+} channels, the functional roles of other subunits are less clear. It was shown that $\alpha_2\delta$ and γ subunits had little effect on skeletal muscle Ca^{2+} channels expressed in murine L cells (Varadi *et al.*, 1991). However, coexpression of skeletal muscle $\alpha_2\delta$ and γ subunits with the cardiac α_1 altered the time course and voltage dependence of activation and inactivation of cardiac Ca^{2+} channels expressed in *Xenopus* oocytes (Mikami *et al.*, 1989; Singer *et al.*, 1991).

The functional properties of L-channels are also modulated in a complex manner by Ca^{2+} channel ligands which act at multiple receptor sites, as described in the following section.

1.3. Pharmacology of L-type Ca^{2+} channels

The original biochemical studies of L-type Ca^{2+} channels benefited from the availability and usefulness of DHP derivatives which specifically bind to these channel proteins with high affinity. To date, at least three discrete sites on L-channels that bind 1,4-DHPs, PAAs, and BTZs have been extensively explored due to the importance of these drugs in the therapy of a variety of cardiovascular disorders (Triggle and Janis, 1987; Triggle, 1994).

1.3.1. Localization of Binding Domains for DHPs, PAAs, and BTZs

1,4-DHPs, PAAs, and BTZs are structurally heterogeneous compounds which have been shown to modulate primarily L-type VDCCs (Triggle *et al.*, 1989).

Photoaffinity labelling studies have demonstrated that the α_1 subunit of L-channels carries high affinity binding sites for each of these classes of drugs (Striessnig *et al.*, 1986, 1987; Naito *et al.*, 1989). These sites are linked allosterically one to the other as shown in radioligand binding and functional studies (Striessnig *et al.*, 1986; Triggle and Janis, 1987).

Different experimental strategies have been applied for determination of the region(s) of α_1 subunit which is (are) critical for high affinity DHP binding. Data from electrophysiological experiments using protonated tertiary DHPs or quaternary DHPs have suggested that DHPs act from the extracellular surface of the L-channels (Kass and Arena, 1989; Kass *et al.*, 1991). Studies that have combined photoaffinity labelling with traditional protein sequencing methods (Regulla *et al.*, 1991) or peptide mapping (Nakayama *et al.*, 1991; Striessnig *et al.*, 1991), however, gave a different view of the localization of the DHP binding sites, suggesting that they occur either in the hydrophilic intracellular C-terminal domain of the α_1 subunit or at the extracellular end of transmembrane segment IIIS6 plus transmembrane segment IVS6. Further studies by construction of chimeric Ca^{2+} channels in *Xenopus* oocytes suggested that the stimulatory effect of a DHP agonist [(+)S202-791] is mediated by a relatively high affinity site which is located in the SS2-S6 linker of domain IV, whereas the inhibitory effect of the DHP antagonist [(-)S202-791] is mediated by another relatively low affinity site that may reside in other regions of domain IV (Tang *et al.*, 1993). Very recent studies combining site-directed mutagenesis with radioligand binding have identified crucial residues in both IIIS6 and IVS6 that are important for high affinity DHP binding (Peterson *et al.*, 1996).

Photoaffinity labelling and peptide mapping studies of the PAA binding site using a photoreactive arylazide PAA, ludopamil, revealed that transmembrane segment S6 in domain IV (IVS6) of the α_1 subunit and several adjacent intracellular and extracellular amino acid residues may contribute to the formation of the PAA receptor site (Striessnig *et*

al., 1987 and 1990). More recently, site-directed mutagenesis studies have identified three amino acid residues (Tyr-1463, Ala-1467, and Ile-1470) in IVS6 that are required for high affinity block of L-type Ca^{2+} channels by the PAA, (-)D888 (Hockerman *et al.*, 1995).

Very recently, the BZT binding site of skeletal muscle L-type channels has also been analyzed by photoaffinity labelling and peptide mapping using benziazem (Kraus *et al.*, 1996) or azidobutyryl clentiazem (Kuniyasu *et al.*, 1996). Results from these studies suggest that the BTZ binding site is located in S6 of domains III and IV or in the loop between S5 and S6 of domain IV and the adjacent S6 of domain IV, respectively.

Thus, binding domains for DHPs, PAAs, and BTZs appear to be located in close proximity to each other and to the pore-forming regions of the channel.

1.3.2. Low Affinity DHP Binding Sites in Skeletal Muscle L-Channels

Sensitivity to DHPs is a distinct characteristic of L-type Ca^{2+} channels. It is generally accepted that DHP binding sites in skeletal muscle are present on the α_1 subunit, to which DHPs bind with high affinity (K_d values of nM range) (Galizzi *et al.*, 1986). These high affinity binding sites have been well studied (see above). However, it has been noticed that the concentrations of DHPs that are pharmacologically active are much greater than those required to saturate the high-affinity sites measured *in vitro* (Schwartz *et al.*, 1985; Triggle and Janis, 1987). Although a similar discrepancy in cardiac muscle may be explained, at least in part, by the voltage-dependence of DHP binding (see below), no voltage-dependence of high affinity DHP binding in skeletal muscle has been detected (Bhat, 1993). Thus, the discrepancy between ligand binding data and pharmacological data in skeletal muscle is not readily explained by the voltage-dependence of binding.

An alternative explanation is that DHP receptors may contain multiple DHP binding sites and that the effects of DHPs on channel function may be due to their binding to

distinct low affinity sites. Evidence that, in addition to high affinity sites for DHPs, low affinity binding sites for DHP drugs may also occur in skeletal muscle membranes was first described by Dunn and Bladen (1991), from their kinetic studies of DHP binding. Several DHP derivatives, at micromolar concentrations, were shown to accelerate the rate of dissociation of [^{3}H]-PN200-110 from its high affinity binding sites (Dunn and Bladen, 1991). The presence of low affinity sites has been further supported by using felodipine, a fluorescent DHP ligand, in direct binding assays. By monitoring the fluorescence changes accompanying felodipine binding, low affinity sites that were specific for DHPs were shown to be localized to the T-tubule membranes (Dunn and Bladen, 1992). It has been suggested that the high and low affinity binding sites are likely to be conformationally linked, such that occupancy of the low affinity sites by DHPs may induce a conformational change in the DHP receptors, thus displacing the radiolabelled ligand from its high affinity sites (Dunn and Bladen, 1991 and 1992). Furthermore, the binding of the DHP agonist, BAY K8644, to low affinity sites appears to be modulated by G protein activation (Dunn and Bladen, 1991). The presence of low affinity binding sites for DHPs may have functional significance since similar concentrations of these ligands are required to affect Ca^{2+} flux. Evidence that T-tubule membranes carry low affinity sites with K_ds in the micromolar range and that these low affinity binding sites are involved in the E-C coupling processes or inhibition of Ca^{2+} channel currents has also been obtained by several other groups using different methods of analysis (Ohkusa *et al.*, 1991; Anderson and Meissner, 1995; Kwan *et al.*, 1995). However, direct biochemical evidence for low affinity DHP binding sites in the purified DHP receptors is lacking.

1.3.3. Complexity of the Pharmacology of L-Type Ca^{2+} Channels

Among the three heterogeneous groups of therapeutically available L-type channel drugs, the DHP series of drugs contains both potent antagonists and potent activators of

Ca^{2+} channels. These drugs, therefore, are of considerable importance as molecular probes for the analysis of the structure and function of Ca^{2+} channels (Triggle and Rampe, 1989; Triggle *et al.*, 1989). It has been suggested that DHP Ca^{2+} channel antagonists and activators may binding to different receptor sites, although the structural differences between DHP antagonists and activators are small and, indeed, both antagonists and activators may exhibit a dual effect, stimulatory or inhibitory, depending on the membrane potential (Brown *et al.*, 1986; Triggle and Rampe, 1989; Vaghy, 1992). In addition, different patterns of state-dependence among these drugs have been reported. Verapamil (PAA) and diltiazem (BTZ) exhibit prominent frequency-dependent interactions whereas nifedipine (and other 1,4-DHPs) exhibits prominent voltage-dependent interaction with cardiac Ca^{2+} channels. In cardiac muscle, verapamil and diltiazem activity increases with increasing frequency of stimulation and nifedipine activity increases with maintained depolarization (Sanguinetti and Kass, 1984a, b; Janis and Triggle, 1991). Moreover, binding of DHPs to L-channels is influenced by divalent cations and auxiliary subunits. Examples of these interactions include the binding of Ca^{2+} in the pore of L-type Ca^{2+} channels which modulates high affinity DHP binding (Peterson and Catterall, 1995; Mitterdorfer *et al.*, 1995) and the ability of the β subunit to increase the affinity of DHP binding sites of the α_1 subunit (Mitterdorfer *et al.*, 1994). In addition, L-type channel antagonists show significant tissue selectivity for cardiovascular tissues despite the widespread distribution of these channels (Triggle, 1994). Thus L-type channels have complex interactions with structurally distinct chemical compounds.

2. STATEMENT OF THE PROBLEM

Skeletal muscle T-tubule membranes are the richest source of L-type Ca^{2+} channels and these channels have been the major biochemical and molecular model for studies of VDCCs (Catterall, 1995; Perez-Reyes and Schneider, 1995). Although the functional significance for their abundance in skeletal muscle remains to be established, it has been proposed that L-channels in skeletal muscle play dual roles. As voltage sensors, L-channels are primarily involved in E-C coupling, communicating the membrane depolarization to the SR triggering release of Ca^{2+} and ultimately muscle contraction by mechanisms that are independent of extracellular Ca^{2+} (Rios and Brum, 1987; Adams and Beam, 1990; Catterall, 1991; Rios and Pizarro, 1991). As functional VDCCs, DHP receptors mediate slow Ca^{2+} currents. This Ca^{2+} entry pathway serves to replenish cellular Ca^{2+} and to increase contractile force (Frank and Oz, 1992; Lamb 1992; Scuptoreanu *et al.*, 1993).

The anatomical inaccessibility of the T-tubule system to direct electrophysiological manipulation *in vivo* in adult skeletal muscle has limited our understanding of the functional roles of these proteins (Fosset *et al.*, 1983). On the other hand, isolated T-tubule vesicles provide a good *in vitro* model to study the properties of VDCCs in their native membrane environment (Hidalgo *et al.*, 1986; Dunn, 1989). However, traditional methods for purifying T-tubule vesicles by equilibrium sucrose density centrifugation is time-consuming (Curtis and Catterall, 1981; Hidalgo *et al.*, 1986; Dunn 1989). In the present study, an attempt has been made to isolate T-tubule membrane vesicles from crude microsomal membranes by a rapid velocity sedimentation method.

L-type channels are the targets for pharmacological agents that have been used successfully in the treatment of a variety of cardiovascular disorders (Tsien *et al.*, 1991). The pharmacology of L-type channels is complex and there is considerable interest, not

only in determining the molecular mechanism of action of these drugs, but also in identifying the molecular sites to which the drugs bind and regulate channel function (Catterall and Striessnig, 1992). There is a quantitative discrepancy between the high concentrations of DHPs required to affect functional properties and the much lower concentrations required to saturate the high affinity sites that are measured in radiolabelled ligand binding studies. This is not readily explained by the voltage-dependence of DHP binding in skeletal muscle (see Introduction). The finding that, in addition to high affinity sites, low affinity sites for DHP drugs also occur in skeletal muscle membranes, suggests that the effects of DHPs on channel function may be due to their binding to distinct low affinity sites. In the present study, the low affinity binding sites have been further identified and characterized by using another fluorescent DHP, amlodipine, and by monitoring changes in the intrinsic protein fluorescence that accompanies ligand binding.

With unique pharmacokinetic properties, amlodipine has been used successfully as a long-duration and once-daily dosage drug in the treatment of hypertension and angina pectoris (Burges, 1992). In contrast to most other DHP derivatives (e.g. PN200-110), amlodipine (pKa 8.7) is ionized (approximately 96%) under physiological conditions. This property makes it an unusual molecular probe for the study of ligand-receptor interactions (Kass and Arena, 1989; Burges, 1992). The pH-dependence of amlodipine binding to skeletal muscle membranes has been further analyzed and compared with that of PN200-110.

3. MATERIALS AND METHODS

3.1. Materials

Amlodipine maleate was a gift from Pfizer Ltd. (Sandwich, Kent) and nicardipine was provided by Syntex Pharmaceuticals (Mississauga, Ontario). Nimodipine was provided by Miles Laboratories, Inc. (Westhaven, CT) and the isomers of PN200-110 by Sandoz Canada Inc. (Dorval, Quebec). (±)Bay K8644 and (±)nitrendipine were from Research Biochemicals International. Nifedipine, diltiazem, verapamil, valinomycin, ruthenium red, digitonin, CHAPS, N-acetyl-D-glucosamine, lectin (WGA)-Sepharose, DEAE-Sephadex, Sephadex G-50-80 and egg phosphatidylcholine (PC) were purchased from Sigma Chemical Company. [^{3}H]-PN200-110 was from Dupont Canada. The anti-α_1 subunit antibody was obtained from Upstate Biotechnology Inc..

3.2. Methods

3.2.1. Preparation of Microsomal Membranes

Microsomal membranes were prepared from the back and hind leg muscles of 2-3 lb New Zealand White rabbits by methods described previously (Dunn, 1989). To prevent protein degradation, all procedures were carried out at 4°C and protease inhibitors [benzamidine, 0.1 mM; iodoacetamide, 1mM; leupeptin, 1 µg/ml; pepstatin A, 1µM; and phenylmethylsuphonyl fluoride (PMSF), 0.1 mM] were included in the homogenization and resuspension buffers. The muscles were cut into small pieces and homogenized in 4 volumes of homogenization buffer (20 mM Tris-HCl, pH 7.4, 0.3 M sucrose, 5 mM EDTA, 1 mM EGTA, 0.02% NaN_3) using five 20-sec bursts of a Waring blender at high speed. Following centrifugation for 20 min at 4,000 x g_{max}, the pellet was discarded and the supernatant was recentrifuged for 20 min at 10,500 x g_{max}. The supernatant was filtered through six layers of cheesecloth and solid KCl was added to a final concentration of 0.5 M to extract contractile fibers. The membrane preparation was mixed by stirring for 30 min at 4°C and then centrifuged for 45 min at 186,000 x g_{max}. The pellets were resuspended in

homogenization buffer with two 20-sec bursts of a Tempest Virtishear homogenizer at a setting of 3. The membranes were washed twice and were finally resuspended in 20 mM Tris-HCl pH 7.4 containing 15% (w/v) sucrose and 0.02% NaN_3 (resuspension buffer). The microsomal membranes were either used immediately or frozen in liquid nitrogen and stored at -80°C.

3.2.2. Preparation of T-tubule Membranes

3.2.2.1. Equilibrium Density Centrifugation Fractionation of T-tubule Membranes

T-tubule membranes were prepared from microsomal membranes by equilibrium discontinuous sucrose density gradient centrifugation by a modification of the method described by Dunn (1989). Sucrose gradients were formed by three 10 ml layers of 35%, 27.5%, and 25% (w/v) sucrose in 20 mM Tris-HCl, pH 7.4, 0.5 M KCl. Each gradient was overlaid with 6 ml microsomal membranes, preequilibrated in 20 mM Tris-HCl, pH 7.4, 0.5 M KCl, 15% (w/v) sucrose. Following centrifugation for 16 hrs in a Beckman SW28 rotor at 22,000 rpm, the floating layer was discarded and the T-tubule membranes were collected from the 15-25% (w/v) sucrose interface. The sucrose and KCl were diluted by the dropwise addition of Tris buffer (20 mM Tris-HCl, pH 7.4) to the membranes which were continuously stirred on ice. The diluted T-tubule membranes were collected by centrifugation at 186,000 x g_{max}, 4°C for 45 min. The membranes were washed once more by resuspension in the same buffer and centrifugation. The final pellet was resuspended in small volume (3-4 ml) of an appropriate buffer using two 20-sec bursts of the Tempest Virtishear homogenizer at a setting of 3 for further studies.

3.2.2.2. Velocity Sedimentation Fractionation of T-tubule Membranes

Preparation of T-tubule membranes by equilibrium density centrifugation is time-consuming. We have, therefore, developed an alternative method to isolate the T-tubule

membrane vesicles rapidly by velocity sedimentation. This technique allows separation of membrane fractions on the basis of their vesicle size rather than equilibrium density.

Microsomal membranes, prepared as above, were diluted 20 fold with velocity fractionation buffer (100 mM sodium phosphate, pH 7.4, 1 mM EDTA, 0.02% NaN_3) and were collected by centrifugation at 186,000 x g_{max} for 30 ~ 45 min. The pellets were resuspended in the same buffer at a protein concentration of 15-20 mg/ml. The suspension (0.2 ml per tube) was layered on linear sucrose gradients prepared in velocity fractionation buffer. The sucrose gradients were formed by the ordered addition of 0.5 ml of 54% (w/v) sucrose to the bottom of the Beckman Ultra-Clear centrifuge tubes (14 x 89 mm) which were precoated with polyvinyl alcohol (Grade 51-05, Dupont), 10.5 ml of 25-15% (w/v) linear sucrose gradient prepared using a Hoefer gradient maker, and an overlay of 1 ml of 2% (w/v) sucrose. The samples were centrifuged at 20,000 rpm in a Beckman SW41 rotor for various times (10-60 min). The floating layer was discarded, and fractions (30 drops) were collected from the bottom of the gradients using a Hoefer fractionator connected to a fraction collector. The efficiency of the isolation of T-tubule membranes from microsomal membranes was evaluated by the distribution of [^{3}H]-PN200-110 binding activity and the protein content in the fractions. In additional experiments, the effects of hypertonic salt (e.g. 0.5 M KCl) on membrane fractionation were examined. Fractions with high [^{3}H]-PN200-110 binding activity but low protein content were pooled, pelleted, washed once with 20 mM Tris-HCl pH 7.4, and finally resuspended in 20 mM Tris-HCl, pH 7.4, 1 mM $CaCl_2$, 0.02% NaN_3. The protein concentration was determined by Bio-Rad protein assay and the binding of [^{3}H]-PN200-110 was measured by a filtration binding assay (see below). Protein compositions of isolated membrane fractions were analyzed by sodium dodecylsulfate polyacrylamide gel electrophoresis (see below).

3.2.3. Purification and Reconstition of DHP Receptor Complex

3.2.3.1. Solubilization and Purification of DHP Receptor Complex

The DHP receptor complex was solubilized and purified from rabbit skeletal muscle by a modified version of the method of Florio *et al.* (1992). Digitonin was used for membrane solubilization. Since commercially available digitonin preparations contain variable amounts of non-water-soluble contaminants, all batches of detergent were first subjected to the following treatment. A 1.5% (w/v) digitonin suspension in distilled water was boiled for 5-10 min with constant stirring. After standing at room temperature for 48 h to permit the formation of a precipitate, the solution was filtered through a 0.22 µm sterile filter. The filtrate was lyophilized using a Virtis freeze-drier. As the pretreated digitonin still tends to form a slight precipitate after dissolving in buffers, all buffers containing digitonin were prepared immediately before use. All purification and reconstitution procedures were performed at 4°C. Microsomal membranes were solubilized in solubilization buffer (10 mM Tris-HCl, pH 7.4, 185 mM KCl, 0.02% NaN_3) containing 1% (w/v) digitonin and protease inhibitors (see above). The final detergent : protein ratio was 5:1 (w/w). After 30 min incubation on ice with gentle stirring, insoluble material was removed by centrifugation at 150,000 x g_{max} for 30 min. The solubilized protein was passed, at a flow rate of 1 ml/min, through a column containing 20 ml lectin-Sepharose pre-equilibrated in the same buffer. The column was then washed at a maximum flow rate (about 8 ml/min) with 10 bed volumes of buffer A [10 mM Tris-HCl, pH 7.4, 185 mM KCl, 0.1% (w/v) digitonin, 0.02% NaN_3) and then buffer B [10 mM Tris-HCl, pH 7.4, 20 mM NaCl, 0.1% (w/v) digitonin, 0.02% NaN_3]. Bound receptors were eluted with 5% (w/v) N-acetyl-D-glucosamine in buffer B at a flow rate of 0.3 ml/min and fractions of 1.2 ml were collected and assayed for [^{3}H]-PN200-110 binding using a polyethylene glycol precipitation (PEG) method (see below). Fractions with high binding activity were pooled and concentrated using Amicon Centricon-100 microconcentrators. The concentrated

lectin-Sepharose-eluate was either used directly in further experiments or was reconstituted into phospholipid vesicles. In some cases, the DHP receptor complex was further purified by DEAE-Sephadex chromatography. The pooled lectin-Sepharose-eluate was passed through a 1.5-2 ml DEAE-Sephadex column preequilibrated in buffer B at a flow rate of 0.5 ml/min. The resin was washed with 10 bed volumes of buffer B at maximum flow rate (8 ml/min). Bound protein was eluted by a 30 ml linear gradient of 20-300 mM NaCl in Buffer B at a flow rated of 0.5 ml/min. Eluted fractions were collected and fractions were assayed for [^{3}H]-PN200-110 binding activity using the PEG method.

The lectin-Sepharose column used for purification was always washed with large volumes of the solubilization buffer without digitonin and stored in the same buffer for further regeneration and reuse as the insoluble contaminants from digitonin irreversibly adhere to Sepharose beads and tend to reduce the purification efficiency and life-time of the column.

3.2.3.2. Reconstitution of DHP Receptor into Phospholipid Vesicles

The partially purified DHP receptor was reconstituted by a modification of the method of Curtis and Catterall (1986) using egg phosphatidylcholine. 100 mg of phosphatidylcholine was dissolved in 1 ml chloroform and was dried under a stream of nitrogen at room temperature and further dried *in vacuo* overnight. To prepare the lipid-detergent mixture, 150 mg of CHAPS, dissolved in 10 ml buffer C (10 mM Hepes-Tris, pH 7.4, 150 mM NaCl, 0.02% NaN_3) was added to the dried lipid and the mixture was sonicated to clarity under nitrogen. Aliquots of 2.2 ml of lipid-detergent solution were either used immediately for reconstitution or were stored at -20°C under nitrogen. For reconstitution, the concentrated lectin-Sepharose-eluate (0.8 ml; 40-400 pmol) was gently mixed with 2.2 ml of lipid-detergent solution, and immediately applied to a 1.5 x 90 cm column of Sephadex G-50-80. The column was eluted with buffer C at 0.5 ml/min. Fractions of 1 ml were collected and the fractions containing reconstituted vesicles, which eluted in the

void volume, were identified by their turbidity. The Sephadex G-50-80 column was previously equilibrated with lipid by applying 1 ml 20 mg/ml asolectin which was suspended by sonication in reconstitution buffer C. The column was washed with a large volume (about 1 L) of buffer C, and this procedure was repeated twice. An aliquot (2.2 ml) of a mixture of the above lipid-detergent solution plus 0.8 ml of 0.1% (w/v) digitonin was then applied to the column, which was then washed with a large volume of buffer C. After each use, the column was washed with large volume of buffer C.

For comparison with digitonin, CHAPS was employed for solubilizing and purifying the DHP receptor by lectin-Sepharose and DEAE-Sephadex chromatography. The procedures and solutions were the same as those described above using digitonin.

3.2.4. SDS-PAGE and Western Blotting

3.2.4.1. SDS-PAGE

Sodium dodecylsulfate polyacrylamide gel electrophoresis (SDS-PAGE) was performed by the method of Laemmli (1970) using 10% polyacrylamide gels under reducing conditions. Samples were dialyzed against ddH_2O overnight at 4°C and then lyophilized. Prior to electrophoresis, samples were dissolved in Laemmli sample buffer i.e. 60 mM Tris buffer, pH 6.8, 2% (w/v) SDS, 5% (v/v) β-mercaptoethanol and 10% (v/v) glycerol and boiled for 5 min. Electrophoresis was performed in electrophoresis buffer (192 mM glycine, 50 mM Tris base and 0.1% SDS) at a constant voltage of 100 V using either a Standard-Protein vertical electrophoresis cell (C.B.S. Scientific Co.) or a mini-gel apparatus (Mini-protean^R II Dual Slab Cell, Bio-Rad Laboratories) with power supply model 1420A (Bio-Rad Laboratories). Gels were stained with Coomassie blue (R-250, Bio-Rad) or kept for electroblotting and Western blot analysis.

3.2.4.2. Western Blot Analysis of DHP Receptor α_1 Subunit of Purified Proteins

In Western blot analysis, the α_1 subunit of the DHP receptor was detected by a specific anti-α_1 subunit monoclonal antibody (primary antibody) and peroxidase-labelled secondary antibodies, followed by visulizing with the chemiluminescent substrate luminol (BM Chemiluminescence Western Blotting Kit, Boehringer Mannheim). SDS-PAGE was performed using a 10% acrylamide gel in a mini-gel apparatus as described above. Electroblotting of proteins from the polyacrylamide gel to PVDF membranes was performed using the protocol of Towbin *et al.* (1979). Briefly, the gels were soaked in electrotransfer buffer [50 mM Tris-HCl, pH 8.3, 192 mM glycine, 20% (v/v) methanol] for 5 min. PVDF membranes of 0.2 μm pore size (Bio-Rad Laboratories) were prewetted in 100% (v/v) methanol for 1 min and were subsequently soaked in electrotransfer buffer for 5 min. Proteins were blotted onto pre-wetted PVDF membranes using a Mini-Trans-Blot Electrophoretic Transfer Cell (Bio-Rad Laboratories) under constant current of 300 mA for 30 min. Rainbow coloured protein molecular weight markers (Amersham, Life Science) were used to ensure the transfer of proteins from the gel to the PVDF membrane. After briefly washing the membrane twice with Tris buffered saline (TBS: 50 mM Tris-HCl, pH 7.5, 150 mM NaCl), excess binding sites on the membrane were blocked by incubation of the blots overnight at 4°C with a blocking solution consisting of TBS and 1% (w/v) blocking reagent (BM Chemiluminescence Western Blotting Kit, Boehringer Mannheim). The membrane was incubated with primary antibody (IgG), mouse-anti-rabbit DHP receptor α_1 subunit monoclonal antibody, 1:2,000 dilution in 0.5% blocking solution [TBS, 0.5% (w/v) blocking reagent] for an hour at room temperature with gentle shaking at 100 rpm. The membrane was washed twice for 10 min each at room temperature with 50 mM Tris-HCl, pH 7.5, 150 mM NaCl, and 0.1% (v/v) Tween-20 (TBST) and then washed twice with 0.5% blocking solution for 10 min each. After washing, the membrane was incubated with 40 mU/ml peroxidase-labelled secondary antibody (anti-mouse

polyclonal antibody, BM Chemiluminescence Western Blotting Kit, Boehringer Mannheim) in 0.5% blocking solution for 30 min at room temperature with gentle shaking. The membrane was then washed four times with large volumes of TBST for 15 min each. Antibody binding was visualized by chemiluminescent detection. Following a brief incubation with the premixed detection reagent (substrate solution A : starting solution B, 100:1, BM Chemiluminescence Western Blotting Kit, Boehringer Mannheim) for 60 s, the excess detection reagent was drained and the membrane was placed between two transparent films. Then the membrane/transparent film sandwich with the protein side up was inserted into a film cassette and covered by a sheet of film (Hyperfilm-ECL, Amersham) in a dark room. Following exposure for 10 to 60 s, the film was developed using a Kodak X-DMAT M35 Processor.

3.2.5. Binding Assays

3.2.5.1. Equilibrium Binding of [^{3}H]-PN200-110 to Membrane Bound DHP Receptors

Measurements of the binding of [^{3}H]-PN200-110 to microsomal membranes and transverse tubule membranes were carried out by filtration assays using a Hoefer manifold filtration apparatus. To minimize ligand photolysis, all experiments were performed in a dim light. Aliquots of membranes (200 µl) were added to different concentrations of [^{3}H]-PN200-110 to give a final protein concentration of 0.075 mg/ml (microsomal membranes) or 0.02 mg/ml (T-tubule membranes) in a total volume of 400 µl in binding assay buffer A (25 mM Hepes-Tris pH 7.4, 1 mM $CaCl_2$ and 0.02% NaN_3). Following 60 min incubation at room temperature, 200 µl aliquots of each sample were rapidly filtered under vacuum through Whatman GF/C glass microfibre filters presoaked in ice cold assay buffer A. The filters were immediately washed with two 4 ml volumes of ice cold assay buffer A. After drying, the filters were extracted in 5 ml of ACS (Amersham, Canada) scintillation

cocktail and counted for [^{3}H] using a Beckman LS6500 Scintillation System. Duplicate 50 µl aliquots of the incubation mixture were counted directly for estimating the total ligand concentration. Non-specific binding of radiolabelled ligand was estimated from parallel measurements of binding in the presence of 1 µM of the unlabelled DHP, nitrendipine.

In order to establish the [^{3}H]-PN200-110 binding profiles of sucrose gradients resulting from velocity sedimentation, fractions from the sucrose gradients were assayed for binding activity by incubation of 50 µl of each fraction with 1 nM of [^{3}H]-PN200-110 in the presence or absence of 1 µM nitrendipine in the binding assay buffer (final volume = 250 µl). Following 60 min incubation at room temperature, 200 µl aliquots of each sample were filtered. After immediate washing with ice-cold assay buffer as described above, the filters were dried and the ligand-receptor complexes were extracted in 5 ml of ACS and counted for [^{3}H]. Non-specific binding was subtracted from the total binding.

3.2.5.2. Equilibrium Binding of [^{3}H]-PN200-110 to Purified DHP Receptor Complex

The binding of [^{3}H]-PN200-110 to the purified DHP receptor complex was measured by the polyethylene glycol precipitation method of Striessnig and Glossmann (1991). Aliquots of 100 µl protein sample were incubated with 1-15 nM of [^{3}H]-PN200-110 for 90 min at room temperature in a final volume of 250 µl in binding assay buffer B [20 mM Tris-HCl, pH 7.4, 20 mM NaCl, 0.01% (w/v) digitonin] containing 0.2 mg/ml bovine serum albumin (BSA). Nonspecific binding was defined in the presence of 5 µM nitrendipine. The incubation mixtures were transferred to an ice bath and 0.1 ml of ice-cold carrier solution (20 mM Tris-HCl, pH 7.4, 5 mg/ml BSA, 5 mg/ml γ-globulin) followed by 3.5 ml of PEG buffer [20 mM Tris-HCl, pH 7.4, 10% (w/v) polyethylene glycol 8000, 10 mM $MgCl_2$) was added. After 3 min incubation, bound and free ligand were separated by rapid filtration through Whatman GF/C filters pre-equilibrated in PEG buffer. Following

two rapid washes with 4 ml of PEG buffer and drying of the filters, the radioactivity was measured as described above.

In purification studies, eluted fractions from both lectin-Sepharose and DEAE-Sepharose columns were assayed for [^{3}H]-PN200-110 binding. Briefly, aliquots of 50 µl of fractions were incubated with 3 nM of [^{3}H]-PN200-110 in the presence or absence of 5 µM nitrendipine in binding assay buffer B (final volume = 250 µl). Again, the polyethylene glycol precipitation method described above was used in the binding assay.

3.2.5.3. Measurements of the Kinetics of [^{3}H]-PN200-110 Dissociation from the Purified DHP Receptor Complex

In these experiments, 8 nM [^{3}H]-PN200-110 was first incubated with the lectin-Sepharose-eluate in binding assay buffer B for 90 min at room temperature. Dissociation was initiated by either a 20-fold dilution of the preformed protein-[^{3}H]-PN200-110 complex into buffer alone or into buffer containing either nitrendipine or amlodipine at final concentrations of 1-30 µM. Aliquots of 10 ml of samples were filtered at the appropriate times and, after washing, the filters were counted for radioactivity as described in 3.2.5.1. Prior to use, the Whatman GF/C filters were soaked in 0.05% (v/v) polyethylenimine (Sigma) solution to reduce nonspecific binding of [^{3}H]-PN200-110 to the filters.

3.2.6. Fluorescence Experiments

Equilibrium fluorescence measurements were made using a Perkin Elmer MPF4 fluorimeter fitted with a magnetically stirred and thermostatted cuvette holder. All measurements were made at 25°C and the samples were continuously stirred during measurements. For membrane-bound receptor preparations (including transverse tubule membranes and reconstituted DHP receptor in phosphatidylcholine vesicles), the binding assay buffer contained 20 mM Tris-HCl, pH 7.4, 150 mM NaCl, 0.02% NaN_3. The

buffer for solubilized and purified receptor preparations was 10 mM Hepes-Tris, pH 7.4, 20 mM NaCl, 0.02% NaN_3 and 0.1% (w/v) digitonin. In amlodipine titration experiments, 2 ml of transverse tubule membranes (5 μg/ml) were equilibrated in quartz cuvettes. Aliquots of 1 μl of concentrated amlodipine solutions in the appropriate binding assay buffer were added and the fluorescence was immediately recorded using an emission wavelength of 450 nm and an emission slit width of 16 nm. The excitation wavelength was either 375 nm (direct excitation) or 290 nm (energy transfer from membrane proteins) and the excitation slit width was 4 nm. Data were corrected for the fluorescence of free amlodipine by using the results of parallel titrations of buffer alone. In competition binding assays, 2 ml of transverse tubule membranes (5 μg/ml) were preincubated with 5 μM amlodipine for 15 min prior to the addition of 1 μl aliquots of concentrated DHP stock solutions in anhydrous Me_2SO (Aldrich Chemical Company). Data were corrected by the fluorescence of control samples in which 5 μM amlodipine was titrated with DHPs in the absence of transverse tubule membranes. The final concentration of Me_2SO did not exceed 1% (v/v).

When the quench of protein intrinsic fluorescence was monitored for measurement of binding of DHPs to their receptors, 2 ml of each preparation in the appropriate buffer was similarly preequilibrated in quartz cuvettes. Aliquots of 1 μl of amlodipine or other DHP stock solutions were added and the fluorescence was immediately recorded using an emission wavelength of 325 nm at a slit width of 16 nm and an excitation wavelength of 290 nm at a slit width of 4 nm. The results were corrected for non-specific effects by parallel titrations of a standard tryptophan solution, which was diluted to give approximately the same initial fluorescence as the membranes or the purified receptor preparation.

3.2.7. Effects of pH on the Binding of [^{3}H]-PN200-110 and Amlodipine to Skeletal Muscle Membranes

A buffer system that is useful over a wide pH range while maintaining constant ionic strength has been used as the binding assay buffer for these studies (Ellis and Morrison, 1982). The buffers contained 50 mM Tris base, 25 mM MES (Sigma), 25 mM sodium acetate (Sigma), and 100 mM NaCl. The pH was adjusted to the appropriate values with either 1 N HCl or 1 N NaOH. Dilutions of both [^{3}H]-PN200-110 and amlodipine were freshly made using buffers at the appropriate pH. The pH-dependence of [^{3}H]-PN200-110 binding to microsomal membranes was measured using the method described in 3.2.5.1..

Competition experiments were used to study the pH-dependence of amlodipine binding to the high affinity binding sites. Variable concentrations (1 nM to 30 μM) of amlodipine in buffers at the appropriate pH were added to 400 μl samples containing 1.5 nM [^{3}H]-PN200-110 and 50 μg/ml microsomal membrane proteins. Samples without added amlodipine were used as controls. Non-specific binding was measured in the presence of 1 μM nitrendipine. Subsequent experimental protocols were as described in 3.2.5.1..

Quench of intrinsic protein fluorescence was used in studies of the pH-dependence of amlodipine binding to the low affinity sites. The detailed procedures are described in 3.2.6..

3.2.8. [$^{45}Ca^{2+}$] Flux Assays

The biochemical properties of T-tubule membranes have been extensively studied in this and other laboratories (Rosemblatt *et al.*, 1981; Hidalgo *et al.*, 1986; Dunn, 1989). More than 90% of the purified transverse tubule membranes prepared from rabbit skeletal muscle have been shown to be sealed in an inside-out orientation, i.e. the surface that is

normally intracellular is exposed extravesicularly. Furthermore, their membrane potential can be manipulated experimentally (Dunn, 1989). Study of the functional responses of VDCCs in the isolated T-tubule vesicles of rabbit skeletal muscle was originally performed using manual filtration techniques, in which the membranes were usually depolarized for 20 sec (Dunn, 1989). More recently, a rapid filtration device has been applied to measure voltage-dependent [$^{45}Ca^{2+}$] flux response on physiologically relevant time scales (Bhat, 1993). In the present study, this system has been further examined.

Because of the inside-out orientation of the sealed T-tubule membrane vesicles, depolarization activated Ca^{2+} flux through the membrane-bound VDCCs was measured by monitoring efflux of [$^{45}Ca^{2+}$] from preloaded vesicles, i.e. in a direction corresponding to the normal influx of Ca^{2+} into the intact cell.

3.2.8.1. Equilibration of T-tubule Membranes in Low Potassium Buffer

To equilibrate the T-tubule membranes in low potassium buffer (10 mM Hepes-Tris, pH 7.4, 145 mM choline chloride, 5 mM potassium gluconate), the membranes were diluted in a large volume of this buffer and washed at least twice by centrifugation and resuspension. Following final suspension in a small volume (3-4 ml) of the same buffer, the membranes were frozen in liquid nitrogen and slowly thawed in a melting ice bath in the cold room (4°C). These procedures have been shown to be sufficient to equilibrate intra- and extravesicular ions (Dunn, 1989). The membranes were frozen in liquid nitrogen and stored at -86°C for use.

3.2.8.2. Loading of Membrane Vesicles with [$^{45}Ca^{2+}$]

The T-tubule membrane vesicles preequilibrated in the low potassium buffer were loaded with [$^{45}Ca^{2+}$] by the addition of one-third volume of isosmatically diluted $CaCl_2$ in the same buffer to give a final total $CaCl_2$ concentration of 5 mM and 50 μCi/ml [$^{45}Ca^{2+}$]. The final membrane protein concentration was about 0.3 mg/ml. The mixture was subject

to two cycles of rapid freezing in liquid nitrogen and slow thawing at 4°C (see above). The [$^{45}Ca^{2+}$] loaded vesicles were kept on ice before use.

3.2.8.3. Repolarization of the T-tubule Membranes

Aliquots of 25 µl of [$^{45}Ca^{2+}$] loaded T-tubule membrane vesicles were diluted with 975 µl of repolarization (high K^+) buffer (10 mM Hepes-Tris, pH 7.4, 150 mM potassium gluconate, 0.166 mM EGTA, 0.1 µM valinomycin) with or without 10 µM ruthenium red. According to the Nernst equilibrium potential for K^+, this dilution into high K^+ buffer generates an estimated extravesicular membrane potential of -86 mV. EGTA included in this solution reduced the extravesicular i.e. corresponding to intracellular Ca^{2+} concentrations to less than 0.1 µM. The use of the K^+ ionophore, valinomycin has been shown to facilitate the development of K^+ gradients across the vesicle membranes (Dunn, 1989). Ruthenium red was used to block Ca^{2+} flux through any contaminating SR membrane vesicles. The repolarization process was allowed to proceed for 5 min. This and the following steps were performed at room temperature. For controls, the repolarization buffer was replaced by the low potassium buffer.

3.2.8.4. Depolarization of T-tubule Membranes and Measurement of [$^{45}Ca^{2+}$] Efflux by Rapid Filtration

Depolarization of T-tubule membranes was established by removing the high K^+ buffer from the extravesicular space followed by washing with depolarizing buffer (10 mM Hepes-Tris, pH 7.4, 5 mM potassium gluconate, 145 mM choline chloride, 0.166 µM EGTA, 0.1 µM valinomycin) for a predetermined time period. According to the Nernst equation, under these conditions the membrane potential will reach about 0 mV. In order to depolarize T-tubule membranes on physiologically relevant time scales, a Biologic rapid filtration device (Biologic, Meykan, France) was used.

After a 5-min incubation at room temperature, aliquots of 0.9 ml of the above membrane vesicle samples were pipetted onto a Whatman GF/C filter which had been preequilibrated in the same repolarization buffer and mounted in the filter holder of the Biologic rapid filtration device. Extravesicular buffer was removed under vacuum, and [$^{45}Ca^{2+}$] efflux was immediately initiated by forced filtration of the filter with appropriate volume of depolarizing low K^+ buffer containing or without the same concentrations of ruthenium red in the filtration syringe. The flux was allowed to proceed for the appropriate time period from 30 msec to 9 sec for both the time-dependence of [$^{45}Ca^{2+}$] flux assay and the effect of ruthenium red on [$^{45}Ca^{2+}$] flux assay. The filters were then dried, extracted with 5 ml of ACS scintillation cocktail and counted for residual [$^{45}Ca^{2+}$] radioactivity.

Samples at all time points were performed in quintuplicate.

3.2.8.5. Nernst Equation for Calculation of Membrane Potential

The values of the membrane potentials indicated in above experiments were predicted from the Nernst equation for the K^+ equilibrium potential at 25°C using the concentrations of K^+ contained in the intra- and extravesicular buffers.

$$E_m = E_k \approx -58\log[K_o/K_i]$$

where K_o = extravesicular concentration

and K_i = intravesicular concentration

All values of membrane potentials given below refer to those in cells with normal orientation i.e. an intracellular membrane potential and, in the inside-out T-tubule membrane vesicles, an extravesicular membrane potential.

3.2.9. Protein Assay

Protein concentrations were estimated using the Bio-Rad Protein Assay (Bio-Rad Laboratories) with bovine serum albumin (BSA) as a protein standard. Dilutions of

samples or 0.1 mg/ml BSA in ddH_2O were prepared in a final volume of 800 µl containing approximately 0-15 µg protein. Bio-Rad reagent (200 µl) was added to each sample. After mixing and incubation in room temperature for 5 min, the absorbance at wavelength of 595 nm (A_{595}) was measured using a Beckman DU-40 spectrophotometer. To establish the protein profiles either for sucrose gradient fractions on velocity centrifugation or for WGA-Sephadex-eluate and DEAE-Sepharose-eluate fractions, aliquots of 50 µl of each fractions were mixed with 750 µl of ddH_2O and 200 µl of Bio-Rad reagent, and the A_{595} was determined.

3.2.10. Data Analysis

All data were analyzed using the Inplot 4 program (GraphPad Software, San Diego, CA). Equilibrium [^{3}H]-PN200-110 binding data were represented as Scatchard plots or a simple binding isotherm i.e. bound = $R_o[L]/(K_d+[L])$, where R_o is the concentration of binding sites and [L] is the ligand concentration. The equation of the competition curve, $Y = \text{bottom}+(\text{top}-\text{bottom})/(1+10^{(\log X-\log EC50)})$, was used for amlodipine competitive binding assays, in which top is the maximum [^{3}H]-PN200-110 binding activity when no displacement by amlodipine occurs, bottom is the binding activity when maximum displacement by amlodipine occurs, EC50 is the amlodipine concentration when 50% of bound radioligand is displaced, X is the concentrations of amlodipine and Y is the measured binding activity. A single exponential decay equation was used for the dissociation binding assay, i.e. $Y = A*\exp(-B*X)+E$, where X is dissociation time, Y is percentage of original binding activity, A is total amplitude of the dissociation reaction, B is the apparent rate of dissociation, and E is the background.

Amlodipine titration data were fit by the equation, $Fl = F_{max}[L]/(K_d+[L])$, where Fl is the observed fluorescence, F_{max} is the maximum fluorescence enhancement, and [L] is amlodipine concentration. Protein quenching data were fit by the similar equation, $Fl\% = 100\%-Q_{max}[L]/(K_d+[L])$, where Fl% is the fluorescence expressed as a percentage of the

original protein fluorescence and Q_{max} is the maximum fluorescence quench (%). Fluorescence competition curves were fit by a simple non-cooperative model.

4. RESULTS AND DISCUSSIONS

4.1. Using Velocity Sedimentation to Isolate T-tubule Membranes from Microsomal Membranes of Rabbit Skeletal Muscle

4.1.1. Results:

DHP-sensitive Ca^{2+} channels are enriched in rabbit skeletal muscle T-tubule membranes which are preferred for both biochemical and functional studies of the Ca^{2+} channels in the native membrane-bound state (Affolter and Coronado, 1985; Curtis and Catterall, 1985; Dunn, 1989). The traditional method for preparing partially purified T-tubule membranes is isopycnic centrifugation; that is, the isolation of transverse tubule membrane vesicles from microsomal vesicles on the basis of their equilibrium density in a discontinuous sucrose gradient (Hidalgo *et al.*, 1986; Dunn, 1989). It is usually necessary to centrifuge overnight to reach equilibrium. Thus, it is time-consuming and there is a high risk of protein denaturation due to the lengthy procedures involved. On the other hand, velocity sedimentation on sucrose gradients has been successfully utilized to quickly fractionate *Torpedo* post-synaptic membranes (Jeng *et al.*, 1981). Such a technique provides an alternative method to rapidly isolate a membrane population that appears to be homogenous in size.

4.4.1.1. The Effects of Various Factors on the Isolation of T-Tubule Vesicles by Velocity Sedimentation

The sucrose gradient and the centrifugation time are the most important parameters to optimize for isolation of membrane populations by velocity sedimentation. In this study, we mainly investigated the effect of the velocity sedimentation time on the isolation of T-tubular vesicles from SR vesicles. A continuous sucrose gradient [15-25% (w/v)] was used. The isolation efficacy was evaluated by the distribution of the [^{3}H]-PN200-110 binding peak (cpm) and the protein peak (A_{595}). The greater the separation between the

binding peak and the protein peak, the better the separation of T-tubule vesicles from contaminating SR vesicles.

It was found that crude microsomal membrane preparations could be fractionated efficiently after centrifugation for 30 min at 20,000 rpm in an SW41 rotor (Figure 2B). The T-tubule membranes were separated into two populations represented by two [^{3}H]-PN200-110 binding peaks. One co-sedimented with SR membranes and was recovered as a dense layer on the 55% sucrose cushion with an overlap between the binding peak and the protein peak. The other was recovered at a sucrose density of about 19-20% (w/v) with high [^{3}H]-PN200-110 binding activity but with low membrane protein content (Fraction 8 and 9 in Figure 2B). As T-tubule membranes account for only a small population in the microsomal membrane preparation (Almers, 1989), these fractions were considered to represent the partially purified T-tubule membranes. Separation was much less efficient using 10 min or 60 min centrifugation. After 10 min centrifugation, the binding peak overlapped with the protein peak at the top of the gradient (Figure 2A) and after 1 hr centrifugation, all the T-tubule membranes were sedimented to the 55% (w/v) sucrose cushion (Figure 2C). As in the case of 15-25% (w/v) linear sucrose gradient, a brief centrifugation (10 min) at the same force (20,000 rpm in a SW41 rotor) on an 8-20% (w/v) linear sucrose gradient failed to separate the T-tubule vesicles from the SR vesicles (Figure 3).

In a study of the possible effect of hypertonic salt (0.6 M KCl) on the isolation of T-tubule vesicles, we found that two [^{3}H]-PN200-110 binding peaks almost overlapped with protein peaks after 30 min centrifugation at 20,000 rpm in an SW41 rotor on a 15-25% (w/v) sucrose gradient (Figure 4A). This profile was maintained even though the spin time was increased to 60 min. (Figure 4B). This suggested that 0.6 M KCl could not improve the isolation efficiency, at least using centrifugation times of 30-60 min.

4.1.1.2. Equilibrium Binding of [^{3}H]-PN200-110 to T-tubule Membranes Isolated by Velocity Sedimentation

The high-affinity binding of [^{3}H]-PN200-110 to T-tubule membranes that had been isolated by velocity sedimentation (Fraction 8 and 9 in Figure 2B) was determined using filtration assays. Scatchard plot analysis indicated that [^{3}H]-PN200-110 specifically binds to a single class of binding sites with K_d of 0.41 nM and a binding density of 55.1 pmol/mg protein (Figure 5B). Isolation of T-tubule membranes from microsomal membranes by velocity sedimentation resulted in an almost a 20-fold increase in the binding density when compared to the crude microsomal membranes (Figure 5A). The resulting enrichment of DHP receptor in this preparation is similar to that found by the traditional equilibrium centrifugation method (Figure 5C).

4.1.1.3. SDS-PAGE Patterns

The partially purified T-tubule membranes prepared by velocity sedimentation was further examined by SDS-PAGE analysis. The main protein bands in the preparation had apparent molecular weights (MW) of 175 kDa, 140 kDa, 100 kDa, 62 kDa and there were several bands from 50 kDa to 30 kDa (lane A in Figure 6). The protein with MW of 175 kDa is a candidate for the α_1 subunit of DHP receptors. The main contamination is the 100 kDa band, likely to be the Ca^{2+}-ATPase from SR (Almers, 1989; Striessnig and Glossmann, 1991). The SDS-PAGE patterns for T-tubule membranes prepared by the different methods are similar (lane A and B in Figure 6).

Comparison of this velocity sedimentation separation with equilibrium density centrifugation system is shown in Table 2.

4.1.2. Discussion:

T-tubules, which are enriched in L-type Ca^{2+} channels or DHP-binding proteins, are delicate invaginations of the sarcolemma membranes (Almers, 1989). They lie deeply within the muscle fiber and are in close contact with the terminal cisternae of the sarcoplasmic reticulum forming a triad-structure (Almers, 1989). T-tubule membranes are 10 times less abundant than SR and occupy only 1% of the skeletal muscle fiber volume (Almers, 1989). Because of structural association between T-tubule and SR membranes and the relatively low content of T-tubule membranes compared to SR membranes, the isolation of T-tubule membranes is quite difficult.

Isolated T-tubule membrane vesicles have been extensively studied and have been shown to be a good model system for studying Ca^{2+} channels in their native membrane-bound state. The successful development of an *in vitro* model for studying VDCCs in their native membrane environment is largely dependent on having a highly purified membrane preparation that is devoid of SR contamination. However, DHP-binding proteins are labile and are susceptible to degradation by proteolytic enzymes present in the membrane preparation mixtures even though they were kept at 0-4°C and were protected by the presence of enzyme inhibitors (Striessnig and Glossmann, 1991). It has been reported that the degradation of DHP-binding proteins is both time-dependent and temperature-dependent (Striessnig and Glossmann, 1991). The longer the preparative procedures, the more likely the DHP-binding proteins will be degraded. The time of T-tubule membrane isolation is, therefore, a key factor for maintaining protein integrity.

By using velocity sedimentation, we have developed a method for isolating T-tubule membrane vesicles from microsomal membranes of rabbit skeletal muscle which is fast, simple and has the same isolation efficiency as traditional procedures (Table 3).

T-tubule membrane vesicles are less dense and smaller than sarcoplasmic membrane vesicles in skeletal muscle microsomal membrane preparation (Lau, 1977; Hidalgo *et al.*, 1986). The different densities of T-tubule vesicles and SR vesicles has been used to fractionate T-tubule membrane by equilibrium centrifugation. The disadvantage of established techniques is the long time that is required to reach equilibrium (16 hours). The mechanism of velocity sedimentation on sucrose gradients depends upon homogenous membrane vesicle size rather than their equilibrium density (Jeng *et al.*, 1981). It only took 30 min to separate T-tubule membrane vesicles from microsomal membrane preparations (Figure 2). As estimated by protein recovery rates, SDS-PAGE analysis and [^{3}H]-PN200-110 binding assays, velocity centrifugation and equilibrium centrifugation are about equally efficient. In each case, binding sites for [^{3}H]-PN200-110 were enriched by about 20-fold over the crude membranes.

It has been previously reported that hypertonic salt (0.6 M KCl) treatment may cause breakage of the triad junction and help to isolate T-tubule membranes from microsomal membranes of skeletal muscle more efficiently (Cadwell and Caswell, 1982). In the present series of experiments, the effects of 0.6 M KCl on isolation of T-tubule membranes were investigated. This was found to have no beneficial effect on isolation efficiency. These results agree with the suggestion that the triads are composite mixtures of breakage-susceptible (weak) and breakage-resistant (strong) triads (Kim *et al.*, 1990) The former is easily disrupted (dissociated) in microsomal membrane preparations by chemical treatment (0.5 M KCl to extract contractile fibers) or by mechanical treatment (homogenization). The latter is resistant to these treatments.

Figure 2. Effect of centrifugation time on the isolation of T-tubule membranes from microsomal membranes by velocity sedimentation. Linear sucrose gradients of 15-25% (w/v) were applied. The distribution of [^{3}H]-PN200-110 binding activity (cpm: ●···●) and protein (A_{595}: O---O) of fractionated the microsomal membrane components after 10 min, 30 min, and 60 min centrifugation at 20,000 rpm in a Beckman SW41 rotor are shown in A, B, and C, respectively. From fraction 1 to 14, the sucrose concentration decreased from 25% to 15%.

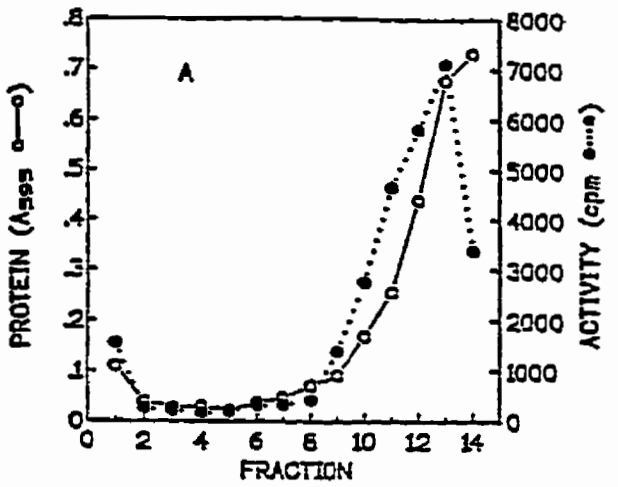
A
PROTEIN (A595 o—o)
ACTIVITY (cpm •···•)
FRACTION
0
1
2
3
4
5
6
7
8
1000
2000
3000
4000
5000
6000
7000
8000
0
2
4
6
8
10
12
14

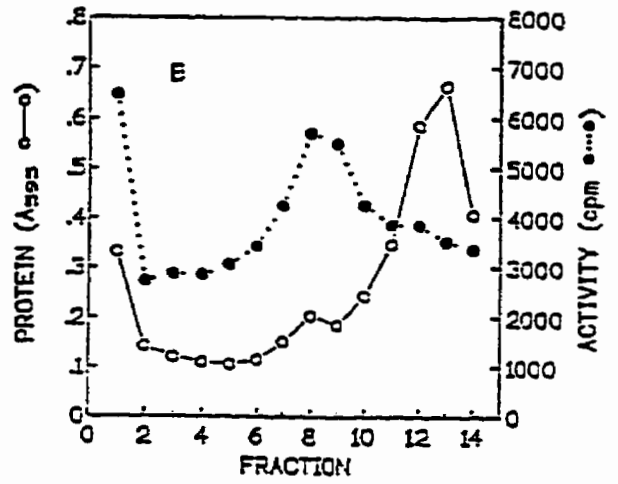
B
PROTEIN (A595 o—o)
ACTIVITY (cpm •···•)
FRACTION
0
1
2
3
4
5
6
7
8
1000
2000
3000
4000
5000
6000
7000
8000
0
2
4
6
8
10
12
14

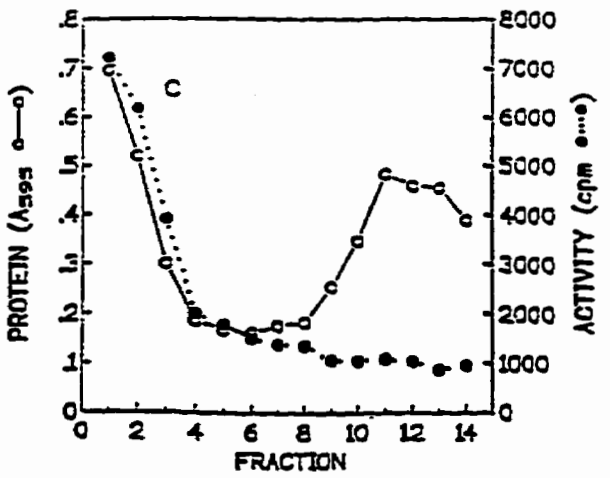
C
PROTEIN (A595 o—o)
ACTIVITY (cpm •···•)
FRACTION
0
1
2
3
4
5
6
7
8
1000
2000
3000
4000
5000
6000
7000
8000
0
2
4
6
8
10
12
14

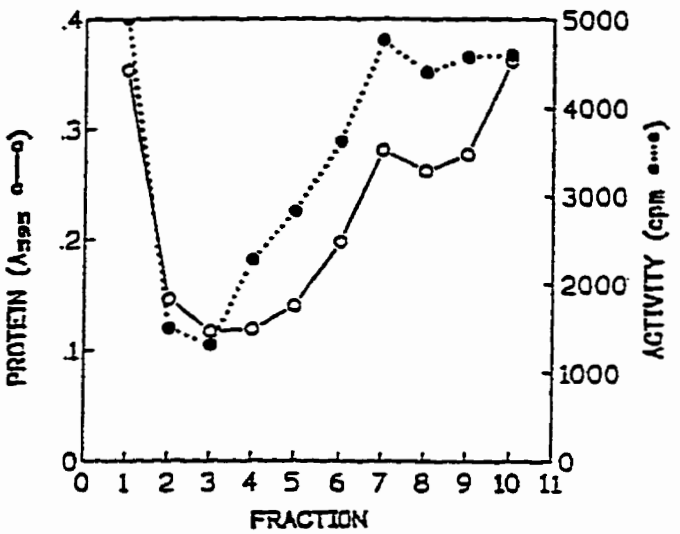

Figure 3. Effect of sucrose gradient on the isolation of T-tubule membranes from microsomal membranes by velocity sedimentation. The [^{3}H]-PN200-110 binding profile (cpm: ●···●) and protein profile (A_{595}: O—O) resulted from 10-min brief centrifugation on 8-20% (w/v) linear sucrose gradients at 20,000 rpm in a Beckman SW41 rotor. From fraction 1 to 10, the sucrose concentrations decreased from 20% to 8%.

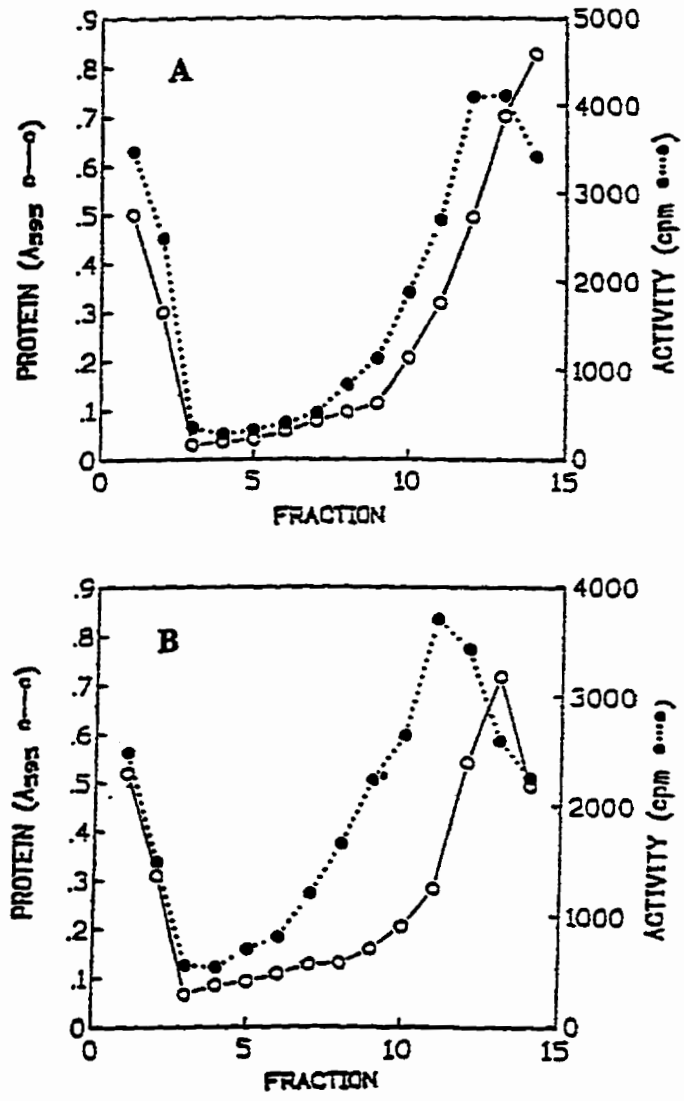

Figure 4. Effect of 0.6 M KCl on the isolation of T-tubule membranes from microsomal membranes by velocity sedimentation. The crude microsomal membranes were pre-incubated in the velocity fractionation buffer containing 0.6 M KCl and the intravesicular medium was equilibrated by a freeze-thaw cycle. The established linear sucrose gradients [15-25% (w/v)] also contained 0.6 M KCl. [^{3}H]-PN200-110 binding profile (cpm: ●···●) and protein profile (A_{595}: O—O) after 10 min and 60 min centrifugation at 20,000 rpm in a Beckman SW41 rotor are shown in Figure A and B, respectively. From fraction 1 to 15, the sucrose concentrations decreased from 25% to 15%.

Figure 5. Representative Scatchard plot analysis of [^{3}H]-PN200-110 binding to microsomal membranes and T-tubule membranes of skeletal muscle. The binding assay was determined by the equilibrium filtration method. The estimated K_ds and B_{max}s were 0.31 nM and 2.9 pmol/mg for microsomal membranes (A), 0.41 nM and 55.1 pmol/mg for the T-tubule membranes purified by velocity sedimentation (B), and 0.92 nM and 56.0 pmol/mg for the T-tubule membranes purified by equilibrium centrifugation (C). Solid lines are linear regression fits of the data. The T-tubule membranes prepared by two different methods resulted in the same extent of enrichment in high affinity [^{3}H]-PN200-110 binding sites. The difference in K_d values listed above was not significant. These results are representative of three individual experiments.

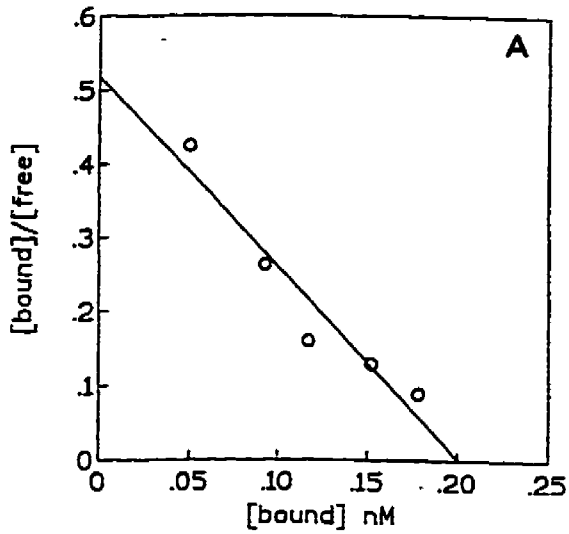
A
[bound]/[free]
.6
.5
.4
.3
.2
.1
0
0
.05
.10
.15
.20
.25
[bound] nM

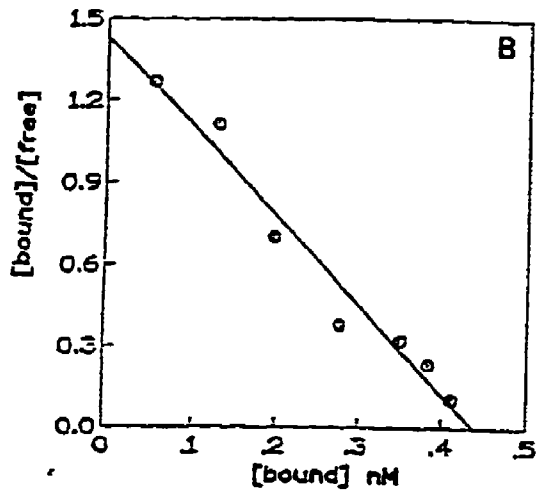
B
[bound]/[free]
1.5
1.2
0.9
0.6
0.3
0.0
0
.1
.2
.3
.4
.5
[bound] nM

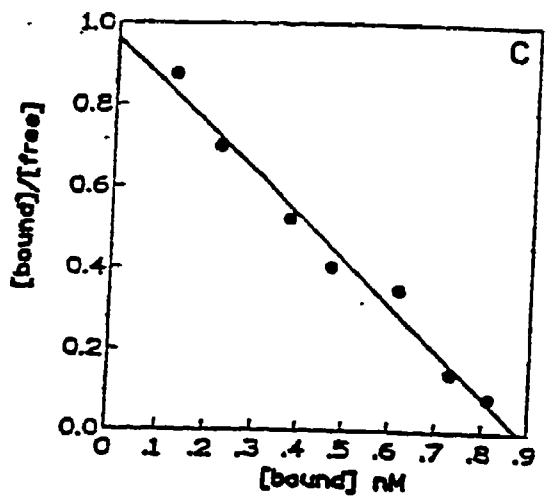
C
[bound]/[free]
1.0
0.8
0.6
0.4
0.2
0.0
0
.1
.2
.3
.4
.5
.6
.7
.8
.9
[bound] nM

Figure 6. SDS-PAGE analysis of skeletal muscle microsomal membranes and the isolated T-tubule membranes. Lane A and lane B both contained 20 μg of T-tubule membrane proteins isolated by either velocity sedimentation (A) or by equilibrium centrifugation (B). Lane C contained 40 μg of microsomal membrane proteins and lane D is molecular weight standards. Electrophoresis was carried out in a 10% polyacrylaminde gel using a Standard-Protein vertical electrophoresis cell at 100 V constant voltage. The gel was stained with Coomassie blue.

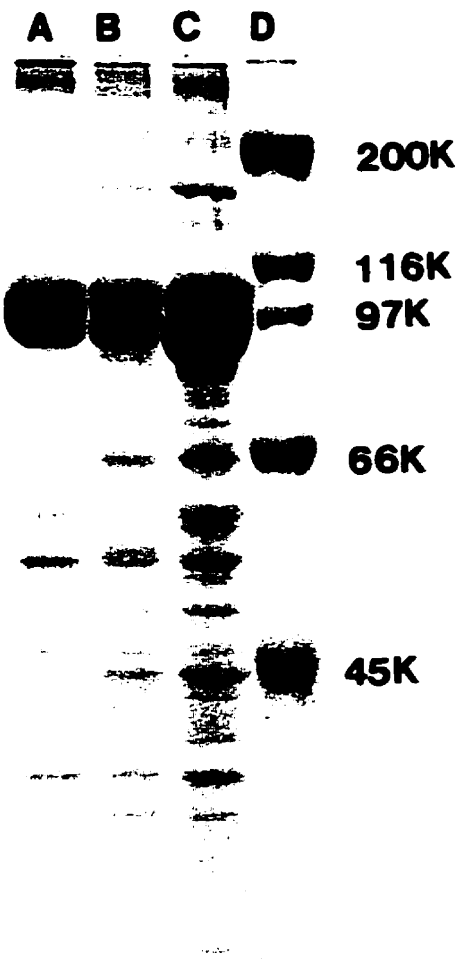
A
B
C
D
200K
116K
97K
66K
45K

Table 2.

Comparison of the Properties of T-tubule Membranes Purified by Velocity Sedimentation or Equilibrium Density Centrifugation

	velocity sedimentation centrifugation	**equilibrium density centrifugation**
separation basis	vesicle size	vesicle density
sucrose gradient	continuous (15-25%)	discontinuous
centrifugation time	30 min	overnight
T-tubule vesicle recovery	19-20% gradient	15%-25% interface
protein recovery	similar (1%)	similar (1%)
SDS-PAGE pattern	similar	similar
[^{3}H]-PN200-110 binding assay (B_{max})	55.1 pmol/mg	56.0 pmol/mg

4.2. Characterization and Identification of Low Affinity DHP-Binding Sites in Skeletal Muscle Membranes

4.2.1. Results:

4.2.1.1. Purification and Reconstitution of DHP Receptor

4.2.1.1.1. [^{3}H]-PN200-110 Binding Characteristics of the Purified and Reconstituted DHP Receptor Complex

The DHP receptor from rabbit skeletal muscle was purified by solubilization with digitonin and sequential chromatography on lectin-Sepharose and DEAE-Sephadex. The binding of [^{3}H]-PN200-110 to the solubilized proteins was measured by the PEG precipitation method. Table 3 shows the DHP binding affinity (K_d) and binding density (B_{max}) of preparations of native microsomal membranes, crude digitonin extract, lectin-Sepharose-eluate and after reconstitution of this extract into PC vesicles. The binding affinity of DHP receptor after solubilization with 1% (w/v) digitonin (K_d=1.21 ± 0.04 nM, n=2) was reduced when compared to that of membrane-bound receptor (K_d=0.40 ± 0.02 nM, n=3), and it was further decreased after purification by lectin-Sepharose chromatography (K_d=6.78 ± 0.45 nM, n=3). This reduction in binding affinity could not be restored by reconstitution into PC vesicles (K_d=15.38 ± 0.74 nM, n=3). On the other hand, a single purification step on lectin-Sepharose chromatography resulted in a reasonable enhancement of specific activity with a B_{max} of 88 pmol/mg protein as compared to a B_{max} of 3.0 pmol/mg protein in the crude digitonin extract. DEAE-Sephadex chromatography resulted in further purification of DHP receptor by about 8-fold (see Figure 7) in the peak of eluted fractions.

The binding characteristics of solubilized and purified DHP receptor has been further investigated by comparing the binding activity of the receptor after solubilization with

digitonin and with CHAPS, the two most frequently used detergents for purification and reconstitution of VDCCs (Hamilton *et al.*, 1989). By comparison of the [^{3}H]-PN200-110 binding and protein profiles of eluates of the lectin-Sepharose and DEAE-Sephadex columns, we found that CHAPS greatly reduced the binding activity of the solubilized DHP receptor. The bound cpm values at similar protein concentration (A_{595}) of either CHAPS-lectin-eluate or CHAPS-DEAE-eluate was much smaller than those of digitonin-lectin-eluate and digitonin-DEAE-eluate, respectively (Figure 7 and Figure 8).

4.2.1.1.2. Immunological Analysis of DHP Receptor α_1 Subunit of the Purified Receptor

Analysis of the DHP receptor α_1 subunit after each purification step has been performed by SDS-PAGE and Western blot analysis. After dialyzing the samples against distilled water to remove salt and sugar, samples were concentrated by lyophylisation. Denatured samples (see sample buffer in Materials and Methods) were separated by SDS-PAGE and electroblotted to PVDF membranes. The DHP receptor α_1 subunit was then detected by a primary antibody, a mouse monoclonal IgG (anti-rabbit DHP receptor α_1 subunit), and peroxidase-labelled anti-mouse secondary antibody. The presence of the α_1 subunit was finally visualized on the X-ray film by the chemiluminescent substrate. Both digitonin-lectin-eluates and digitonin-DEAE-eluates were enriched in the DHP receptor α_1 subunit. After lectin-Sepharose chromatography, DEAE-Sephadex chromatography resulted in a further purification of the receptor α_1 subunit as measured by the density of the bands of the same amount of digitonin-lectin-eluate and digitonin-DEAE-eluate (Lane C and D in Figure 9). This result is consistent with that obtained from comparison of binding and protein profiles after each purification step (Figure 7). The α_1 subunit was also clearly present in Western blots of the receptor purified by lectin affinity chromatography in the presence of CHAPS (Lane E in Figure 9). This suggests that the poor [^{3}H]-PN200-110

binding activity observed in CHAPS eluates (see above) is due to protein inactivation rather than poor solubilisation efficiency.

Under the experimental conditions used, we have been unable to clearly visualize the full sized α_1 subunit (MW ~212 kDa) of DHP receptor in either digitonin or CHAPS solubilized and further purified receptor proteins using this anti-α_1 subunit monoclonal antibody (Upstate Biotechnology Incorporated). Thus, in agreement with previous results, the full sized subunit, if present, is only a minor component of purified DHP receptor.

4.2.1.2. Low Affinity DHP Binding Sites

4.2.1.2.1. Fluorescence Properties of Amlodipine and T-tubule Membranes

Like felodipine, amlodipine, in aqueous solution, is highly fluorescent with broad excitation and emission maxima at about 370 nm and 450 nm, respectively (Figure 10). Addition of T-tubule membranes results in an enhancement of amlodipine fluorescence with a slight shift of the emission maximum to lower wavelength. This fluorescence enhancement can be reversed by the addition of excess nitrendipine (Figure 11A). In addition, the T-tubule membranes are themselves highly fluorescent when excited at 290 nm with the fluorescence of a 5 μg/ml suspension being similar to that of about 5 μM tryptophan ((i) in Figure 11B). The binding of amlodipine (10 μM) quenches the protein fluorescence at 330 nm and a new peak appears in the emission spectrum at about 440 nm ((ii) in Figure 11B). As the fluorescence of 10 μM amlodipine alone is negligible using an excitation wavelength of 290 nm (data not shown), this result indicates that the excitation of amlodipine fluorescence is via energy transfer from protein aromatic amino acid residues.

4.2.1.2.2. Equilibrium Binding of Amlodipine to T-tubule Membranes

As shown in the spectra in Figure 12, the binding of amlodipine to T-tubule membranes can be monitored in three ways: (a) by the enhancement of the amlodipine fluorescence, (b) by energy transfer from membrane protein, and (c) by the quench in the intrinsic fluorescence of the protein. The data in Figure 13 are representative equilibrium fluorescence titrations using each of these methods. In each case, the changes in fluorescence are saturable and conform to a simple binding isotherm. Estimated K_ds were 10.8 ± 2.6 μM (n=13) by direct excitation of amlodipine (Figure 12A), 4.9 ± 0.8 μM (n=7) by energy transfer (Figure 12B), and 3.6 ± 1.7 μM (n=4) by protein quenching (Figure 12C). Thus, K_d values obtained by the changes in amlodipine fluorescence were consistently higher than when excitation was via protein fluorescence.

4.2.1.2.3. Equilibrium Binding of Amlodipine to Solubilized, Purified, and Reconstituted DHP Receptor

The ability of amlodipine to quench the intrinsic protein fluorescence has been exploited to follow the low affinity DHP binding sites during each step of purification and reconstitution of the DHP receptor. Like the T-tubule membranes, the purified DHP receptor is highly fluorescent and this protein fluorescence is sensitive to the binding of amlodipine (Figure 13). Figure 14 shows that the low affinity amlodipine binding sites are maintained after solubilization in 1% digitonin, after purification by lectin-Sepharose chromatography and after reconstitution in phosphatidylcholine vesicles. The apparent K_d is somewhat increased in the solubilized protein (12.8 ± 0.7 μM, n=3) and this is not significantly affected by further purification (12.3 ± 4.1 μM, n=3) or reconstitution (11.8 ± 2.3 μM), suggesting that the lipid environment of the T-tubule membrane is important in conferring slightly higher affinity (3.6 ± 1.7 μM, in Figure 12C). Further purification of the receptors by DEAE-Sephadex had no effect on the fluorescence changes observed (Figure 13 inset).

4.2.1.2.4. Binding of Non-fluorescent DHPs to T-tubule Membranes

The enhancement of amlodipine fluorescence upon it binding to the T-tubule membranes can be reversed by the addition of excess nitrendipine (Figure 11A). Detailed studies have shown that micromolar concentrations of several other DHPs are able to reverse the enhancement of amlodipine fluorescence in a concentration-dependent manner (Figure 15A). Furthermore, the binding of non-fluorescent DHPs has also been measured directly by their ability to quench the protein fluorescence. Figure 15B shows the concentration-dependence of the quench of fluorescence of T-tubule membranes by titration with several DHPs including Bay K8644, nicardipine, nitrendipine and nifedipine. Estimated dissociation constants obtained directly from the quench in protein fluorescence or indirectly by displacement of amlodipine are given in Table 4. Although, for most DHPs, estimated K_d values were very similar, values for nimodipine and nifedipine were consistently higher when monitored indirectly by displacement of amlodipine.

4.2.1.2.5. Dissociation Kinetic Studies of the Partially Purified DHP Receptor Complex

The observation that micromolar concentrations of nitrendipine and other DHPs could accelerate the dissociation of [^{3}H]-PN200-110 from its high affinity sites in microsomal membrane proteins provided the first evidence that, in addition to high affinity binding sites for DHPs, low affinity binding sites for DHP drugs also exist in skeletal muscle membranes (Dunn and Bladen, 1991). Similarly, in the present study, the purified protein was first incubated with 8 nM [^{3}H]-PN200-110 to form the high affinity receptor-DHP complex. Dissociation was then induced by 20-fold dilution into buffer alone or into buffer containing 1-30 μM amlodipine or nitrendipine. As shown in the Figure 16, dilution of the complex into 1 μM of either amlodipine or nitrendipine, a concentration sufficient to prevent any rebinding of radiolabelled ligand to its high affinity sites but too low to occupy the low affinity sites significantly (amlodipine, K_d=10.8 ± 2.6 μM; nitrendipine, K_d=11.4 ±

2.9 μM), had no effect on the dissociation rate. However, when 30 μM amlodipine or nitrendipine was included in the dilution buffer, the rate was significantly increased, from 0.069 min^{-1} to 0.11 min^{-1} and 0.099 min^{-1}, respectively. These data suggest that, not only are the low affinity sites present in the purified receptor protein, but that they are also allosterically linked to the high affinity DHP sites.

4.2.1.3. [$^{45}Ca^{2+}$] Flux Studies

Purified skeletal muscle T-tubules have been used for functional studies of Ca^{2+} channels in their native membrane-bound state (Affolter and Coronado, 1985; Dunn, 1989). It has been demonstrated that the isolated T-tubule vesicles contain functional DHP-sensitive VDCCs which are able to mediate [$^{45}Ca^{2+}$] flux in response to membrane depolarization (Dunn, 1989). More recently, a rapid filtration technique was developed to measure [$^{45}Ca^{2+}$] flux responses on physiologically relevant time scales (Bhat, 1993).

Due to the prolonged depolarization of the membranes that occurs during their preparation, VDCCs in isolated T-tubule vesicles appear to be in an inactivated state. Thus, a two-step procedure has been developed to perform [$^{45}Ca^{2+}$] flux measurements using isolated T-tubule vesicles (Dunn, 1989). Vesicles loaded with [$^{45}Ca^{2+}$] are first diluted into the high K^+ buffer designed to generate a membrane potential mimicking the resting state of the cell and to reduce the extravesicular Ca^{2+} to sub-micromolar levels. [$^{45}Ca^{2+}$] efflux is then measured upon subsequent depolarization. Changes in potential across T-tubule membrane vesicles are induced by establishing potassium gradients across the membrane (in the presence of valinomycin) by isosmotic exchange of choline chloride for potassium gluconate. In the present study, we have measured the time course of [$^{45}Ca^{2+}$] flux and have also investigated the possible contribution to the observed [$^{45}Ca^{2+}$] flux arising from the presence of contaminating SR vesicles in the T-tubule membrane preparation.

The results in Figure 17 show that even in the control samples (without repolarization before depolarization), there is a considerable decrease in the amount of [$^{45}Ca^{2+}$] retained by the vesicles with increasing time of depolarization. Thus, specific [$^{45}Ca^{2+}$] flux is defined as the difference of retained [$^{45}Ca^{2+}$] between the repolarized sample and the control. The time-course of [$^{45}Ca^{2+}$] flux shows that the greatest amount of specific depolarization-induced [$^{45}Ca^{2+}$] flux occurs within the first 300 ms after initiation of depolarisation. These results, which are similar to those reported previously (Bhat, 1993), are consistent with the time taken for slow VDCCs to reach peak current amplitude in voltage-clamp recordings of intact skeletal muscle fibers (Beaty *et al.*, 1987).

Ruthenium red, an antagonist of Ca^{2+} release channels in SR, has been used to block [$^{45}Ca^{2+}$] flux via this source. Figure 17 also shows that the possible interference due to the contaminating SR is negligible because specific [$^{45}Ca^{2+}$] flux measured as above i.e. the difference between amount of [$^{45}Ca^{2+}$] retained by control membrane vesicles and those that had undergone the repolarisation-depolarisation procedures, were unaffected by the presence of ruthenium red. As Ca^{2+} release from the skeletal muscle SR is sensitive to the depolarization of the dihydropyridine receptor (Anderson and Merssner, 1995), this result suggests that any contaminating SR vesicles in this membrane preparation are uncoupled from the T-tubule membranes.

In the present study, attempts were made to measure the dose-dependence of DHP effects on depolarisation-induced [$^{45}Ca^{2+}$] efflux responses. Unfortunately, as has been found in many previous studies (see Dunn, 1989), the results were erratic, possibly reflecting the dual effects of DHPs which can act as both agonists and antagonists, complications arising from the racemic mixtures of some of the DHPs used in this study and possible voltage-dependence in the modes of actions of these drugs. Thus further experiments are required before it will be possible to correlate binding occupancy with effects of DHPs on VDCC function.

4.2.2. Discussion:

The presence of low affinity DHP-binding sites which are colocalized with the well studied high affinity sites in skeletal muscle T-tubule membranes have been reported previously by Dunn and Bladen (1991 and 1992). In these earlier studies, however, it was not demonstrated that both high and low affinity sites were associated with the same protein i.e. the L-type Ca^{2+} channel or the DHP receptor. Purification of the receptor protein from solubilized membranes is an important step toward clarifying this point.

Consistent with reports from other laboratories (Striessnig and Glossmann, 1991; Florio *et al.*, 1992), a single step purification by lectin affinity chromatography after solubilizing crude microsomal membranes with digitonin results in a high recovery of DHP receptor which is enriched in the α_1 subunit and retains high affinity DHP binding. Thus, this preparation is suitable for further studies of low affinity binding sites and their interaction with the high affinity sites. After solubilisation there is a decrease in affinity for radiolabelled DHPs suggesting that lipids may play an important role in stabilizing these high affinity sites. Our inability to observe the full-length form of the α_1 subunit in the purified protein may be due to the proteolytic cleavage by calpain since specific inhibitors of calpain were not included in the preparation buffers.

In addition to digitonin, CHAPS has also been commonly used to solubilize and purify the L-type channel protein (Borsotto *et al.*, 1985; Barhanin *et al.*, 1987). However, there are controversial reports that CHAPS causes loss of the high affinity sites in the purified protein (Barhanin *et al.*, 1987; Hamilton *et al.*, 1989; Gutierrez *et al.*, 1991). Our study shows that the use of CHAPS does result in an almost complete loss of high affinity sites in the purified protein. We suggest that this is due to inactivation of the high affinity binding sites on the α_1 subunit rather than the dissociation of α_1 subunit from the highly glycosylated α_2 subunit which underlies the basis of lectin affinity chromatography, since this subunit was easily detected in the purified protein by Western blot analysis. This

suggestion is supported by the previous observation that CHAPS accelerates dissociation of [^{3}H]-PN200-110 from the receptor complex (Curtis and Catterall, 1986).

Due to the relatively high K_d values (3-21 μM) of the low affinity DHP binding sites and the nature of its dissociation kinetics (Dunn and Bladen, 1992), direct measurements using a radiolabelled ligand, such as [^{3}H]-PN200-110, are precluded in the study of low affinity DHP binding sites. The fluorescent DHP derivative, felodipine, has previously been used in direct measurements of low affinity DHP binding sites in skeletal muscle membranes (Dunn and Bladen, 1992).

Amlodipine has similar fluorescence properties to felodipine. This is likely to be due to the structural similarity between amlodipine and felodipine, i.e. neither contains an aromatic nitro group which, in general, is known to impart poor fluorescence properties (Ghosh and Whitehouse, 1968). The greater water solubility of amlodipine than felodipine makes it a better probe for studies of low affinity DHP binding sites in T-tubule membranes. However, as was previously found using felodipine, we have been unable to use amlodipine fluorescence to detect low affinity sites after membrane solubilization. This is due to large spectral artifacts in the presence of detergent when amlodipine is excited directly and complications in energy transfer measurements arising from some direct excitation of amlodipine fluorescence at high concentrations.

T-tubule membranes are themselves highly fluorescent, as is the purified receptor protein. Protein fluorescence, which arises mainly from the presence of tryptophan residues, is often environmentally sensitive and has frequently been used to monitor ligand-induced changes in protein conformation (Bradshaw and Harris, 1987). Since protein fluorescence is sensitive to the binding of DHPs, studies of the low affinity sites are not restricted to the use of fluorescent derivatives and low affinity sites for other non-fluorescent DHPs can be directly measured. Furthermore, by monitoring the quench in

protein fluorescence, we have been able to study the low affinity binding sites in purified receptor protein.

The present study shows that DHPs bind to a saturable, homogeneous population of low affinity sites in skeletal muscle T-tubule membranes with K_d values in the μM range. Other DHPs compete for the same sites as amlodipine as shown by the ability of micromolar concentrations of these drugs to reverse the enhancement of amlodipine fluorescence. The non-DHP Ca^{2+} channel ligands, diltiazem and verapamil, did not inhibit the amlodipine fluorescence enhancement on binding to T-tubule membranes and also had no specific effects on the protein intrinsic fluorescence (Dunn and Bao, manuscript in preparation). These results suggest that the low affinity binding sites are specific for DHPs and this is consistent with a previous report by Dunn and Bladen (1992).

DHPs have previously been shown to bind with low affinity to a number of proteins that are unrelated to Ca^{2+} channels, including peripheral benzodiazepine receptors, calmodulin, nucleoside transporters, Na^+-K^+ ATPase and the multidrug-resistance related P-glycoprotein (Dunn and Bladen, 1992). Our present study demonstrates that the purified Ca^{2+} channel protein also carries low affinity sites. Although previous reports identified low affinity DHP binding sites that were colocalized with the high affinity sites in T-tubule membranes, this is the first report demonstrating that the sites are present on the purified Ca^{2+} channel complex and not on another, interacting but unrelated, protein.

Our kinetic studies have shown that the rate of dissociation of [^{3}H]-PN200-110 previously bound to its high affinity sites on the purified protein is accelerated by the presence of other DHPs (e.g. amlodipine and nitrendipine, Figure 17) at concentrations of 10-30 μM. As described using native T-tubule membranes, these results suggest that occupancy of the low affinity sites has an allosteric effect on the high affinity DHP sites to increase the apparent rate of dissociation, presumably as a result of decreased affinity due to protein conformation change (Dunn and Bladen, 1991). These data clearly demonstrate

that not only are the low affinity sites present in the purified DHP receptor complex, but also that they are allosterically coupled to the high affinity DHP binding sites. Our studies also show that although the low affinity DHP binding sites are maintained in the purified protein, the binding affinity is decreased after solubilization and purification and this decrease cannot be recovered by subsequent reconstitution into phospholipid vesicles. This suggests that the lipid environment of the T-tubule membranes is important in conferring slightly higher affinity of these sites. This is in agreement with a previous suggestion that the low affinity sites are located at a lipid-protein interface (Dunn and Bladen, 1992), a suggestion that has been further supported by recent report of the unusual stability of the low affinity sites to proteolysis or heat denaturation (Dunn and Bladen, manuscript in preparation).

In many experiments, we have found that measurements of the low affinity DHP sites are more reliably monitored by the quench in intrinsic protein fluorescence. Direct excitation of amlodipine fluorescence is affected by the presence of detergents and energy transfer measurements are complicated by some direct excitation of amlodipine fluorescence that occurs at high concentrations (Dunn and Bao, manuscript in preparation). In addition, the monitoring of protein fluorescence eliminates interference from lipid-specific effects on amlodipine fluorescence (Dunn and Bladen, manuscript in preparation) which may account for the observation that K_d values for some DHPs were consistently higher when monitored indirectly by displacement of amlodipine.

Our functional study of [$^{45}Ca^{2+}$] fluxes using the isolated T-tubule preparation further confirms the presence of slow voltage-dependent Ca^{2+} channels in these membranes. We also provide evidence that contaminating SR vesicles in this preparation do not contribute to the observed flux responses. By using automated rapid filtration techniques, we were able to measure voltage-dependent [$^{45}Ca^{2+}$] flux responses on physiologically relevant time scales (10-300 ms). Previously, the activity of T-tubule Ca^{2+}

channels has been investigated after their purification and reconstitution into phospholipid vesicles or planar bilayers (Affolter and Coronado, 1985; Curtis and Catterall, 1986). However, during purification, channel proteins may be denatured and loss of structurally and functionally associated molecules has been reported (Florio *et al.*, 1992). An advantage of using native vesicle preparations is that they permit parallel measurements of ligand binding and functional responses of the channel population as a whole. As noted above, further flux studies will be necessary to determine the dose-dependence of DHP effects on Ca^{2+} channel function.

Figure 7. Distribution of [^{3}H]-PN200-110 binding activity and protein after digitonin-lectin-Sepharose (A) and digitonin-DEAE-Sephadex (B) chromatography. ● (cpm): [^{3}H]-PN200-110 binding activity; ○ (A_{595}): protein absorbance at wavelength of 595 nm. The bound receptor complex was eluted from the lectin-Sepharose column with 5% (w/v) N-acetyl-D-glucosamine and from the DEAE-Sephadex column with a 20-300 mM linear NaCl gradient. Fractions containing the receptor complex were identified by [^{3}H]-PN200-110 binding activity. DHP receptor complex purified by affinity lectin chromatography overlapped with the protein peak, and the receptor complex further purified by DEAE ion exchange chromatography was recovered in a single peak at about 200 mM NaCl.

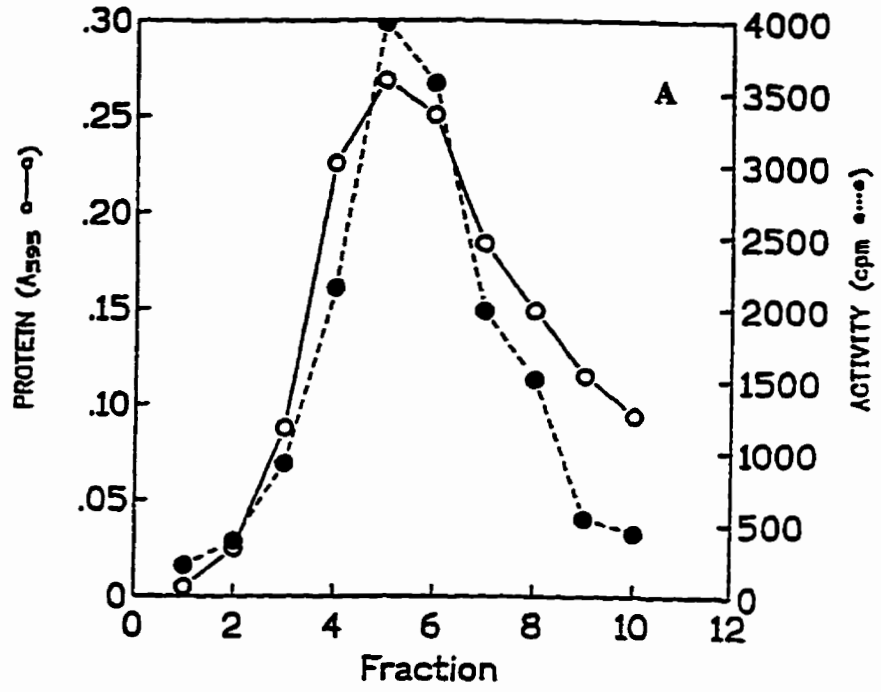
A
PROTEIN (A595 o—o)
ACTIVITY (cpm •···•)
Fraction
.30
.25
.20
.15
.10
.05
0
4000
3500
3000
2500
2000
1500
1000
500
0
0 2 4 6 8 10 12

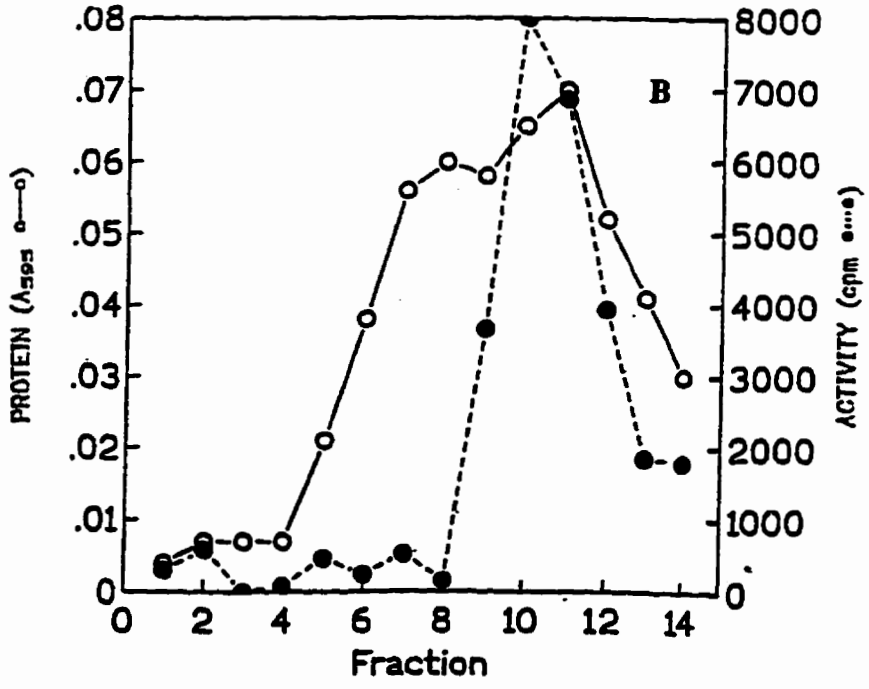
B
PROTEIN (A595 o—o)
ACTIVITY (cpm •···•)
Fraction
.08
.07
.06
.05
.04
.03
.02
.01
0
8000
7000
6000
5000
4000
3000
2000
1000
0
0 2 4 6 8 10 12 14

Figure 8. Distribution of [^{3}H]-PN200-110 binding activity and protein after CHAPS-lectin-Sepharose (A) and CHAPS-DEAE-Sephadex (B) chromatography. ● (cpm): [^{3}H]-PN200-110 binding activity; ○ (A_{595}): protein absorbance at wavelength of 595 nm. The bound receptor complex was eluted from the lectin-Sepharose column with 5% (w/v) N-acetyl-D-glucosamine and from the DEAE-Sephadex column with a 20-300 mM linear NaCl gradient. Fractions containing the receptor complex were identified by [^{3}H]-PN200-110 binding activity. It shows that the binding ability of the purified protein was greatly decreased.

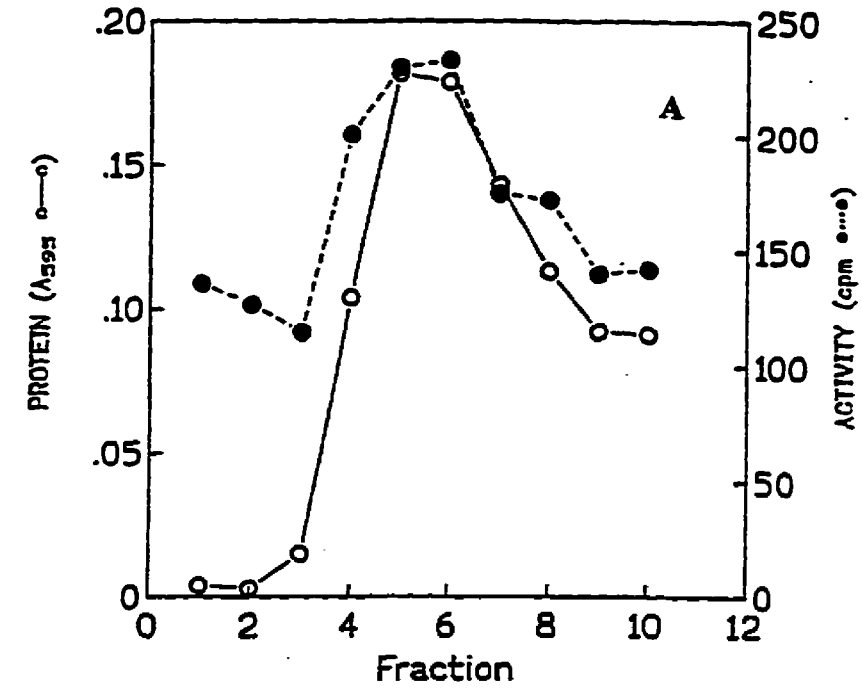
A
PROTEIN (A595 o—o)
ACTIVITY (cpm •···•)
.20
.15
.10
.05
0
250
200
150
100
50
0
0 2 4 6 8 10 12
Fraction

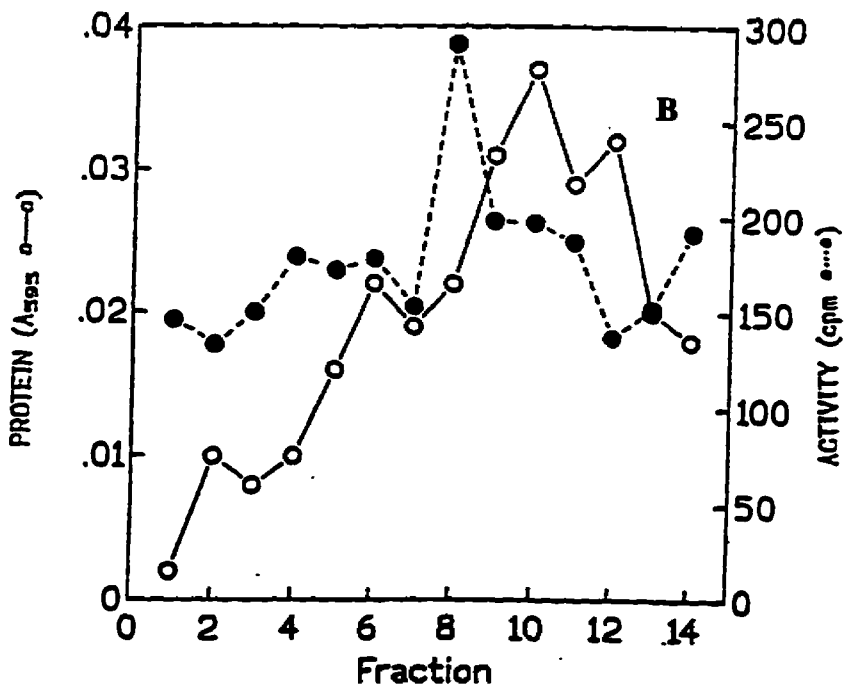
B
PROTEIN (A595 o—o)
ACTIVITY (cpm •···•)
.04
.03
.02
.01
0
300
250
200
150
100
50
0
0 2 4 6 8 10 12 14
Fraction

Figure 9. Western blot analysis of the DHP receptor α_1-subunit of purified proteins. Crude microsomal membrane proteins (20 μg, Lane A), partially purified T-tubule membrane proteins (5 μg, Lane B), and purified membrane proteins either by digitonin-lectin-Sepharose (5 μg, Lane C), digitonin-DEAE-Sephadex (5 μg, Lane D) or CHAPS-lectin-Sepharose (5 μg, Lane E) were resolved by a 10% denaturing polyacrylamide gel electrophoresis, and electrotransferred onto a PVDF membrane. The membrane was incubated with an anti-rabbit skeletal muscle DHP receptor α_1-subunit monoclonal antibody at a dilution of 1:2,000. Following incubation with peroxidase-labelled secondary antibody, specific bands were visualized by chemiluminescent substrate luminol as described in 3.2.4. of materials and methods. Arrow indicates the position of α_1-subunit with molecular weight of 175 kDa.

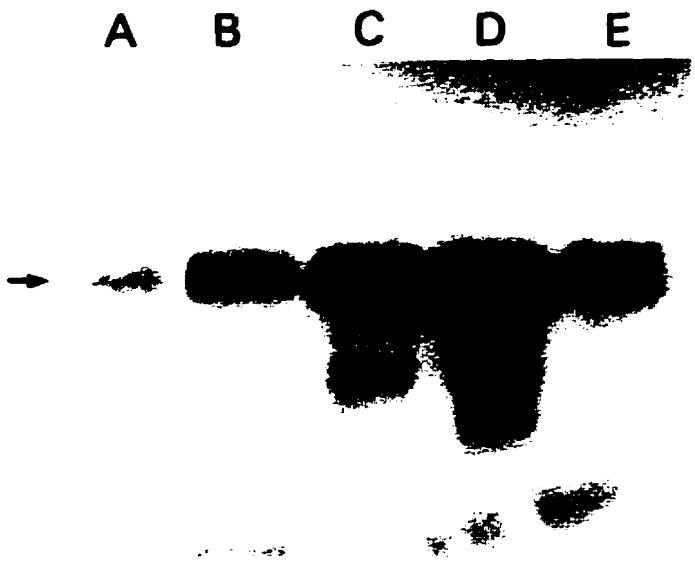
A
B
C
D
E

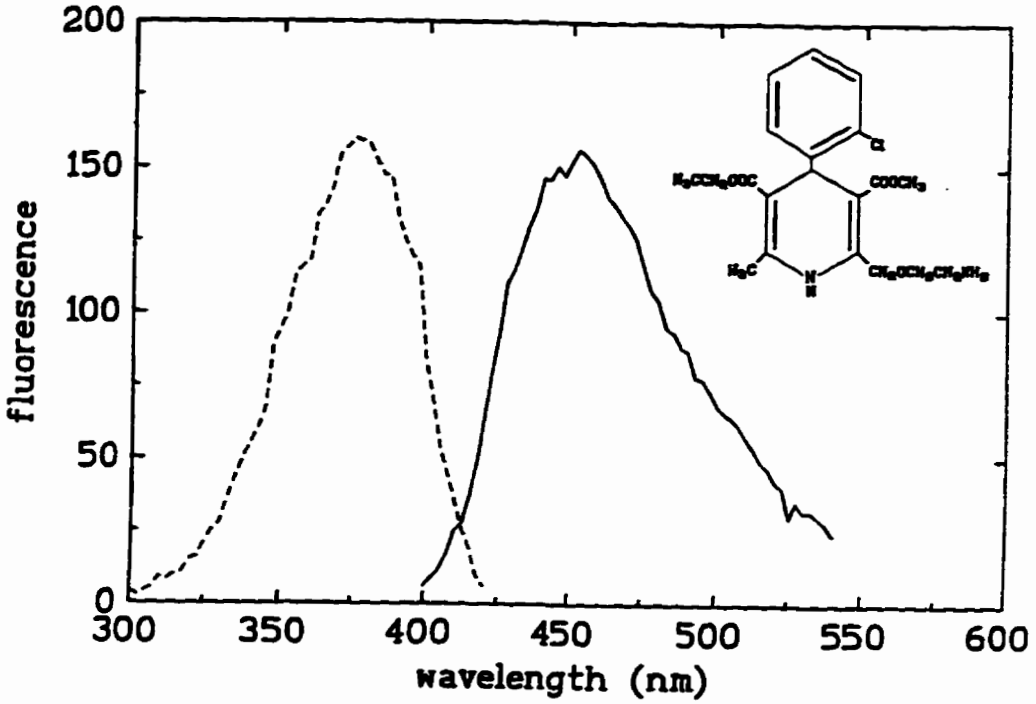

Figure 10. Fluorescence properties of amlodipine maleate. Spectra of a 10 μM solution of amlodipine maleate in 20 mM Tris-HCl pH 7.4, 1 mM $CaCl_2$ were recorded in a thermostatted cuvette at 25°C. The excitation spectrum (dashed curve) was recorded using an emission wavelength of 450 nm and the excitation wavelength used for the emission spectrum (solid curve) was 375 nm. The inset shows the structure of amlodipine.

Figure 11. Fluorescence changes on binding of amlodipine to T-tubule membranes and the intrinsic protein fluorescence of T-tubule membranes. In (A), the emission spectrum of 10 μM solution of amlodipine were shown in (i) (excited at 375 nm). Addition of 5 μg/ml of T-tubule membranes resulted in the enhancement of amlodipine fluorescence (ii). 50 μM of nitrendipine reversed the enhancement in amlodipine fluorescence (iii). In (B), the emission spectrum (i) of 5 μg/ml T-tubule membranes was recorded while excited at 290 nm. Spectrum (ii) was recorded after the addition of 10 μM amlodipine and illustrates the quench in protein fluorescence maxima at about 330 nm and the appearance of a new peak of amlodipine fluorescence at about 440 nm, excited via energy transfer from the membrane proteins. At this concentration, the fluorescence of amlodipine alone is negligible using an excitation wavelength of 290 nm (data not shown).

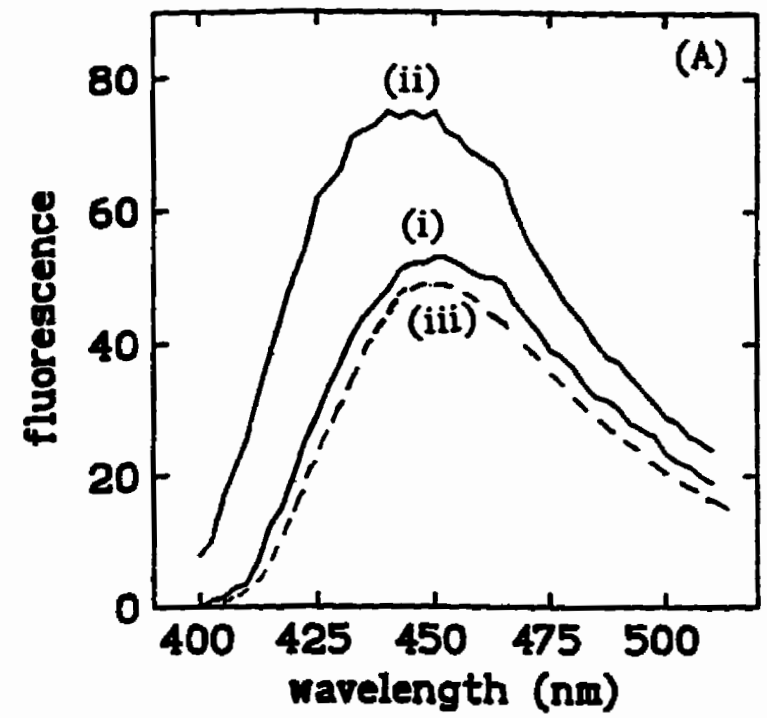
(A)
(ii)
(i)
(iii)
80
60
40
20
0
fluorescence
400
425
450
475
500
wavelength (nm)

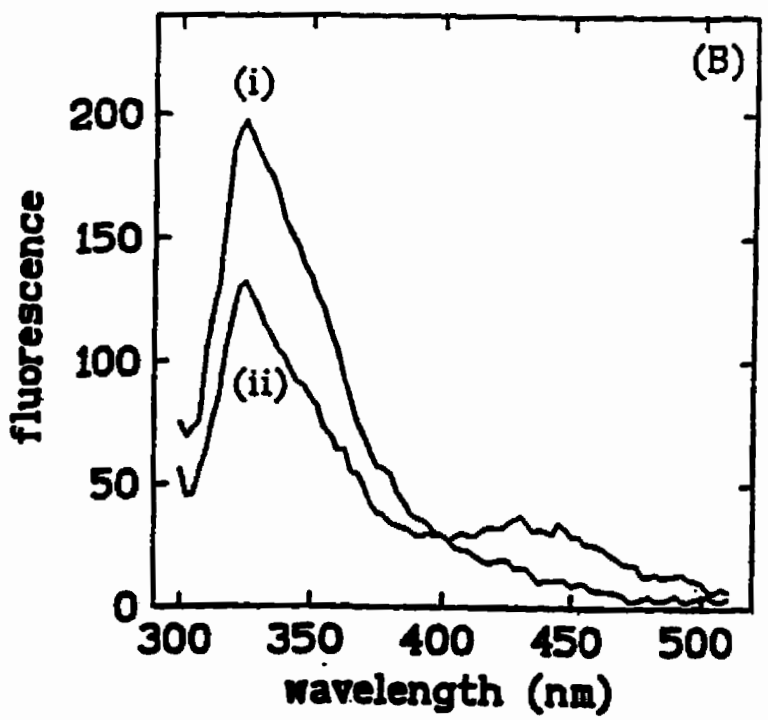
(B)
(i)
(ii)
200
150
100
50
0
fluorescence
300
350
400
450
500
wavelength (nm)

Figure 12. Equilibrium fluorescence titrations of T-tubule membranes (5 μg/ml) monitored by changes in (A) amlodipine fluorescence, (B) energy transfer fluorescence or (C) protein intrinsic fluorescence. Excitation and emission wavelengths were 370/450 nm (A), 290/450 nm (B), and 290/330 nm (C), respectively. The curves in (A) and (B) show the specific fluorescence enhancement accompanying binding of amlodipine to membranes. The insets in these panels show fluorescence in the presence of membranes (upper curves) and the fluorescence on adding amlodipine to buffer alone (lower curve). In (C), the upper curve is the fluorescence change occurring on the addition of amlodipine to the control tryptophan solution (dilution effect) and the lower curve is the fluorescence quench on the binding of amlodipine to T-tubule membranes. The open symbols represent the difference between the two curves, showing the specific fluorescence quench on binding. K_d values obtained from fitting by a simple binding model were (A) 9.2 μM, (B) 5.4 μM, and (C) 2.1 μM.

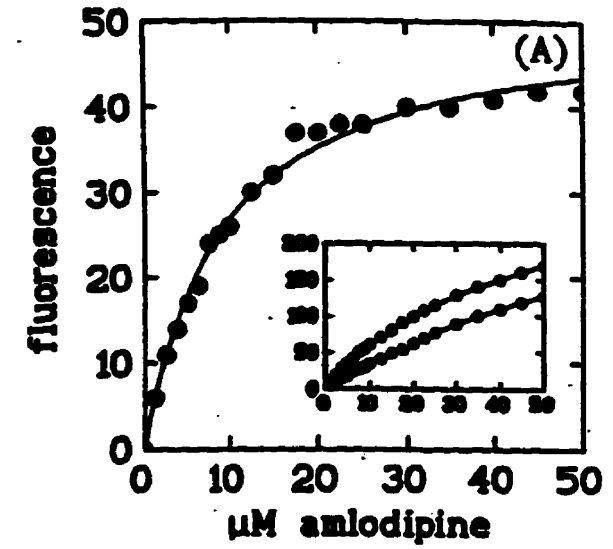
(A)
fluorescence
0
10
20
30
40
50
µM amlodipine

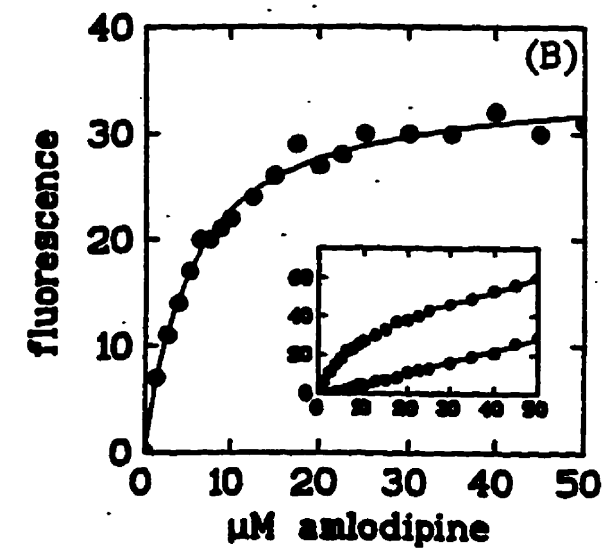
(B)
fluorescence
0
10
20
30
40
50
µM amlodipine

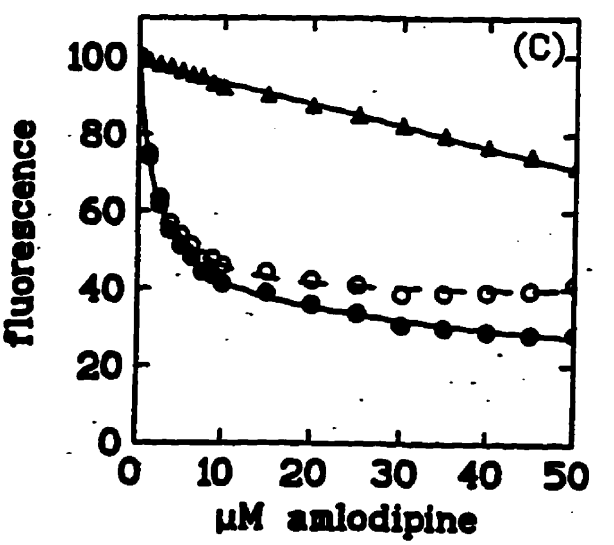
(C)
fluorescence
0
20
40
60
80
100
0
10
20
30
40
50
µM amlodipine

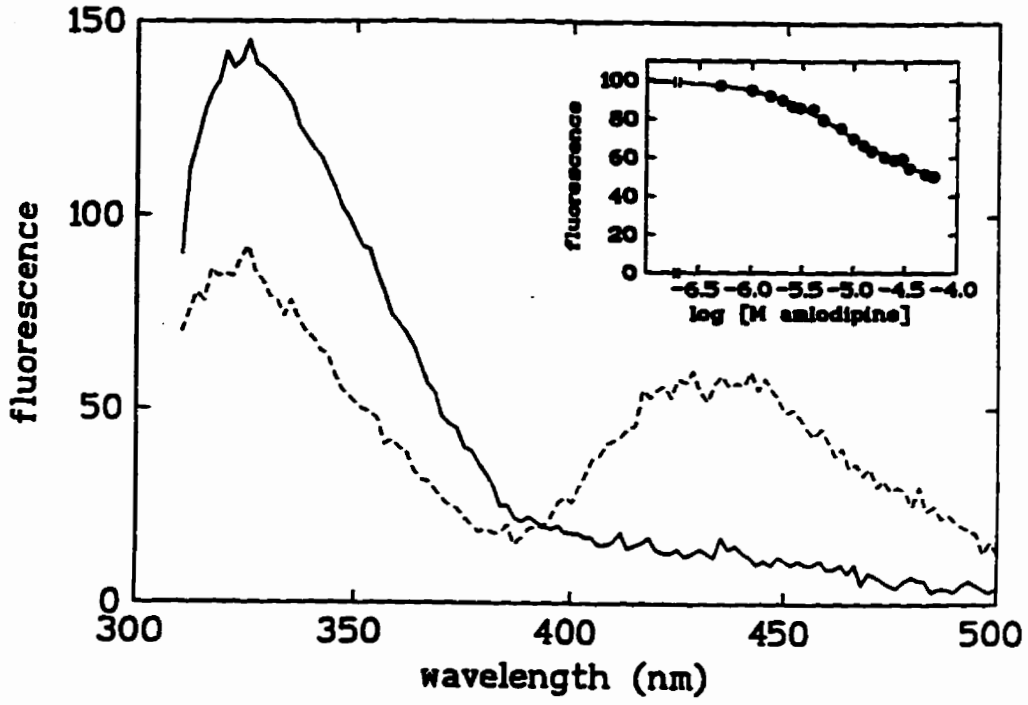

Figure 13. Fluorescence properties of the purified DHP receptor. Receptor protein was purified by solubilization with digitonin and subsequent purification with lectin affinity chromatography and DEAE ion exchange chromatography. Solid curve shows emission spectrum of purified protein with excitation at 290 nm. Dashed curve is the spectrum after addition of 10 μM amlodipine, illustrating the quench of protein fluorescence and the appearance of energy transfer fluorescence at longer wavelength. Inset shows the concentration-dependence of the quench in protein fluorescence giving an estimated K_d of 9 μM in this experiment.

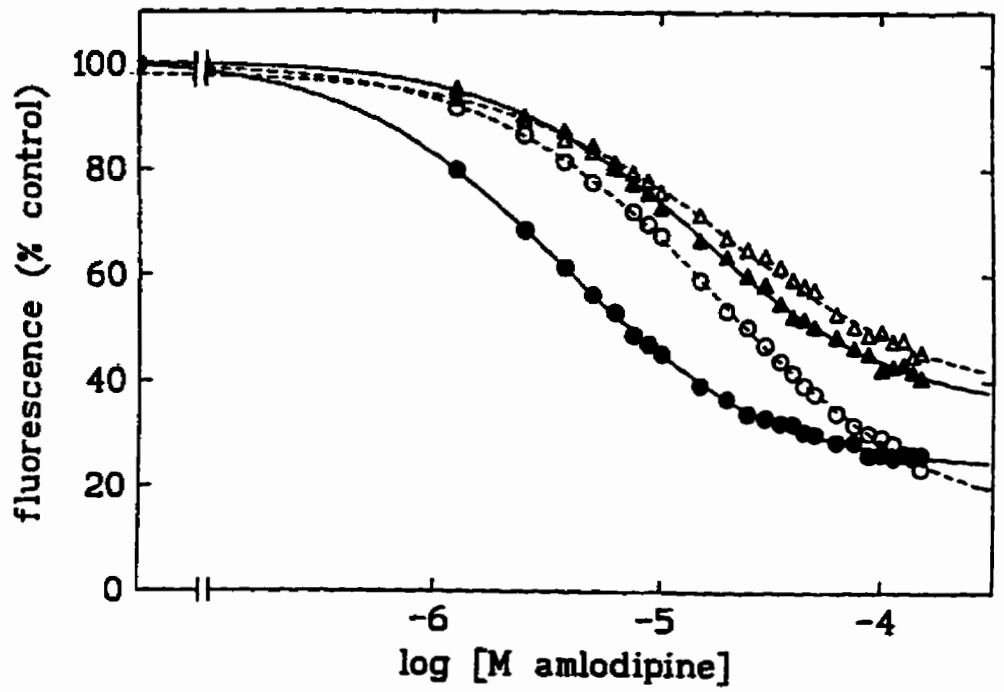

Figure 14. Low affinity DHP binding sites measured by the quench in protein fluorescence (ex/em, 290/330 nm) in T-tubule membranes (●), after solubilization in 1% digitonin (▲), after WGA-Sepharose chromatography (Δ) and after reconstitution in phospholipid vesicles (○). Membranes, solubilized and purified receptor were used at a protein concentration of 5 μg/ml. The concentration of reconstituted protein was adjusted to the same initial protein fluorescence. The buffers used in these titration were 10 mM Hepes-Tris, pH 7.4, 150 mM NaCl, 0.02% NaN_3 (●, ○) and 10 mM Hepes-Tris, pH 7.4, 20 mM NaCl, 0.1% (w/v) digitonin, 0.02% NaN_3 (▲,Δ). Curve fitting gave K_d values of 3.6 μM, 13.8 μM, 14.7 μM and 12.2 μM for the membrane, solubilized, purified and reconstituted samples, respectively.

Figure 15. Low affinity binding of non-fluorescent dihydropyridines. In (A), T-tubule membranes (5 μg/ml) were equilibrated with 5 μM amlodipine and the complex was titrated with Bay K8644 (●), nicardipine (△), nitrendipine (▲), and nifedipine (○). Displacement of bound amlodipine were monitored by changes in its fluorescence using excitation and emission wavelengths of 370 and 450 nm. Estimated IC_{50} values were 2.9 μM, 3.0 μM, 12.3 μM, and 45.7 μM, respectively. (B) Effect of Bay K8644 (●), nicardipine (△), nitrendipine (▲), and nifedipine (○) on the intrinsic fluorescence of T-tubule membranes (5 μg/ml) monitored using excitation and emission wavelengths of 290 and 330 nm. Estimated K_d values were 3.7 μM, 2.1 μM, 9.5 μM, and 10.7 μM, respectively.

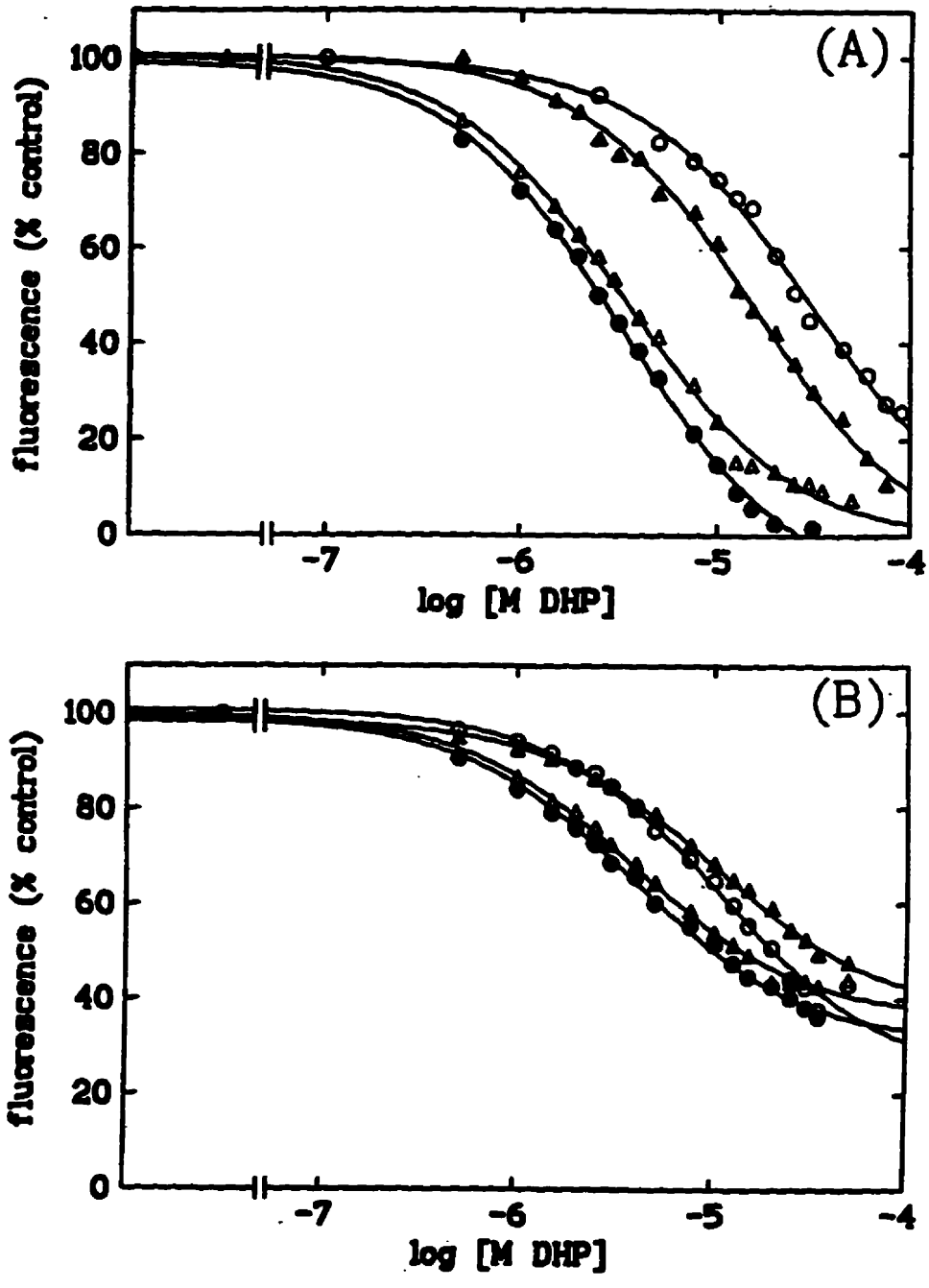
(A)
fluorescence (% control)
100
80
60
40
20
0
-7
-6
-5
-4
log [M DHP]
(B)
fluorescence (% control)
100
80
60
40
20
0
-7
-6
-5
-4
log [M DHP]

Figure 16. Evidence that the low affinity amlodipine binding sites are allosterically coupled to the high affinity DHP sites. Purified receptor (20 μg/ml) was first equilibrated with 8 nM [^{3}H]-PN200-110 and dissociation was initiated by 20-fold dilution into buffer alone (△), 1 μM amlodipine (○) or 30 μM amlodipine (□) in A. Estimated apparent rates of dissociation from fitting by a simple exponential decay were 0.069 min^{-1} by 20-fold buffer dilution alone, 0.066 min^{-1} in the presence of 1 μM amlodipine and 0.11 min^{-1} in the presence of 30 μM amlodipine. B shows that nitrendipine has a similar accelerating effect on the rate of [^{3}H]-PN200-110 dissociation. Estimated apparent rates of dissociation were 0.069 min^{-1} by 20-fold buffer dilution alone (▲), 0.065 min^{-1} in the presence of 1 μM nitrendipine (●) and 0.099 min^{-1} in the presence of 30 μM nitrendipine (■).

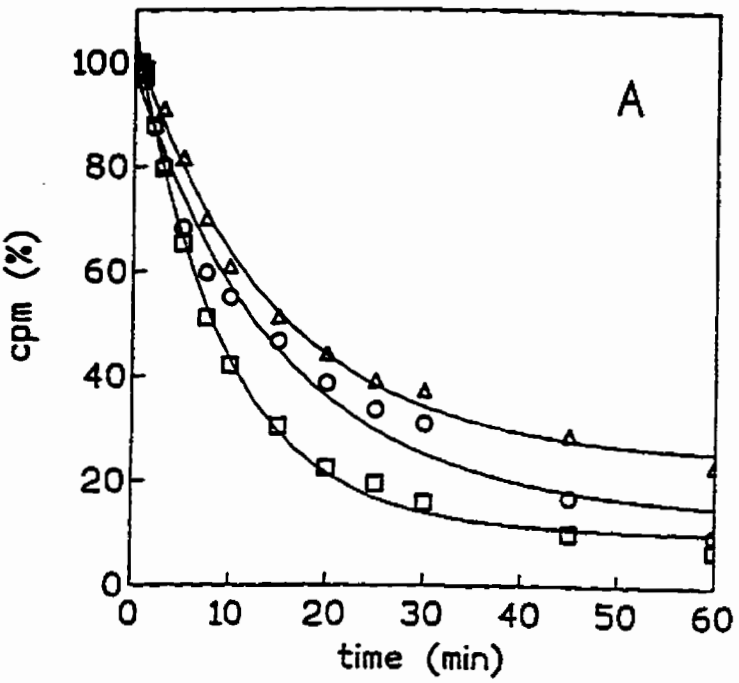
A
100
80
60
40
20
0
cpm (%)
0
10
20
30
40
50
60
time (min)

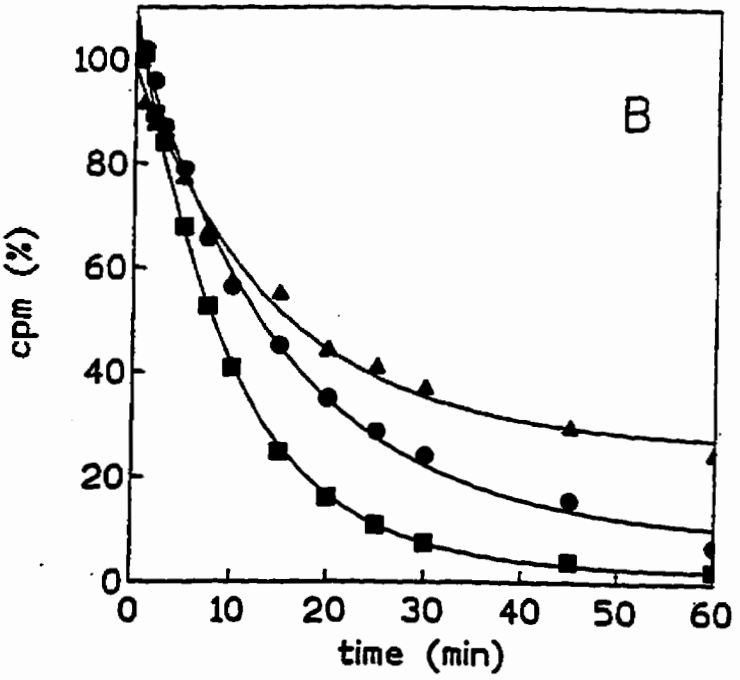
B
100
80
60
40
20
0
cpm (%)
0
10
20
30
40
50
60
time (min)

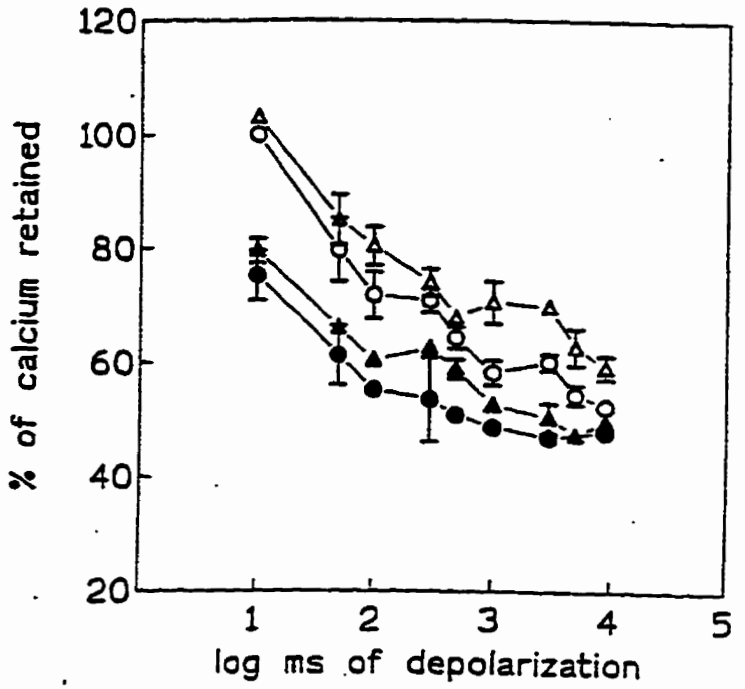

Figure 17. Time course and ruthenium red effect on [$^{45}Ca^{2+}$] flux in the isolated T-tubule vesicles. Partially purified T-tubule membrane vesicles preequilibrated in low K^+ buffer and loaded with $^{45}Ca^{2+}$ were diluted 40-fold in a nonrepolarizing buffer (0 mV, △) or a repolarizing buffer (-86 mV, ▲). Following 5 min incubation, aliquots of 900 µl were mounted in a Biologic Rapid Filtration device and filtered under vacuum for an appropriate time with a depolarizing buffer (0 mV). The difference between these two groups gives specific voltage-dependent [$^{45}Ca^{2+}$] flux. In parallel experiments, [$^{45}Ca^{2+}$] flux in the isolated T-tubule vesicles was measured in the presence of 1 µM of ruthenium red (0 mV, ○; -86 mV, ●). The data represent the results from three quintuplicate experiments.

Table 3.

Binding of [^{3}H]-PN200-110 to Different Preparations of Skeletal Muscle VDCCs

preparation	K_d (nM)	B_{max} (pmol/mg)
Microsomal Membranes	0.40 ± 0.02	2.91 ± 0.08
Digitonin Extract	1.21 ± 0.04	3.01 ± 0.28
Lectin-Sepharose-Eluate	6.78 ± 0.45	84 ± 5.9
Reconstituted Vesicles	15.38 ± 0.74	ND*

*: not determined.

Table 4.

Binding of Non-fluorescent DHPs to Low Affinity Sites in Skeletal Muscle T-tubule Membranes

DHP	K_i (μM) amlodipine competition	K_d (μM) protein quench
Bay K8644	2.7 ± 0.9	4.2 ± 0.3
Nifedipine	29.9 ± 1.4	8.6 ± 2.0
Nimodipine	25.5 ± 4.4	4.8 ± 0.9
Nitrendipine	11.4 ± 2.9	9.0 ± 0.2
Nicardipine	2.0 ± 0.2	2.9 ± 0.6
(+)PN200-110	8.2 ± 0.8	7.4 ± 0.6
(-)PN200-110	11.2 ± 1.8	11.7 ± 0.8

Chapter 3. pH-dependence of Amlodipine Binding to the Skeletal Muscle Membranes

A variety of dihydropyridine drugs have proved to be not only powerful therapeutic tools for treatment of cardiovascular diseases but also key molecular probes of L-type Ca^{2+} channels. Although much attention has focused on the study of drug binding domains, current reports are controversial and the precise location of the functional DHP binding sites remains unknown due to the complexity of the ligand-receptor interactions and the technical limitations in site identification (see Introduction).

The slow onset and long duration of action of amlodipine makes it a unique DHP drug which is widely prescribed for hypertension and angina pectoris. Its pharmacokinetic properties allow once-daily dosing and many side effects associated with other DHPs are avoided (Burges, 1992). In addition, the physiochemical properties of amlodipine may be useful in studies of the ligand-receptor interactions. Unlike many other DHP derivatives, amlodipine contains a basic aminoethoxymethyl side chain rather than a methyl group at position 2 of the dihydropyridine ring (Burges, 1992). Under physiological conditions, amlodipine (pKa = 8.7) is positively charged (protonated), whereas many other DHP drugs (e.g. PN200-110) are neutral. Furthermore, the relative amount of protonated amlodipine can be simply manipulated by changes in solution pH, whereas PN200-110 is neutral over a wide pH range (5-10) (Kass *et al.*, 1989a, b). In the present study, the pH-dependence of amlodipine binding to its receptors has been investigated and compared with that of the neutral DHP, PN200-110.

1. Results:

Figure 18 shows the effect of pH on [^{3}H]-PN200-110 binding to its high affinity sites in skeletal muscle membranes. Over the pH range of 6-10, neither the K_d (0.9-1.2

nM) nor density of sites displayed any pH sensitivity. At pH 5 there was a decrease in the density of sites and no [^{3}H]-PN200-110 binding was measurable at pH 4 or pH 11.

Table 5 shows the effect of pH on the K_d of amlodipine binding to its high and low affinity binding sites of skeletal muscle determined by competitive binding assays (i.e. displacement of [^{3}H]-PN200-110) and protein fluorescence quench experiments, respectively. The binding of amlodipine to its high affinity sites is pH-sensitive. The binding affinity is highest at a pH of 8-10, and decreases at lower pH. The binding of amlodipine to its low affinity sites is less pH-sensitive and although there is a significant decrease of affinity at extremes of pH (4, 10.66), there is little pH dependence over the range of 5-9.

2. Discussion:

In studies of the pH-dependence of ligand binding, two components may be pH-sensitive. One is the ligand molecule if it has an ionizable group over the pH range of interest, and the other is the presence of ionizable groups within the protein binding domain. The effect of pH on the binding of [^{3}H]-PN200-110 to its high affinity sites shows that it is pH-insensitive over the range in which the [^{3}H]-PN200-110 molecules are neutral (i.e. pH of 6-10). This suggests that over this pH range, ionizable amino acids within the binding domain do not contribute significantly to the binding interaction. The changes in the binding density seen at extremes of pH (pH<6, pH>10) may be due to protein denaturation (Hill, 1965). Our studies have also shown that the binding of amlodipine to its high affinity sites is pH-sensitive over the range in which the degree of protonation of amlodipine is expected to change. Amlodipine has a pKa of 8.7, and thus is mostly charged (protonated) at physiological pH and neutral in more alkaline solutions. Our studies show that the binding affinity is high when most of the amlodipine molecules are neutral and is reduced when the protonated portion of amlodipine molecules increases. Since [^{3}H]-PN200-110 binding was unaffected over this pH range, it is unlikely that

changes in the ionization of amino acids within the binding sites contribute to the observed effects. The pH-dependence of amlodipine binding occurs at lower pH than would be predicted from its pKa value (8.7). This lack of direct correlation between binding affinity and the relative amount of protonated species may be due to a change in the pKa of amlodipine when bound. In comparison with high affinity binding, the effect of pH on the binding of amlodipine to its low affinity sites is much less. Within a wide pH range (e.g. pH of 5-9), there was little pH dependence although the binding affinity was greatly reduced when the solution was either very acidic (pH = 4) or very basic (pH = 10.66). This effect in the binding affinity at extremes of pH may be due to partial protein denaturation as observed in studies of [^{3}H]-PN200-110 binding (see above).

As mentioned in the Introduction, the location of the high affinity DHP binding sites within the primary structure of the L-channel α_1 subunit has been probed using several biochemical and molecular approaches and a consensus remains to be reached. To resolve the location of the binding sites in native L-channels, electrophysiological studies using permanently charged DHP antagonists have provided very useful information. The DHP binding sites have been shown to be accessible from the extracellular, but not intracellular, side of the cardiac ventricular cell membrane (Kass *et al.*, 1991). Further studies using variable length, permanently charged DHPs have shown that the DHP binding domain is not on the extracellular membrane surface but is probably within the lipid bilayer, approximately 11-14 Å from the extracellular surface (Bangalore *et al.*, 1994). This finding is consistent with the membrane bilayer pathway theory of DHP ligand-receptor interactions proposed by Rhodes *et al.* (1985). According to this theory, the drug first partitions into the membrane and then diffuses laterally through the bilayer to reach its specific receptor sites. The asymmetrical intramembrane location of the binding sites may explain the phenomena we observed in the pH-dependence of amlodipine binding to its high affinity sites. The protonated species, predominating at low pH, may have restricted accessibility to its intramembrane binding sites and thus have reduced affinity.

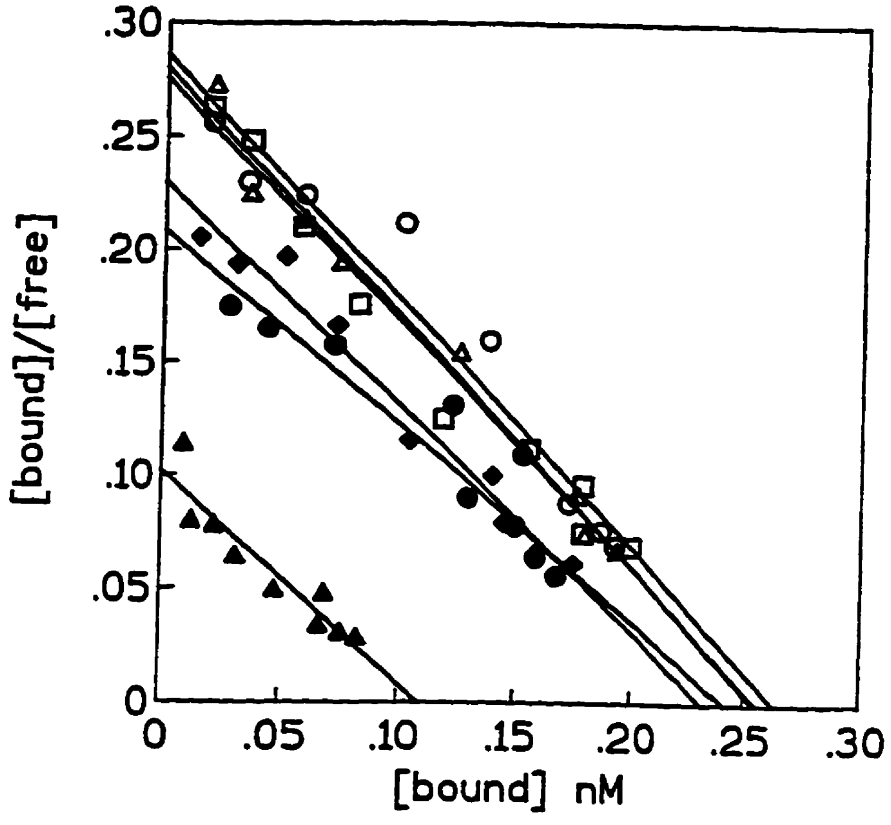

Figure 18. pH-dependence [^{3}H]-PN200-110 binding to skeletal muscle microsomal membranes. Equilibrium binding assay was performed by the filtration method. The binding assay buffer contained 50 mM Tris, 25 mM MES, 25 mM sodium acetate, and 100 mM NaCl. The pH was adjusted to appropriate values with 1 N HCl or 1 N NaOH. K_d values were 1.07 ±0.19 nM, 1.01 ± 0.09 nM, 0.91 ± 0.05 nM, 0.92 ± 0.07 nM, 0.93 ± 0.06 nM, and 1.16 ± 0.11 nM for buffers with pH values of 5 (▲), 6 (◆), 7 (△), 8 (○), 9 (□), and 10 (●), respectively. Correspondingly, the B_{max} values were 0.109 ± 0.018 nM, 0.231 ± 0.022 nM, 0.248 ± 0.019 nM, 0.261 ± 0.021 nM, 0.252 ± 0.017 nM, and 0.239 ± 0.023 nM. The data are representative of three experiments.

Table 5.

Effects of pH on the Binding of Amlodipine to Skeletal Muscle Membranes

pH	K_i (nM)	K_d (μM)
4	ND	6.78 ± 0.48
5	58.49 ± 5.32	3.91 ± 0.31
6	83.13 ± 2.02	2.42 ± 0.10
7	30.26 ± 1.69	1.88 ± 0.05
8	11.08 ± 0.86	1.67 ± 0.06
9	7.06 ± 0.35	1.62 ± 0.05
10/10.66*	11.8 ± 0.55	6.04 ± 0.18*

5. GENERAL DISCUSSION

The best studied of the voltage-dependent Ca^{2+} channels are the L-type channels which are sensitive to 1,4-dihydropyridine derivatives. It has been proposed that, in skeletal muscle, the L-channels may function both as voltage-sensors and as voltage-dependent Ca^{2+} channels. However, the significance of the abundance of these channels in skeletal muscle T-tubules remains to be established.

Specific 1,4-dihydropyridine derivatives have been used as key molecular probes of L-type channels and as powerful therapeutic tools to treat a wide range of cardiovascular disorders (Janis and Triggle, 1990). The underlying ligand-receptor interactions are, however, complex and far from understood.

In skeletal muscle, DHPs appear to affect both the voltage sensor and Ca^{2+} channel functions of the L-channels (Lamb, 1992). However, there is a discrepancy between the high concentrations of DHPs required to affect functional properties and the much lower concentrations required to saturate the high affinity sites that are measured in radiolabelled ligand binding studies (Triggle and Janis, 1987). This cannot readily be explained by a state-dependence of DHP-binding as is found in cardiac muscle (Janis and Triggle, 1990).

Our present studies confirm previous reports of the presence of low affinity DHP binding sites which are allosterically coupled to the high affinity sites in skeletal muscle T-tubule membranes. More importantly, we provide solid evidence that the sites are present on the purified Ca^{2+} channel protein complex and not on another, interacting but unrelated, protein. Thus, an alternative explanation for the discrepancy between functional studies and the binding data is the presence of the multiple binding sites in skeletal muscle, whose occupancy has different effects on Ca^{2+} channel function.

The functional significance of both high and low affinity sites remains to be established. A previous finding that different concentrations of DHPs were required to block charge movements and Ca^{2+} conductance suggests the possibility that the high and low affinity sites modulate voltage sensors and Ca^{2+} channels, respectively (Rios and Pizarro, 1991). In addition, other studies have suggested that low affinity DHP sites may be involved in modulating the Ca^{2+} released from the SR (Ohkusa, *et al.*, 1991).

Isolated T-tubule membrane vesicles are useful for studies of Ca^{2+} channels in their native membrane-bound state. Extensive studies have shown that isolated T-tubule membrane vesicles are sealed in an inside-out orientation, the membrane potential can be manipulated experimentally, and the membranes contain endogenous protein kinases and G-proteins that may be important for channel modulation (Dunn, 1989). In the present study, an alternative procedure to purify T-tubules by velocity sedimentation has been developed. This procedure is much faster than traditional equilibrium density centrifugation but has similar separation efficiency. Measurements of [$^{45}Ca^{2+}$] fluxes using isolated T-tubule vesicles with rapid filtration techniques suggest that this system is useful for studies of functional responses of the Ca^{2+} channel population as a whole. In order to determine functional significance of multiple DHP binding sites, it will be important to establish the dose-dependence of DHP effects on channel function.

Our current studies on ligand-receptor interactions have exploited both protein fluorescence properties and the unique physiochemical properties of amlodipine. The high fluorescence of the purified Ca^{2+} channel protein and its specific sensitivity to DHP binding suggest that it may be possible to develop spectroscopic techniques to monitor conformational transitions that are associated with voltage-sensing and/or Ca^{2+} channel function (Dunn and Bao, manuscript in preparation). This will be important in gaining further insight into the precise roles of L-channels in skeletal muscle.

6. SUMMARY AND CONCLUSIONS

1. By using velocity sedimentation, T-tubule membrane vesicles have been rapidly (30 min) purified from microsomal membranes of rabbit skeletal muscle with similar efficiency as the traditional equilibrium density centrifugation method.

2. Digitonin is a better detergent than CHAPS for use in solubilizing, purifying and reconstituting the DHP-sensitive Ca^{2+} channel of skeletal muscle.

3. Amlodipine, in aqueous solution, is highly fluorescent with excitation and emission maxima at 375 nm and 450 nm, respectively. T-tubule membranes are themselves highly fluorescent when excited at 290 nm, as is the purified Ca^{2+} channel protein.

4. Low affinity binding of amlodipine to T-tubule membranes can be monitored in three ways: (a) by the enhancement of the amlodipine fluorescence, (b) by energy transfer from membrane protein, and (c) by the quench in the intrinsic fluorescence of protein.

5. Low affinity DHP binding sites with K_d values in the micromolar range are present on the Ca^{2+} channel protein complex and are allosterically coupled to the high affinity binding sites.

6. The intrinsic protein fluorescence of DHP-sensitive Ca^{2+} channels is specifically sensitive to the binding of DHP derivatives. Thus, low affinity binding of non-fluorescent DHPs can be determined by monitoring the changes in protein fluorescence.

7. Binding of amlodipine to its high affinity sites is pH-sensitive while binding of amlodipine to its low affinity is much less pH-dependent.

8. Functional responses of DHP-sensitive Ca^{2+} channels can be studied by using rapid filtration techniques to monitor voltage-dependent [$^{45}Ca^{2+}$] flux responses of isolated T-tubule vesicles on physiologically relevant time scales.

9. In conclusion, we have used fluorescence techniques to demonstrate the presence of low affinity DHP binding sites in the skeletal muscle Ca^{2+} channel. These sites are allosterically coupled to the high affinity sites. The low affinity binding of non-fluorescent DHP derivatives can be directly monitored by their ability to quench the fluorescence of the Ca^{2+} channel protein. T-tubule membranes, enriched in DHP-sensitive Ca^{2+} channels, can be quickly and efficiently isolated from skeletal muscle microsomal membranes. Isolated T-tubule membranes are useful for studies of ligand binding and VDCC function.

7. REFERENCES

Adams, B. A., T. Tanabe, A. Mikami, S. Numa, and K. G. Beam. 1990. Intramembrane charge movement restored in dysgenic skeletal muscle by injection of dihydropyridine receptor cDNAs. *Nature.* **346:**569-72.

Adams, B. A., and K. G. Beam. 1990. Muscular dysgenesis in mice: a model system for studying excitation-contraction coupling. *Faseb J.* **4:**2809-16.

Affolter, H., and R. Coronado. 1985. Agonists Bay-K8644 and CGP-28392 open calcium channels reconstituted from skeletal muscle transverse tubules. *Biophys J.* **48:**341-7.

Almers, W. 1989. Excitation-contraction coupling in skeletal muscle. In: *Textbook of Physiology.* (Eds: Patton, H. D., A. F. Fuchs, B. Hille, A. M. Scher, and R. Steiner.). W. B. Saunders Company. 21st Ed. pp156-170.

Anderson, K., and G. Meissner. 1995. T-tubule depolarization-induced SR Ca^{2+} release is controlled by dihydropyridine receptor- and Ca^{2+}-dependent mechanisms in cell homogenates from rabbit skeletal muscle. *J Gen Physiol.* **105:**363-83.

Armstrong, C. M., F. M. Bezanilla, and P. Horowicz. 1972. Twitches in the presence of ethylene glycol bis(-aminoethyl ether)-N,N'-tetracetic acid. *Biochim Biophys Acta.* **267:**605-8.

Arreola, J., J. Calvo, M. C. Garcia, and J. A. Sanchez. 1987. Modulation of calcium channels of twitch skeletal muscle fibres of the frog by adrenaline and cyclic adenosine monophosphate. *J Physiol (Lond).* **393:**307-30.

Bangalore, R., N. Baindur, A. Rutledge, D. J. Triggle, and R. S. Kass. 1994. L-type calcium channels: Asymmetrical intramembrane binding domain revealed by variable length, permanently charged 1,4-dihydropyridines. *Mol Pharmacol..* **46:**660-666.

Barhanin, J., T. Coppola, A. Schmid, M. Borsotto, and M. Lazdunski. 1987. The calcium channel antagonists receptor from rabbit skeletal muscle. Reconstitution after purification and subunit characterization. *Eur J Biochem.* **164:**525-31.

Beam, K. G., C. M. Knudson, and J. A. Powell. 1986. A lethal mutation in mice eliminates the slow calcium current in skeletal muscle cells. *Nature.* **320:**168-170.

Beam, K. G., B. A. Adams, T. Niidome, S. Numa, and T. Tanabe. 1992. Function of a truncated dihydropyridine receptor as both voltage sensor and calcium channel. *Nature.* **360:**169-71.

Bean, B. P. 1989. Classes of calcium channels in vertebrate cells. *Annu Rev Physiol.* **51:**367-84.

Beaty, G. N., G. Cota, L. Nicola Siri, J. A. Sanchez, and E. Stefani. 1987. Skeletal muscle Ca^{2+} channels. In: *Structure and Physiology of the Slow Inward Calcium Channel.* (Eds: Venter, J. C. and D. J. Triggle.). Alan R. Liss. New York. pp123-140.

Belles, B., J. Hescheler, W. Trautwein, K. Blomgren, and J. O. Karlsson. 1988. A possible physiological role of the Ca-dependent protease calpain and its inhibitor calpastatin on the Ca current in guinea pig myocytes. *Pflugers Arch.* **412:**554-6.

Benham, C. D., and R. W. Tsien. 1987. A novel receptor-operated Ca^{2+}-permeable channel activated by ATP in smooth muscle. *Nature.* **328:**275-8.

Bertolino, M., and R. R. Llinas. 1992. The central role of voltage-activated and receptor-operated calcium channels in neuronal cells. *Annu Rev Pharmacol Toxicol.* **32:**399-421.

Bhat, M. B. 1993. DHP-binding proteins of skeletal muscle. *M.Sc. thesis.*

Bird, G. S., M. F. Rossier, A. R. Hughes, S. B. Shears, D. L. Armstrong, and J. W. Putney, Jr. 1991. Activation of Ca^{2+} entry into acinar cells by a non-phosphorylatable inositol trisphosphate [see comments]. *Nature.* **352:**162-5.

Borsotto, M., J. Barhanin, M. Fosset, and M. Lazdunski. 1985. The 1,4-dihydropyridine receptor associated with the skeletal muscle voltage-dependent Ca^{2+} channel. Purification and subunit composition. *J Biol Chem.* **260:**14255-63.

Bosse, E., S. Regulla, M. Biel, P. Ruth, H. E. Meyer, V. Flockerzi, and F. Hofmann. 1990. The cDNA and deduced amino acid sequence of the gamma subunit of the L-type calcium channel from rabbit skeletal muscle. *FEBS Lett.* **267:**153-6.

Bradshaw, C. R. and D. A. Harris. 1987. Measure of ligand binding to protein, In: *Spectrophotometry and spectrofluorimetry, a practical approach* (Eds: D. A. Harris and C. L. Bashford.). IRL Press. Oxford. pp91-113.

Brown, A. M., D. L. Kunze, and A. Yatani. 1986. Dual effects of dihydropyridines on whole cell and unitary calcium currents in single ventricular cells of guinea-pig. *J Physiol (Lond).* **379:**495-514.

Brown, A. M., A. Yatani, Y. Imoto, J. Codina, R. Mattera, and L. Birnbaumer. 1989. Direct G-protein regulation of Ca^{2+} channels. *Ann N Y Acad Sci.* **560:**373-86.

Burges, R. A. 1992. Review of the pharmacology of amlodipine. *J Cardiovasc Pharmacol.* **20(Suppl.A):**S1-S5.

Cadwell, J. J., and A. H. Caswell. 1982. Identification of a constituent of the junctional feet linking terminal cisternae to transverse tubules in skeletal muscle. *J Cell Biol.* **93:**543-50

Campbell, K. P., A. T. Leung, and A. H. Sharp. 1988. The biochemistry and molecular biology of the dihydropyridine-sensitive calcium channel. *Trends Neurosci.* **11:**425-30.

Carafoli, E. 1987. Intracellular calcium homeostasis. *Annu Rev Biochem.* **56:**395-433.

Carbone, E., and D. Swandulla. 1989. Neuronal calcium channels: kinetics, blockade and modulation. *Prog Biophys Mol Biol.* **54:**31-58.

Catterall, W. A. 1988. Structure and function of voltage-sensitive ion channels. *Science.* **242:**50-61.

Catterall, W. A. 1991. Structure and function of voltage-gated sodium and calcium channels. *Curr Opin Neurobiol.* **1:**5-13.

Catterall, W. A. 1994. Molecular properties of a superfamily of plasma-membrane cation channels. *Current Opinion in Cell Biology.* **6:**607-15.

Catterall, W. A., and J. Striessnig. 1992. Receptor sites for Ca^{2+} channel antagonists. *Trends in Pharmacological Sciences.* **13:**256-62.

Catterall, W. A. 1995. Structure and function of voltage-gated ion channels. *Annual Review of Biochemistry.* **64:**493-531.

Chad, J. E. 1989. Inactivation of calcium channels. *Comp. Biochem. Physio.* **93A:**95-105.

Curtis, B. M., and W. A. Catterall. 1984. Purification of the calcium antagonist receptor of the voltage-sensitive calcium channel from skeletal muscle transverse tubules. *Biochemistry.* **23:**2113-8.

Curtis, B. M., and W. A. Catterall. 1985. Phosphorylation of the calcium antagonist receptor of the voltage-sensitive calcium channel by cAMP-dependent protein kinase. *Proc Natl Acad Sci U S A.* **82:**2528-32.

Curtis, B. M., and W. A. Catterall. 1986. Reconstitution of the voltage-sensitive calcium channel purified from skeletal muscle transverse tubules. *Biochemistry.* **25:**3077-83.

De Jongh, K. S., D. K. Merrick, and W. A. Catterall. 1989. Subunits of purified calcium channels: a 212-kDa form of alpha 1 and partial amino acid sequence of a phosphorylation site of an independent beta subunit. *Proc Natl Acad Sci U S A.* **86:**8585-9.

De Jongh, K. S., C. Warner, and W. A. Catterall. 1990. Subunits of purified calcium channels. Alpha 2 and delta are encoded by the same gene. *J Biol Chem.* **265:**14738-41.

De Jongh, K. S., C. Warner, A. A. Colvin, and W. A. Catterall. 1991. Characterization of the two size forms of the alpha 1 subunit of skeletal muscle L-type calcium channels. *Proc Natl Acad Sci U S A.* **88:**10778-82.

De Jongh, K. S., A. A. Colvin, K. K. Wang, and W. A. Catterall. 1994. Differential proteolysis of the full-length form of the L-type calcium channel alpha 1 subunit by calpain. *Journal of Neurochemistry.* **63:**1558-64.

Dirksen, R. T., and K. G. Beam. 1995. Single calcium channel behavior in native skeletal muscle. *J Gen Physiol.* **105:**227-47.

Dulhunty, A. F., and P. W. Gage. 1988. Effects of extracellular calcium concentration and dihydropyridines on contraction in mammalian skeletal muscle. *J Physiol (Lond).* **399:**63-80.

Dunn, S. M. J. 1989. Voltage-dependent calcium channels in skeletal muscle transverse tubules. Measurements of calcium efflux in membrane vesicles. *J Biol Chem.* **264:**11053-60.

Dunn, S. M. J., and C. Bladen. 1991. Kinetics of binding of dihydropyridine calcium channel ligands to skeletal muscle membranes: evidence for low-affinity sites and for the involvement of G proteins. *Biochemistry.* **30:**5716-21.

Dunn, S. M. J., and C. Bladen. 1992. Low-affinity binding sites for 1,4-dihydropyridines in skeletal muscle transverse tubule membranes revealed by changes in the fluorescence of felodipine. *Biochemistry.* **31:**4039-45.

Dunn, S. M. J., M. B. Bhat, and M. A. Oz. 1993. Molecular structure and gating of calcium channels. In: *Ion Channels and Ion Transport.* (Eds: Foa, P. P. and Walsh, M.). Springer-Verlag, New York. pp1-18.

Dunn, S. M. J. and D. Bao. manuscript preparation. Amlodipine binding to skeletal muscle transverse tubule membranes: Evidence for low affinity 1,4-dihydropyridine binding sites associated with L-type calcium channels.

Dunn, S. M. J. and C. Bladen. manuscript preparation. Stability of high and low affinity sites for 1,4-dihydropyridines in skeletal muscle transverse tubule membranes: Implication for binding site locations.

El-Hayek, R., B. Antoniu, J. Wang, S. L. Hamilton, and N. Ikemoto. 1995. Identification of calcium release-triggering and blocking regions of the II-III loop of the skeletal muscle dihydropyridine receptor. *J Biol Chem.* **270:**22116-8.

Ellis, K. J. and J. F. Morrison. 1982. Buffers of constant ionic strength for studying pH-dependent processes. *Methods Enzymol.* **87**:405-426.

Ellis, S. B., M. E. Williams, N. R. Ways, R. Brenner, A. H. Sharp, A. T. Leung, K. P. Campbell, E. McKenna, W. J. Koch, A. Hui, and et al. 1988. Sequence and expression of mRNAs encoding the alpha 1 and alpha 2 subunits of a DHP-sensitive calcium channel. *Science.* **241**:1661-4.

Felder, C. C., D. Singer-Lahat, and C. Mathes. 1994. Voltage-independent calcium channels. Regulation by receptors and intracellular calcium stores. *Biochem Pharmacol.* **48**:1997-2004.

Flockerzi, V., H. J. Oeken, F. Hofmann, D. Pelzer, A. Cavalie, and W. Trautwein. 1986. Purified dihydropyridine-binding site from skeletal muscle T-tubules is a functional calcium channel. *Nature.* **323**:66-8.

Florio, V., J. Striessnig, and W. A. Catterall. 1992. Purification and reconstitution of skeletal muscle calcium channels. *Methods in Enzymology.* **207**:529-46.

Fosset, M., E. Jaimovich, E. Delpont, and M. Lazdunski. 1983. [^{3}H]nitrendipine receptors in skeletal muscle. *J Biol Chem.* **258**:6086-92.

Fox, A. P., M. C. Nowycky, and R. W. Tsien. 1987a. Single-channel recordings of three types of calcium channels in chick sensory neurones. *J Physiol (Lond).* **394**:173-200.

Fox, A. P., M. C. Nowycky, and R. W. Tsien. 1987b. Kinetic and pharmacological properties distinguishing three types of calcium currents in chick sensory neurones. *J Physiol (Lond).* **394**:149-72.

Frank, G. B. 1982. Roles of extracellular and "trigger" calcium ions in excitation--contraction coupling in skeletal muscle. *Can J Physiol Pharmacol.* **60**:427-39.

Frank, G. B., and M. Oz. 1992. The functional role of t-tubular calcium channels in skeletal muscle contractions. *Adv Exp Med Biol.* **311**:123-36.

Galizzi, J. P., M. Borsotto, J. Barhanin, M. Fosset, and M. Lazdunski. 1986. Characterization and photoaffinity labeling of receptor sites for the Ca^{2+} channel inhibitors d-cis-diltiazem, (+/-)-bepridil, desmethoxyverapamil, and (+)-PN 200-110 in skeletal muscle transverse tubule membranes. *J Biol Chem.* **261**:1393-7.

Ghosh, P. B. and M. W. Whitehouse. 1968. 7-Chloro-4-nitrobenzo-2-oxa-1,3-diazole: A new fluorigenic agent for amino acids and other amines. *Biochem J.* **108**:155-156.

Gonzalez Burgos, G. R., F. I. Biali, B. D. Cherksey, M. Sugimori, R. R. Llinas, and O. D. Uchitel. 1995. Different calcium channels mediate transmitter release evoked by transient or sustained depolarization at mammalian sympathetic ganglia. *Neuroscience.* **64**:117-23.

Gutierrez, L. M., R. M. Brawley, and M. M. Hosey. 1991. Dihydropyridine-sensitive calcium channels from skeletal muscle I. roles of subunits in channel activity. *J Biol Chem.* **266:**16387-16394.

Hamilton, S. L., M. J. Hawkes, K. Brush, and R. Cook. 1989. Subunit composition of the purified dihydropyridine binding protein from skeletal muscle. *Biochemistry.* **28:**7820-7828.

Hamilton, S. L., J. Codina, M. J. Hawkes, A. Yatani, T. Sawada, F. M. Strickland, S. C. Froehner, A. M. Spiegel, L. Toro, E. Stefani, and et al. 1991. Evidence for direct interaction of Gs alpha with the Ca^{2+} channel of skeletal muscle. *J Biol Chem.* **266:**19528-35.

Heinemann, S. H., T. Schlief, Y. Mori, and K. Imoto. 1994. Molecular pore structure of voltage-gated sodium and calcium channels. *Braz J Med Biol Res.* **27:**2781-802.

Hess, P. 1990. Calcium channels in vertebrate cells. *Annu Rev Neurosci.* **13:**337-56.

Hidalgo, C., C. Parra, G. Riquelme, and E. Jaimovich. 1986. Transverse tubules from frog skeletal muscle: purification and properties of vesicles sealed with the inside-out orientaion. *Biochem Biophys Acta.* **855:**79-88.

Hill, R. L. 1965. Hydrolysis of protein. *Adv Protein Chem.* **20:**37-107.

Hillman, D., S. Chen, T. T. Aung, B. Cherksey, M. Sugimori, and R. R. Llinas. 1991. Localization of P-type calcium channels in the central nervous system. *Proc Natl Acad Sci U S A.* **88:**7076-80.

Hockerman, G. H., B. D. Johnson, T. Scheuer, and W. A. Catterall. 1995. Molecular determinants of high affinity phenylalkylamine block of L-type calcium channels. *Journal of Biological Chemistry.* **270:**22119-22.

Hoffman, E. P. 1995. Voltage-gated ion channelopathies: inherited disorders caused by abnormal sodium, chloride, and calcium regulation in skeletal muscle. *Annu Rev Med.* **46:**431-41.

Hofmann, F., M. Biel, and V. Flockerzi. 1994. Molecular basis for Ca^{2+} channel diversity. *Annu Rev Neurosci.* **17:**399-418.

Hosey, M. M., and M. Lazdunski. 1988. Calcium channels: molecular pharmacology, structure and regulation. *J Membr Biol.* **104:**81-105.

Hymel, L., J. Striessnig, H. Glossmann, and H. Schindler. 1988. Purified skeletal muscle 1,4-dihydropyridine receptor forms phosphorylation-dependent oligomeric calcium channels in planar bilayers. *Proc Natl Acad Sci U S A.* **85:**4290-4.

Isom, L. L., K. S. De Jongh, and W. A. Catterall. 1994. Auxiliary subunits of voltage-gated ion channels. *Neuron.* **12:**1183-94.

Jahn, H., W. Nastainczyk, A. Rohrkasten, T. Schneider, and F. Hofmann. 1988. Site-specific phosphorylation of the purified receptor for calcium-channel blockers by cAMP- and cGMP-dependent protein kinases, protein kinase C, calmodulin-dependent protein kinase II and casein kinase II. *Eur J Biochem.* **178:**535-42.

Janis, R. A. and D. J. Triggle. 1990. Drugs acting on calcium channels. In: *Calcium Channels: Their Properties, Functions, Regulation and Clinical Relevance.* (Eds: Hurwitz, L., Partridge, L. D. and Leach, J. F.). CRC Press. Boca Raton, FL. pp195-249.

Jay, S. D., S. B. Ellis, A. F. McCue, M. E. Williams, T. S. Vedvick, M. M. Harpold, and K. P. Campbell. 1990. Primary structure of the gamma subunit of the DHP-sensitive calcium channel from skeletal muscle. *Science.* **248:**490-2.

Jay, S. D., A. H. Sharp, S. D. Kahl, T. S. Vedvick, M. M. Harpold, and K. P. Campbell. 1991. Structural characterization of the dihydropyridine-sensitive calcium channel alpha 2-subunit and the associated delta peptides. *J Biol Chem.* **266:**3287-93.

Jeng, A. Y., P. A. St. John, and J. B. Cohen. 1981. Fractionation by velocity sedimentation of *Torpedo* nicotinic post-synaptic membranes. *Biochi Biophy Acta.* **646:**411-421.

Kass, R. S., and J. P. Arena. 1989. Influence of pHo on calcium channel block by amlodipine, a charged dihydropyridine compound. Implications for location of the dihydropyridine receptor. *J Gen Physiol.* **93:**1109-27.

Kass, R. S., J. P. Arena, and S. Chin. 1989. Modulation of calcium channels by charged and neutral dihydropyridines. *Ann N Y Acad Sci.* **560:**189-97.

Kass, R. S., J. P. Arena, and S. Chin. 1991. Block of L-type calcium channels by charged dihydropyridines. Sensitivity to side of application and calcium. *J Gen Physiol.* **98:**63-75.

Kim, K. C., A. H. Caswell, J. P. Brunschwig, and N. R. Brandt. 1990. Identification of a new subpopulation of triad junctions isolated from skeletal muscle; morphological correlations with intact muscle. *J Membr Biol.* **113:**221-35.

Kostyuk, P. G. 1989. Diversity of calcium ion channels in cellular membranes. *Neuroscience.* **28:**253-61.

Kraus, R., B. Reichl, M. Grabner, S. D. Kimball, B. J. Murphy, W. A. Catterall, and J. Striessnig. 1996. Identification of benzothiazepine binding regions within L-type calcium channel alpha1 subunits. *Society for Neuroscience.* **22:**344 (Abstract 140.6).

Kuniyasu, A., N. Yoshida, H. Yabana, K. Naito, K. Itagaka, A. Schwartz, and H. Nakayama. 1996. Identification of benzothiazepine regions within the α_1 subunit of calcium channels. *Society for Neuroscience.* **22:**344 (Abstract 140.8).

Kwan, Y. W., R. Bangalore, M. Lakitsh, H. Glossmann, and R. S. Kass. 1995. Inhibition of cardiac L-type calcium channels by quaternary amlodipine: implications for pharmacokinetics and access to dihydropyridine binding site. *J Mol Cell Cardiol.* **27:**253-62.

Laemmli, U.K. 1970. Cleavage of structural proteins during the assembly of the head of bacteriophage T4. *Nature.* **227:**680-5.

Lacerda, A. E., H. S. Kim, P. Ruth, E. Perez-Reyes, V. Flockerzi, F. Hofmann, L. Birnbaumer, and A. M. Brown. 1991. Normalization of current kinetics by interaction between the alpha 1 and beta subunits of the skeletal muscle dihydropyridine-sensitive Ca^{2+} channel. *Nature.* **352:**527-30.

Lai, Y., M. J. Seagar, M. Takahashi, and W. A. Catterall. 1990. Cyclic AMP-dependent phosphorylation of two size forms of alpha 1 subunits of L-type calcium channels in rat skeletal muscle cells. *J Biol Chem.* **265:**20839-48.

Lai, Y., B. Z. Peterson, and W. A. Catterall. 1993. Selective dephosphorylation of the subunits of skeletal muscle calcium channels by purified phosphoprotein phosphatases. *Journal of Neurochemistry.* **61:**1333-9.

Lamb, G. D. 1991. Ca^{2+} channels or voltage-sensors? *Nature.* **352:**113.

Lamb, G. D. 1992. DHP receptors and excitation-contraction coupling. *J Muscle Res Cell Motil.* **13:**394-405.

Lau, Y. H., A. H. Caswell, and J. P. Brunschwig. 1977. Isolation of transverse tubules by fractionation of triad junctions of skeletal muscle. *J Biol Chem.* **252:**5565-74.

Llinas, R. R. 1988. The intrinsic electrophysiological properties of mammalian neurons: insights into central nervous system function. *Science.* **242:**1654-64.

Llinas, R. R., M. Sugimori, and B. Cherksey. 1989. Voltage-dependent calcium conductances in mammalian neurons. The P channel. *Ann N Y Acad Sci.* **560:**103-11.

Ma, J., C. Mundina-Weilenmann, M. M. Hosey, and E. Rios. 1991. Dihydropyridine-sensitive skeletal muscle Ca channels in polarized planar bilayers. 1. Kinetics and voltage dependence of gating. *Biophys J.* **60:**890-901.

McCleskey, E. W. 1994. Calcium channels: cellular roles and molecular mechanisms. *Curr Opin Neurobiol.* **4:**304-12.

Melzer, W., M. F. Schneider, B. J. Simon, and G. Szucs. 1986. Intramembrane charge movement and calcium release in frog skeletal muscle. *J Physiol (Lond).* **373:**481-511.

Mikami, A., K. Imoto, T. Tanabe, T. Niidome, Y. Mori, H. Takeshima, S. Narumiya, and S. Numa. 1989. Primary structure and functional expression of the cardiac dihydropyridine-sensitive calcium channel. *Nature.* **340:**230-3.

Miller, R. J. 1992. Voltage-sensitive Ca^{2+} channels. *J Biol Chem.* **267:**1403-6.

Mintz, I. M., V. J. Venema, K. M. Swiderek, T. D. Lee, B. P. Bean, and M. E. Adams. 1992. P-type calcium channels blocked by the spider toxin omega-Aga-IVA. *Nature.* **355:**827-9.

Mitterdorfer, J., M. Froschmayr, M. Grabner, J. Striessnig, and H. Glossmann. 1994. Calcium channels: the beta-subunit increases the affinity of dihydropyridine and Ca^{2+} binding sites of the alpha 1-subunit. *FEBS Lett.* **352:**141-5.

Mitterdorfer, J., M. J. Sinnegger, M. Grabner, J. Striessnig, and H. Glossmann. 1995. Coordination of Ca^{2+} by the pore region glutamates is essential for high-affinity dihydropyridine binding to the cardiac Ca^{2+} channel alpha 1 subunit. *Biochemistry.* **34:**9350-5.

Mori, Y., T. Friedrich, M. S. Kim, A. Mikami, J. Nakai, P. Ruth, E. Bosse, F. Hofmann, V. Flockerzi, T. Furuichi, and et al. 1991. Primary structure and functional expression from complementary DNA of a brain calcium channel. *Nature.* **350:**398-402.

Mundina-Weilenmann, C., C. F. Chang, L. M. Gutierrez, and M. M. Hosey. 1991. Demonstration of the phosphorylation of dihydropyridine-sensitive calcium channels in chick skeletal muscle and the resultant activation of the channels after reconstitution. *J Biol Chem.* **266:**4067-73.

Naito, K., E. McKenna, A. Schwartz, and P. L. Vaghy. 1989. Photoaffinity labeling of the purified skeletal muscle calcium antagonist receptor by a novel benzothiazepine, [3H]azidobutyryl diltiazem. *J Biol Chem.* **264:**21211-4.

Nakai, J., R. T. Dirksen, H. T. Nguyen, I. N. Pessah, K. G. Beam, and P. D. Allen. 1996. Enhanced dihydropyridine receptor channel activity in the presence of ryanodine receptor. *Nature.* **380:**72-5.

Nakayama, H., M. Taki, J. Striessnig, H. Glossmann, W. A. Catterall, and Y. Kanaoka. 1991. Identification of 1,4-dihydropyridine binding regions within the alpha 1 subunit of skeletal muscle Ca^{2+} channels by photoaffinity labeling with diazipine. *Proc Natl Acad Sci U S A.* **88:**9203-7.

Nishimura, S., H. Takeshima, F. Hofmann, V. Flockerzi, and K. Imoto. 1993. Requirement of the calcium channel beta subunit for functional conformation. *FEBS Lett.* **324**:283-6.

Nunoki, K., V. Florio, and W. A. Catterall. 1989. Activation of purified calcium channels by stoichiometric protein phosphorylation. *Proc Natl Acad Sci U S A.* **86**:6816-20.

O'Callahan, C. M., and M. M. Hosey. 1988. Multiple phosphorylation sites in the 165-kilodalton peptide associated with dihydropyridine-sensitive calcium channels. *Biochemistry.* **27**:6071-7.

O'Callahan, C. M., J. Ptasienski, and M. M. Hosey. 1988. Phosphorylation of the 165-kDa dihydropyridine/phenylalkylamine receptor from skeletal muscle by protein kinase C. *J Biol Chem.* **263**:17342-9.

Ohkusa, T., A. D. Carlos, J. J. Kang, H. Smilowitz, and N. Ikemoto. 1991. Effects of dihydropyridines on calcium release from the isolated membrane complex consisting of the transverse tubule and sarcoplasmic reticulum [published erratum appears in Biochem Biophys Res Commun 1991 Apr 15;176(1):549]. *Biochem Biophys Res Commun.* **175**:271-6.

Olivera, B. M., W. R. Gray, R. Zeikus, J. M. McIntosh, J. Varga, J. Rivier, V. de Santos, and L. J. Cruz. 1985. Peptide neurotoxins from fish-hunting cone snails. *Science.* **230**:1338-43.

Pelzer, D., A. O. Grant, A. Cavalie, S. Pelzer, M. Sieber, F. Hofmann, and W. Trautwein. 1989. Calcium channels reconstituted from the skeletal muscle dihydropyridine receptor protein complex and its alpha 1 peptide subunit in lipid bilayers. *Ann N Y Acad Sci.* **560**:138-54.

Pelzer, D., S. Pelzer, and T. F. McDonald. 1990. Properties and regulation of calcium channels in muscle cells. *Rev Physiol Biochem Pharmacol.* **114**:107-207.

Perez-Reyes, E., H. S. Kim, A. E. Lacerda, W. Horne, X. Y. Wei, D. Rampe, K. P. Campbell, A. M. Brown, and L. Birnbaumer. 1989. Induction of calcium currents by the expression of the alpha 1-subunit of the dihydropyridine receptor from skeletal muscle. *Nature.* **340**:233-6.

Perez-Reyes, E., and T. Schneider. 1995. Molecular biology of calcium channels. *Kidney Int.* **48**:1111-24.

Peterson, B. Z., and W. A. Catterall. 1995. Calcium binding in the pore of L-type calcium channels modulates high affinity dihydropyridine binding. *Journal of Biological Chemistry.* **270**:18201-4.

Peterson, B. Z., T. N. Tanada, and W. A. Catterall. 1996. Molecular determinants of high affinity dihydropyridine binding in L-type calcium channels. *Journal of Biological Chemistry.* **271:**5293-6.

Plummer, M. R., D. E. Logothetis, and P. Hess. 1989. Elementary properties and pharmacological sensitivities of calcium channels in mammalian peripheral neurons. *Neuron.* **2:**1453-63.

Pragnell, M., M. De Waard, Y. Mori, T. Tanabe, T. P. Snutch, and K. P. Campbell. 1994. Calcium channel beta-subunit binds to a conserved motif in the I-II cytoplasmic linker of the alpha 1-subunit [see comments]. *Nature.* **368:**67-70.

Regulla, S., T. Schneider, W. Nastainczyk, H. E. Meyer, and F. Hofmann. 1991. Identification of the site of interaction of the dihydropyridine channel blockers nitrendipine and azidopine with the calcium-channel alpha 1 subunit. *Embo J.* **10:**45-9.

Rhodes, D. G., J. G. Sarmiento, and L. G. Herbette. 1985. Kinetics of binding of membrane-active drugs to receptor sites. Diffusion limited rateds for a membrane bilayer approach of 1,4-dihydropyridine calcium channel antagonist to their active site. *Mol Pharmacol.* **27:**612-623.

Rios, E., and G. Brum. 1987. Involvement of dihydropyridine receptors in excitation-contraction coupling in skeletal muscle. *Nature.* **325:**717-20.

Rios, E., and G. Pizarro. 1991. Voltage sensor of excitation-contraction coupling in skeletal muscle. *Physiol Rev.* **71:**849-908.

Romanin, C., M. Reinsprecht, I. Pecht, and H. Schindler. 1991. Immunologically activated chloride channels involved in degranulation of rat mucosal mast cells. *Embo J.* **10:**3603-8.

Rosemblatt, M., C. Hidalgo, C. Vergara, and N. Ikemoto. 1981. Immunological and biochemical properties of transverse tubule membranes isolated from rabbit skeletal muscle. *J Biol Chem.* **256:**8140-8148.

Ruth, P., A. Rohrkasten, M. Biel, E. Bosse, S. Regulla, H. E. Meyer, V. Flockerzi, and F. Hofmann. 1989. Primary structure of the beta subunit of the DHP-sensitive calcium channel from skeletal muscle. *Science.* **245:**1115-8.

Sanguinetti, M. C., and R. S. Kass. 1984a. Regulation of cardiac calcium channel current and contractile activity by the dihydropyridine Bay K 8644 is voltage-dependent. *J Mol Cell Cardiol.* **16:**667-70.

Sanguinetti, M. C., and R. S. Kass. 1984b. Voltage-dependent block of calcium channel current in the calf cardiac Purkinje fiber by dihydropyridine calcium channel antagonists. *Circ Res.* **55:**336-48.

Schneider, M. F., and W. K. Chandler. 1973. Voltage dependent charge movement of skeletal muscle: a possible step in excitation-contraction coupling. *Nature.* **242:**244-6.

Schwartz, L. M., E. W. McCleskey, and W. Almers. 1985. Dihydropyridine receptors in muscle are voltage-dependent but most are not functional calcium channels. *Nature.* **314:**747-51.

Sculptoreanu, A., E. Rotman, M. Takahashi, T. Scheuer, and W. A. Catterall. 1993. Voltage-dependent potentiation of the activity of cardiac L-type calcium channel alpha 1 subunits due to phosphorylation by cAMP-dependent protein kinase. *Proc Natl Acad Sci U S A.* **90:**10135-9.

Singer, D., M. Biel, I. Lotan, V. Flockerzi, F. Hofmann, and N. Dascal. 1991. The roles of the subunits in the function of the calcium channel. *Science.* **253:**1553-7.

Snutch, T. P., and P. B. Reiner. 1992. Ca^{2+} channels: diversity of form and function. *Curr Opin Neurobiol.* **2:**247-53.

Stanley, E. F., and A. H. Atrakchi. 1990. Calcium currents recorded from a vertebrate presynaptic nerve terminal are resistant to the dihydropyridine nifedipine. *Proc Natl Acad Sci U S A.* **87:**9683-7.

Starr, T. V., W. Prystay, and T. P. Snutch. 1991. Primary structure of a calcium channel that is highly expressed in the rat cerebellum. *Proc Natl Acad Sci U S A.* **88:**5621-5.

Striessnig, J., K. Moosburger, A. Goll, D. R. Ferry, and H. Glossmann. 1986. Stereoselective photoaffinity labelling of the purified 1,4-dihydropyridine receptor of the voltage-dependent calcium channel. *Eur J Biochem.* **161:**603-9.

Striessnig, J., H. G. Knaus, M. Grabner, K. Moosburger, W. Seitz, H. Lietz, and H. Glossmann. 1987. Photoaffinity labelling of the phenylalkylamine receptor of the skeletal muscle transverse-tubule calcium channel. *FEBS Lett.* **212:**247-53.

Striessnig, J., H. Glossmann, and W. A. Catterall. 1990. Identification of a phenylalkylamine binding region within the alpha 1 subunit of skeletal muscle Ca^{2+} channels. *Proc Natl Acad Sci U S A.* **87:**9108-12.

Striessnig, J., F. Scheffauer, J. Mitterdorfer, M. Schirmer, and H. Glossmann. 1990. Identification of the benzothiazepine-binding polypeptide of skeletal muscle calcium channels with (+)-cis-azidodiltiazem and anti-ligand antibodies. *J Biol Chem.* **265:**363-70.

Striessnig, J., B. J. Murphy, and W. A. Catterall. 1991. Dihydropyridine receptor of L-type Ca^{2+} channels: identification of binding domains for [^{3}H](+)-PN200-110 and [^{3}H]azidopine within the alpha 1 subunit. *Proc Natl Acad Sci U S A.* **88:**10769-73.

Striessnig, J. and H. Glossmann. 1991. Purification of L-type calcium channel drug receptors. *Methods in Neurosciences.* **4**:210-228.

Takahashi, M., M. J. Seagar, J. F. Jones, B. F. Reber, and W. A. Catterall. 1987. Subunit structure of dihydropyridine-sensitive calcium channels from skeletal muscle. *Proc Natl Acad Sci U S A.* **84**:5478-82.

Tanabe, T., H. Takeshima, A. Mikami, V. Flockerzi, H. Takahashi, K. Kangawa, M. Kojima, H. Matsuo, T. Hirose, and S. Numa. 1987. Primary structure of the receptor for calcium channel blockers from skeletal muscle. *Nature.* **328**:313-8.

Tanabe, T., K. G. Beam, J. A. Powell, and S. Numa. 1988. Restoration of excitation-contraction coupling and slow calcium current in dysgenic muscle by dihydropyridine receptor complementary DNA. *Nature.* **336**:134-9.

Tanabe, T., A. Mikami, S. Numa, and K. G. Beam. 1990a. Cardiac-type excitation-contraction coupling in dysgenic skeletal muscle injected with cardiac dihydropyridine receptor cDNA. *Nature.* **344**:451-3.

Tanabe, T., K. G. Beam, B. A. Adams, T. Niidome, and S. Numa. 1990b. Regions of the skeletal muscle dihydropyridine receptor critical for excitation-contraction coupling. *Nature.* **346**:567-9.

Tang, C. M., F. Presser, and M. Morad. 1988. Amiloride selectively blocks the low threshold (T) calcium channel. *Science.* **240**:213-5.

Tang, S., A. Yatani, A. Bahinski, Y. Mori, and A. Schwartz. 1993. Molecular localization of regions in the L-type calcium channel critical for dihydropyridine action. *Neuron.* **11**:1013-21.

Towbin, H., T. Staehelin, and J. Gordon. 1979. Electrophoretic transfer of proteins from polyacrylamide gels to nitrocellulose sheets: procedure and some applications. *Proc Natl Acad Sci USA.* **76**:50-59.

Triggle, D. J. 1992. Calcium-channel antagonists: mechanisms of action, vascular selectivities, and clinical relevance. *Cleveland Clinic Journal of Medicine.* **59**:617-27.

Triggle, D. J. 1994. Molecular pharmacology of voltage-gated calcium channels. *Ann N Y Acad Sci.* **747**:267-81.

Triggle, D. J. and R. A. Janis. 1987. Calcium channel ligands. *Ann Rev Pharmacol Toxicol.* **27**:347-369.

Triggle, D. J., and D. Rampe. 1989. 1,4-Dihydropyridine activators and antagonists: structural and functional distinctions. *Trends Pharmacol Sci.* **10**:507-11.

Triggle, D. J., and R. A. Janis. 1989. Recent development in calcium channel antagonists. *Magnesium.* **8**:213-22.

Triggle, D. J., D. A. Langs, and R. A. Janis. 1989. Ca^{2+} channel ligands: structure-function relationships of the 1,4-dihydropyridines. *Med Res Rev.* **9:**123-80.

Tsien, R. W., P. T. Ellinor, and W. A. Horne. 1991. Molecular diversity of voltage-dependent Ca^{2+} channels. *Trends Pharmacol Sci.* **12:**349-54.

Vaghy, P. L. 1992. Modulated multisubsite receptors fro calcium-channel ligands: unique binding of amlodipine. *J Cardiovasc Pharmacol.* **20(Suppl.A):**S17

Varadi, G., P. Lory, D. Schultz, M. Varadi, and A. Schwartz. 1991. Acceleration of activation and inactivation by the beta subunit of the skeletal muscle calcium channel. *Nature.* **352:**159-62.

Westenbroek, R. E., T. Sakurai, E. M. Elliott, J. W. Hell, T. V. Starr, T. P. Snutch, and W. A. Catterall. 1995. Immunochemical identification and subcellular distribution of the alpha 1A subunits of brain calcium channels. *J Neurosci.* **15:**6403-18.

Wheeler, D. B., A. Randall, and R. W. Tsien. 1994. Roles of N-type and Q-type Ca^{2+} channels in supporting hippocampal synaptic transmission [see comments]. *Science.* **264:**107-11.

Yatani, A., Y. Imoto, J. Codina, S. L. Hamilton, A. M. Brown, and L. Birnbaumer. 1988. The stimulatory G protein of adenylyl cyclase, Gs, also stimulates dihydropyridine-sensitive Ca^{2+} channels. Evidence for direct regulation independent of phosphorylation by cAMP-dependent protein kinase or stimulation by a dihydropyridine agonist. *J Biol Chem.* **263:**9887-95.